Small-scale biomass power plant for distributed energy generation

Politecnico di Bari

Department of Mechanics, Mathematics and Management

MECHANICAL AND MANAGEMENT ENGINEERING
Ph.D. Program

SSD: ING-IND/08–FLUID MACHINERY

Final Dissertation

Small-scale biomass power plant for distributed energy generation

by

Arianna Sorrentino

Supervisors:

Prof. Ing. Sergio M. Camporeale

Prof. Ing. Vinicio Magi

Ing. Giacobbe Braccio

Ing. Emanuele Fanelli

Coordinator of Ph.D. Program:

Prof. Ing. Giuseppe P. Demelio

Course n°32, 01/11/2016-31/10/2019

List of Contents

PART I

LIST OF FIGURES

PART I

ABSTRACT

Nowadays concern about climate change is gaining more importance not only in the scientific community but also in the public opinion, which is pushing for having policies oriented to encourage the use and the development of renewable energies. In order to contribute to the spreading and evolution of renewable energy, the approach to the distribution of the energy is changed from centralized to distributed generation (DG). In this frame, Combined Heat and Power (CHP) systems are becoming crucial, thanks to their capability to satisfy at the same time heat and power demand with a relatively high efficiency. One of the main advantages of these new solutions is that they can give a boost to the spreading of renewables and developments of green technologies. However, the selection and installation of the best performing renewable plants is never trivial due to the inherently intermittent nature of some renewables (as wind or solar energy) and so, their need to be integrated with energy storage and programmable generation systems in order to match energy demand.

This thesis deals with the integration of energy produced by biomass, mainly woody, with other small-scale power plants, such as Organic Rankine Cycle (ORC), and Thermal Energy Storage (TES), in a DG approach that exploits cogeneration to reduce energy waste. Two different scenarios are the main line of the following work: a hybrid plant, where biomass integrates solar energy, and a pure biomass boiler fed system, where the biomass supply heat to different power generations technologies. Tools such as optimization algorithms and thermo-economics analysis have been used to quantify the

effect of some of the many variables on the efficiency and profitability of such systems.

In the hybrid biomass-solar plant case, the effect of coupling this system with an external combustion gas turbine is analayzed. The turbine is fed by biomass to overcome the main limits of solar energy, i.e. energy intermittence. The coupling between the two systems is done by means of a TES that receives heat from both systems. In turn, the TES transfers heat to an ORC, which will be the element that supplies energy to the end-user. Concerning this layout, the performances, the effects of the use of different organic fluids in the plant ORC and the variation in economic profitability depending on the geographical location of the plant are analyzed.

The second case analyzes different layouts all with a biomass boiler. The furnace is here coupled with systems such as TES, steam plants and ORC in different configurations. Real input data from a biomass boiler installation and heat demand have been applied to the systems. The analysis has been performed by implementing hourly energy costs and electricity feed-in tariff. The aim is to evaluate the effect of TES and/or ORC installation in a biomass system and eventually select the best performing size and operating conditions of the plant components.

The two studies highlight that, in general, (i) coupling the biomass boiler with a TES allows the boiler to work at higher part-load conditions and at a higher global energy efficiency; (ii) profitability of ORC installation could increase with flexible plant, where the heat demand is satisfied also by the other component such as a TES: in this case, a smaller ORC size could be selected, increasing equivalent operating hours and reducing investment costs; (iii) investment profitability increases in the presence of a dedicated subsidy framework such as the one available in the Italian energy market. The future steps of this research will focus on the quantification of the techno-economic

advantages of the proposed system configurations in terms of higher generation flexibility and implementation of demand response strategies.

Introduction

Nowadays awareness of climate change is growing day by day. The public opinion is pushing governments around the world to adopt policies oriented to encourage the use and development of renewable energy. One of the main examples of this new attitude is the international school strike for climate, also known as “Fridays for future”, where students take time off from class to participate in demonstrations aiming at demand action to prevent further global warming and climate change.

Scientific research is focused since years in finding new solutions that can convert clean energy sources in usable energy and in increasing the efficiency of the existing technologies.

In order to contribute to the spreading and evolution of renewable energy, the approach to the distribution of the energy is changed from centralized to distributed, due to the decentralized nature that renewable sources have. A Large number of terms and definitions is used in relation to Distributed Generation (DG) (Ackermann et al. 2001) but loosely, it can be defined as small-scale electricity generation where the electricity is supplied to customers in the close neighborhood of the generation plant (Papermans et al.2005), in contrast to the traditional centralized electricity plant. International Energy Agency (IEA) listed DG among the five factors that contribute to renewable energy growing (IEA 2002).

DG implementation in the distribution system has many benefits, in addition to the elimination or reduction of output process emissions. These are:

- *Economic benefits*, because the systems can be considered modular, easily assembled and operated immediately and separately. Every module is not affected by other modules' failure. Moreover, DG systems has no location restriction with a positive effect on energy prices since DG system can be placed almost anywhere;

- *Operational benefits*, because the distribution network power losses are reduced; system continuity and reliability are increased, as DG systems are many generation spots, not only one centralized large generation (El-Khattam & Salama 2004).

The emergence of DG gave a boost to the development of Combined Heat and Power systems (CHP), due to the need to satisfying both thermal and power demand of residential, commercial or industrial buildings. Conventionally, electricity is purchased from the local grid and heat is generated by burning fuel in a boiler (Wu & Wang 2006). CHP, also known as cogeneration, consists in the simultaneous production of useful heat and electricity from a single energy source. A cogeneration plant has a higher efficiency compared to a conventional power plant since the heat produced during electricity generation is not wasted but captured and used to produce heating and hot water (COGEN 2001). CHP technologies, when applied to renewable power plants, help them to compete against fossil fuel plants because it has been proved that sustainable sources are incapable to take advantage of a big part of the available energy (Kooreneus et al. 2003).

One of the biggest limits of renewables, like wind or sun, is discontinuity because they are influenced by natural and meteorological conditions. Increasing penetration of intermittent sources is currently one of the main scientific and technological challenges (Teleke et. al. 2010). One method to overcome this inconvenience is to integrate solar or wind power generation technologies with power sources that can ensure continuous 24-hour power supply, such as diesel (Kyoungsoo Ro & Saifur Rahman 1998) or gas backup. In this frame, aiming at a full renewable power production, biomass can be a valid alternative to traditional fossil fuel and, also promoted by DG approach, renewable system could reach a full predictable system (Pérez-Navarro et al. 2010).

A second solution is to couple renewables plant with energy storage, that can supply energy independently from the moment it was produced. To store electric energy, it must be transformed at first into another form of storable energy and then transformed back when needed. There are many possible techniques for energy

storage, found in practically all forms of energy: mechanical, chemical and thermal. (Hibrahim et al. 2008).

This thesis deals with the integration of energy produced by biomass, mainly woody, with other small-scale power plants, such as Organic Rankine Cycle (ORC), and Thermal Energy Storage (TES), in a DG approach that exploit cogeneration to reduce energy waste. Two different scenarios are the main lines of the following work: a hybrid plant, where biomass integrates solar energy, and a pure biomass boiler fed system, where the biomass supply heat to different power generations technologies. Tools such as optimization algorithms and thermo-economics analysis have been used to quantify the effect of some of the many variables on the efficiency and profitability of such a system.

CHAPTER 1

This chapter consists of a literature review on the three macro-topics that are analysed in this thesis: Biomass and the methods to convert it into energy, ORC plants, and Energy Storage technologies. For each topic are also listed the reasons why they are scientifically interesting and their inherent limits, representing the current and future challenges for the scientific research.

1.1 Biomass and biomass energy conversion processes

Among alternative sources, biomass can be a secure energy supplier if managed properly (Huang et al. 2017). Biomass represents any organic matter which is derived from plant. It is a general term which includes Phyto-mass or plant biomass and zoomass or animal biomass.

Figure 1.1 Different sources of biomass fuel (APO 2010)

Biomass fuel is a more specific term that includes wood, short-rotation woody crops, agricultural wastes, short-rotation herbaceous species, wood wastes, bagasse, industrial residues, municipal solid waste, bio-solids, grass, waste from food processing, aquatic plants, algae animal wastes and a host of other materials (Demirbas 2004), see Figure 1.

The three products that can be obtained by conversion of biomass are energy in the form of power and heat, fuel for transportation and chemical feedstock. The method used to convert biomass is selected mainly on the basis of the biomass characteristics, but also on end-use requirements, environmental standards, economic conditions (McKendry 2002). Biomass can be converted by mean of three mechanisms: thermal conversion, biochemical conversion, and mechanical extraction process.

Mechanical extraction process

Mechanical extraction method has biodiesel as the main product. Biodiesel is a fuel used in Europe, US and many other countries. Chemically, biodiesel is composed of fatty acid methyl esters (Knothe 2008) and it is historically obtained from edible and no-edible plant oils. Mechanical extraction consists in cell disruption to extract lipids from the cellular (Halim et al. 2006). The oils available after this process undergo then transesterification, a process where oil or fat is reacted with a monohydric alcohol in the presence of a catalyst (Meher et. al 2006). The resulting biodiesel shows energy efficiency comparable to that of conventional diesel fuel ones and it is 98% biodegradable in 28 days, against conventional fuels that show a biodegradability of 20-30%. However, biodiesel has been considered not competitive with fossil fuel due to the high costs in terms of land, water, manpower and other resources required for cultivation. In recent years, food waste has been analyzed as a no-value and non-edible resource and can be used to develop a cost-effective process to produce biofuels (Karmee 2016).

Biochemical conversion

Biochemical processes exploit microorganisms during fermentation, anaerobic and aerobic digestion, hydrolysis, bio photolysis, and esterification in order to release energy from the biomass (Caputo et al. 2005). Those methods are primarily used for biomass that has a carbon-nitrogen ratio lower than 30 and moisture content at the harvesting higher than 30%. Thanks to biochemical conversion methods it is possible to obtain biogas, ethanol, and hydrogen.

Anaerobic digestion is used to produce biogas. In this process the waste is kept without oxygen for approximately 2-8 weeks at 310 K. The gas obtained is composed of 65-70% methane, 35-30% carbon dioxide and negligible traces of other gases (e.g. H2S and H2) and has an approximate heating value of about 26 MJ/m (Küçük and Demirbaş 1997).

Ethanol is produced through fermentation and it is widely used as a partial gasoline replacement, especially in the USA. Fermentation is a biological process in which organic material is converted by microorganisms to simpler compounds, such as sugars. These compounds are then fermented by other microorganisms to produce ethanol and CO2 (Lin and Tanaka 2005). Even if ethanol showed similar characteristics to fossil fuel in terms of efficiency and power, it cannot compete with them in terms of costs if produced from edible crop, since the land to farm it competes with the limited agricultural land needed for food and feed production (Sun and Chen 2002). To overcome this limit agro-residues biomass has been proposed as renewable resources for cost-effectively bioethanol production. Quality of the ethanol produced with this alternative method is lower than the one obtained from sugar and stark, but agro-residues are less expensive and in large quantities available (Gupta and Verma 2015).

Hydrogen is traditionally derived from non-renewable natural gas and petroleum. It can be theoretically also generated from renewable resources such as biomass or water but the main challenges of this process are the low efficiency of extraction process of hydrogen from water and that the technologies for hydrogen extraction from biomass are complex and have a low hydrogen production rate (Cortrig et al

2002). Anyway, due to the high potential of hydrogen as alternative energy technologies, much research has been focused on improving hydrogen production method from biomass, since it can be considered as the best option and it has the largest potential (Balat and Kirtay 2010). The methods available for hydrogen production from biomass are mainly divided into thermochemical and biological methods. Thermochemical processes, such as pyrolysis and gasification (for further details on these technologies see Chapter 1.1.3), have the advantages of a high overall efficiency and a low production cost (Patel et al. 2005) but they lead to the decomposition of the biomass feedstock leading to char and tar formation (Swami et al. 2008). Biological methods are bio photolysis, photo- fermentation, and dark-fermentation. These processes demonstrated to be more environmental-friendly and less energy-intensive then thermo-chemical one (Das and Veziroglu 2001).

Thermo-chemical conversion

Thermochemical conversion processes are direct combustion, pyrolysis, gasification, and Steam Explosion (SE). Those methods are normally selected for biomass with a humidity content lower than 30%. Although technologies such as pyrolysis and gasification are certainly not the most important options at present, combustion is responsible for over 97% of the world's bioenergy production (2009). Combustion is the most important and mature technologies nowadays available for biomass utilization. The most favorable biofuel for combustion is wood thanks to its low nitrogen content, which is a source of NOx, and ash components, such K and Cl, that leads to particulate emissions (Nussbaumer 2003). The burning of biomass is used to convert chemical energy to heat, in the form of hot gases at a temperature of 800-1000 °C, that can be stored or used to produce electricity or mechanical power. The biomass combustion techniques can be classified into three main types, namely gate-firing, fluidized bed and pulverized fuel (Rosendahl 2013).

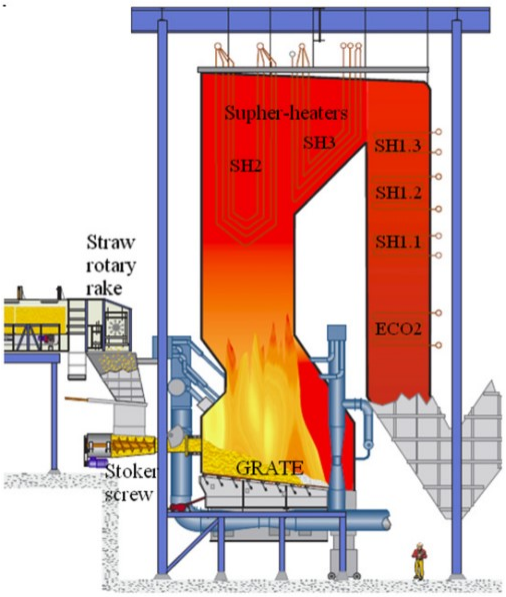

Figure 1.2 Grate-fired boiler burning biomass (Yin et al. 2008)

Grate-firing systems and fluidized bed combustors have both a good fuel flexibility and can be fuelled entirely by biomass or co-fired with coal. (Subramanian and Marwaha 2006). Suspension or pulverized burners are often used to co-fire milled biomass pellets or raw biomass with pulverized coal or natural gas (Werther et al. 2000).

Modern grate-fired boilers consist of four key elements: a fuel feeding system, a grate assembly, a secondary air (including over-fire air or OFA) system and an ash discharge system, in fig 1.2. The grates are mainly classified into stationary sloping grates, travelling grates, reciprocating grates, and vibrating grates (Yin et al. 2008). Among the different types of grates, vibrating gates may have the longest life and highest availability (Jørgensen 2007). The general combustion mechanism can be summarized as follows: after ignition, a reaction front propagates from the surface of the bed downwards to the grate against the direction of the primary air. The reaction front generates and transports heat against the combustion air flow and dries and devolatilizes the raw fuel. Reaction front is kept narrow thanks to the opposing directions of the heat flow and the air flow. If oxygen is still present in the reaction front, a char layer can be formed above the reaction front. When the reaction front reaches the surface of the grate, a secondary reaction front burns the char layer previously formed (Van der Lans et al. 2000).

Gasification is a process for the thermo-chemical conversion of biomass, where it is converted, in the presence of a gasifying agent, to a multifunctional gaseous mixture, usually called syngas or synthesis gas (Molino et al. 2018). Syngas consists of a

mixture of CO, H2, CO2, CH4 (primary components) and H2O, H2S, NH3, tar, and other trace species (secondary components) (Ahmad at al. 2016). It can be used to produce energy (heat and/or electricity generation), chemicals (ammonia) and biofuels (Molino et. al 2013). Usually, there are four steps in the gasification process: drying (endothermic step), pyrolysis (endothermic step), oxidation (exothermic stage), and reduction (endothermic stage). Eventually, Tar-reforming can also be added as a step that produces light hydrocarbons from large tar molecules (Kumar et al. 2009). The main biomass characteristics that can affect gasification performance are: (i) biomass type, because the syngas yield is related to the proportion between cellulose and hemicellulose; (ii) moisture content, that should be kept low to increase energy efficiency, syngas quality, and Higher Heating Value and to decrease conversion emissions (Sikarwar et al 2016); (iii) particle size, that is fundamental to select the correct gasification technology (Parthasarathy and Narayanan 2014); (iv) ash content, that influences the gasifier operating temperature (Sansaniwal et al. 2017). Biomass gasification technologies are normally classified as fixed bed gasifiers, fluidized bed gasifiers, and entrained flow gasifiers. Processes in every reactor are always drying, pyrolysis, reduction, and finally combustion but the sequence of those steps is different. In fluidized bed gasifier, a cyclone separator at the outlet of the reactor is required to separate bad material from the syngas produced (Molino et al. 2016).

Pyrolysis is the thermal decomposition of biomass that takes place in the absence of oxygen (Maschio et al. 1992). It produces (i)solid components, so-called char, that can be used as either a slurry fuel, a soil-improving agent or as the activated carbon in industrial applications; (ii) liquid mixture, called bio-oil, used for producing different chemicals such as levoglucosan and acetic acid, upgraded motor fuel and electricity; (iii) gaseous products that can be utilized for producing solvents such as acetone and methanol, and other gaseous substances such as syngas (Balat et al. 2009). It is normally classified in “fast” pyrolysis, characterized by high heating rates and short vapour residence times, and “slow” pyrolysis, characterized by a gentle heating of relatively larger solid particles for longer vapour residence times and

usually a lower temperature than fast pyrolysis (Sharma et al. 2015). Pyrolysis process can be modified by using catalysts and the application of different catalysts in biomass pyrolysis process can lead to an upgradation of pyrolysis products (Bridgwater 1996). They can decrease decomposition temperature, promote formation of coke, increase releasing of CO and CO2, and other effects.

Steam Explosion is a thermo-mechanic chemical pre-treatment which allows the breakdown of lignocellulosic structural components by the action of heating, formation of organic acids during the process, and shearing forces resulting in the expansion of the moisture (Jacquet et al. 2015). This method was developed to open the complex structure of lignocellulose, one of the major components presents in biomass materials, and so make biomass polymer more accessible for subsequent processes. In general, steam explosion is a process in which biomass is treated with hot steam (180 to 240 °C) under pressure (1 to 3.5 MPa) followed by an explosive decompression of the biomass that results in a rupture of the biomass fibers rigid structure (Stelte 2013). Major parameters of steam explosion processes are the particle size, temperature, and residence time (Overend and Chornet 1987). It is recently used for the pre-treatment of wood prior pelletization since it showed an increased heating value and pelletizing properties while decrease moisture absorption (Lam et al 2011).

Energy from biomass: Life Cycle Analysis

Biomass is considered a carbon neutral source of energy: the CO2 produced during complete combustion is equal to the amount absorbed from the atmosphere in the growing stage (OECD 1991). Therefore, interest in bioenergy and biofuel is continuously growing and their use is pushed by many regulations of emissions in the USA and Europe.

With time some questions about biomass sustainability were raised. Petrou and Pappis (2009) analyzed the main economic, environmental, and social impacts of biofuels, measuring the pros and cons of their use in energy production. In their study, some problems are listed such as the increase of food market prices due to the

increased use of cultivation land for biomass, or the negative impact concerning the supply chain of solid biofuels production that emits heavy metal (Pb, Hg, etc.) and dioxin. Tabatabaie and Murthy (2016) focused on the environmental impact of biofuels considering biomass location, production practices and proved that the variations in weather and soil characteristics are important factors in determining the overall field emissions. To assess the sustainability of biomass and biofuel is used the Life Cycle Assessment (LCA).

LCA is a technique for assessing the environmental aspects associated with a product over its life cycle. It is made by four steps: 1) definition of scope goal to identify the size of product life cycle to assess and the final aim, 2) definition of material and energy fluxes, called inventory analysis, and their interaction with the environment, 3) impact assessment, where each category defined in phase 2 is normalized and a certain importance has been assigned to them, 4) data interpretation. Even if these four steps are constant in every LCA application, there are several ways to approach LCA of a product: it can be done from "cradle-to-grave", when it starts from manufacture (cradle) through the to the disposal phase (grave), from "cradle-to-cradle" where the end-of-life of the product is a recycling process, until you get to Life cycle energy analysis (LCEA) where is considered not only direct energy inputs during manufacture, but also all energy inputs required to produce components and services needed for the manufacturing process (Muralikrishna and Manickam 2017). LCA technique is gaining in significance as a tool that evaluates the environmental impacts of bioenergy chains. It helps to identify the most critical parts of the chain (geographic location, transport, conversion technologies…) and it focuses on how to improve it.

As regards woody biomass considered in this thesis, fertilizer production and application result in some of the big contributors to global warming applying LCA. Therefore, it is possible to reduce this negative impact using plant species that require low maintenance and low agrochemical inputs (Patel et al. 2016). Post-combustion ashes are also a problematic product to deal with when biomass direct combustion is considered. However, the application of ashes as a soil quality

improver is an alternative that can lead to a decreasing use of fertilizers (Boschiero et al. 2016). Production of energy from direct combustion in a biomass boiler can show a negative balance of the greenhouse gas (GHG) emissions, as analyzed by Tagliaferri et al. (2018). They apply LCA to Heathrow energy center biomass plant and it shows environmental impact can be reduced by coupling biomass furnace to a steam turbine and an even more reduction can be obtained by ORC. Considering biomass plant in CHP configuration is very important too (Bartocci et al. 2018).
In conclusion, there are still many ways to improve the application of biomass as renewables but most LCA studies found a significant net reduction in GHG emissions when bioenergy replaces fossil energy (Cherubini and Strømman 2011). Moreover, it is generally accepted that biofuels offer several advantages: sustainable energy production, regional development, agricultural and social development (Taylan et al. 2017).

1.2 Organic Rankine Cycle

ORC is a concept based on standard steam Rankine Cycle, that uses alternative working fluids able to efficient recovering low enthalpy heat at T<370 °C. (Hung et al. 1997).
ORC is technically composed of the same equipment present in a steam Rankine cycle: a pump, two or more Heat Exchanger (HE), an expander, and a power generator. The pump compresses the working fluid in order to reach the thermodynamic conditions at the evaporator entrance; it is normally selected a multistage centrifugal pump.
Heat exchangers have several tasks:

1. introducing heat into the system. Architecture of this HE depends on the type of fluids and on the characteristics of the thermodynamic cycle. It normally consists of economizer, evaporator, and superheater (if required);
2. release in the environment the remaining heat in the fluid after the turbine expansion, in a so-called condenser;

3. eventually recover the thermal energy available after the turbine discharged, in a recuperative configuration of the ORC. This HE, called regenerator, is selected based on the temperature of the heat source.

Most common HEs are Shell and Tubes. Those are made by a bundle of tubes enclosed in a shell: one stream flows in the tubes, the other in the shell with a direction almost perpendicular to the tubes. HEs have to be selected with particular attention, due to the relatively low efficiency of the ORC and their large fraction of power block cost.

The expander is a key component of an ORC. It converts the enthalpy drop available into torque that will be in turn converted into electrical energy by the power generator. It is selected based on plant size and type of fluid; expander can mainly be a turbomachine or a volumetric device (Macchi and Astolfi 2016). A recuperative layout is shown in Figure. 2a, where the thermal oil loop resents here the low-grade heat-transfer fluid which extracts energy from different sources.

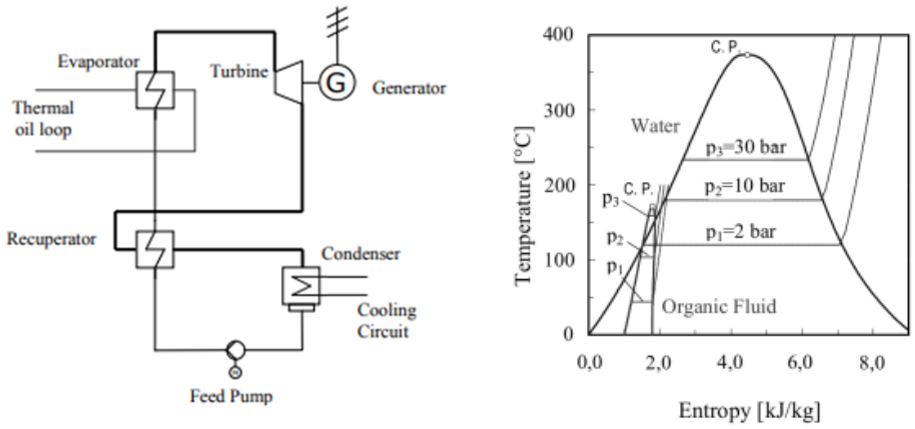

Figure 1.3 a) Recuperative Organic Rankine Cycle layout. b) Comparison between steam and a generic organic fluid saturation curves. (Karellas and Schuster 2008)

ORC gained with time a growing interest, due to its ability to produce electricity in a bottoming cycle, virtually requiring no fuel. ORC first design in 1970s was powered by thermal energy of the exhaust of one diesel truck engine (Patel 1976). From that moment, many studies have been done in ORC automotive applications

driven by the desire of overcome many challenges (the system must be small and light, organic fluid must satisfy environmental and technological requirements) to recover the wasted heat discharged in the environment, that is approximately equal to the 66% of the fuel energy content (Lang et al. 2016). Nowadays there are unfortunately no commercial ORC for automotive applications, but several and robust solutions have been developed for power plants in DG purpose. As regards ORC systems coupled to renewables plants, state of the art applications includes CHP production from biomass combustion and combination with heat produced by geothermal heat sources. Other innovative uses are driving stand-alone solar desalinization system by exploiting solar radiation, recovering waste heat from biogas digestion plants, and producing power in a range of few kW_{el}, if coupled with micro-gas turbine or biomass fired boiler in Micro-CHP plant (Schuster et. al 2009). ORCs owe their success to some characteristics of the organic medium used, which have several advantages in recovery low-temperature heat sources respect to steam. Indeed, these fluids can be used at a much lower evaporation temperature and pressure than in a conventional steam cycle (Figure 2b), and still achieve a competitive electric efficiency or perform even better at low temperatures (Vankeirsbilck et al. 2011).

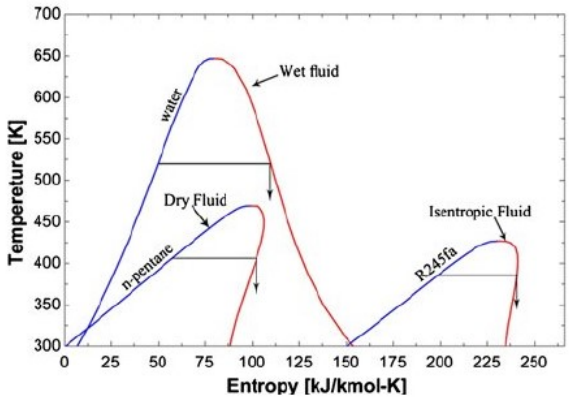

Figure 1.4 T-s diagram of dry, isentropic and wet type organic fluid (Bahram et al. 2013)

Organic fluid can be classified as wet, dry and isentropic (Figure 3) and this definition is based on the slope of their curve in the saturated region in a Temperature-Entropy plane, also called T-s plane. A wet fluid has a positive saturation vapor curve. This fluid can condensate during the expansion process and damage the turbine. Isentropic fluids with vertical saturation curves and dry fluids with a negative slope in the saturation region have no fluid condensation problems during expansion (Ebrahimi et al. 2017).

The selection of the working fluid is crucial in ORC design process since it affects the efficiency of the system, size of components, system stability and environmental impact (Bao and Zhao 2013). As described before, a first selection can be done considering the slope of the saturation vapor curve. The use of a wet fluid is normally avoided in ORC application, due to the saturated liquid content during the expansion phase that leads to turbine damages and reduction of turbine isentropic efficiency. Albeit superheating the turbine inlet fluid can increase the minimum dryness fraction at the outlet of a turbine, this solution is hard to implement because often the heat sources cannot supply enough temperature driving force or, if the heat is available at high temperature, the HE required to reach such thermodynamic conditions could be pretty expensive and reduce the profitability of the complete system (Desai and Bandyopadhyay 2009). Select a "too dry" fluid can be also tricky since it will run the risk to have at the turbine outlet a superheated fluid, which is not only a waste but it also will increase the load at the condenser (Chen et al. 2010). In this case, a regenerator could be a viable solution, since it will reclaim these exhaust vapor to increase the cycle efficiency even with a slight increase of the system's initial price. Further selection can be done considering other thermo-physical properties such as specific and latent heat, density and critical point. Chen et al. (2010) demonstrated that a performing working fluid shall have a high density, low liquid specific heat, and high latent heat since they are expected to give high turbine work output. As regards critical points, they should be normally not lower than 300 K due to the technical limitation of the condensation temperature and not too high to overpass in a supercritical Rankine cycle.

Other important organic fluids characteristics are chemical stability, environmental impact, and safety.

When it comes to organic fluid, it must be considered their chemical decomposition at high temperature, that also leads to a limit to the maximum cycle temperature (Pasetti et al. 2014). The fluid should be chemically stable over the whole employed temperature range. Chemical decomposition of the fluid can produce non-condensable gases which lower the heat transfer rate in the condenser, as well as compounds, which have corrosive effects on the materials of the system (Badr et al. 1985).

As regards the environmental impact, the substance potential to contribute to ozone degradation and global warming is indicated by Ozon Depletion Potential (ODP) and Global Warming Potential (GWP). ODP is the relative amount of degradation to the ozone layer that a chemical compound can cause, with trichlorofluoromethane (R-11 or CFC-11) being fixed at an ODP of 1.0; GWP consists in the amount of heat trapped by a certain mass of the gas in question to the amount of heat trapped by a similar mass of carbon dioxide and is expressed as a factor of carbon dioxide (whose GWP is standardized to 1). Due to environmental concerns, some working fluids have been phased out, such as R-11 or R-113, but this is pushing researchers to develop new fluids with zero-ODP and low (<10) GWP (Kontomaris 2012).

Ultimately, the level of danger of organic fluids can be found in the ASHRAE refrigerant safety classification (ASHRAE 2013). Generally, characteristics like noncorrosive, non-flammable, and non-toxic are expected. The maximum allowable concentration and the explosion limit should also be under consideration.

Although ORCs are considered a proven technology, there are still key research challenges: the identification of high-performance working fluids, the corresponding optimal design configuration and operating characteristics of the thermodynamic cycle and the optimum integration of the ORCs with the available heat sources (Linke et al. 2015). The literature regarding optimization methods applied to ORC is therefore extensive. Thermodynamic and economic optimization of a small-scale

ORC in waste heat recovery application has been carried out by Quoilin et al. (2011). In this work a sizing model of the ORC is proposed, capable of predicting the cycle performance with different working fluids and different components sizes. Madhawa et al. (2007) applied the steepest descent method to optimize a binary Organic Rankine power cycle using low-temperature geothermal resources. The used optimization criterion is the ratio of heat transfer area to net power produced, which is a good measure of the total power plant cost. Wang et al. (2012) presented a working fluid selection and parametric optimization using a multi-objective optimization model by simulated annealing algorithm. In their study 13 working fluids are compared, showing that the boiling temperature of working fluids will greatly affect the optimal evaporating pressure. Many conventional optimization methods, like steepest descendent, are easy to converge to sub-optimal solutions during the process of searching for the optimal values, especially for complicated problems. Different from many optimization methods, genetic algorithm (GA) method involves several individuals in a population when starting searching, which could avoid converging to sub-optimal solutions effectively (Xi et al. 2013). ORC has indeed many parameters that are varied together, presenting a multi-dimensional surface on which an optimum can be found. GA is employed by Dai et al. (2009) to examine the effects of turbine inlet pressure and temperature on the cycle performance. They proved that under fixed waste heat condition cycle with organic working fluids are much better than the cycle with water and, among organic fluids, the ones with non-positive saturation vapor curve slope have the best performance property with saturated vapor at the turbine inlet. The main limit of GA application is that it is not able to optimize problems that require the simultaneous satisfaction of several different and often conflicting objectives, also known as multi-objective problems (Wang et al. 2013). The Non-dominated Sorting Genetic Algorithm (NSGA) is an extension of the GA for multiple objectives function optimization. The flexibility of this algorithm is proved by several authors. Hajabdollahi et. al (2013) optimized an ORC for diesel engine waste heat recovery using NSGA to maximize the thermal efficiency and minimize the total annual cost simultaneously, while

Imran et al. (2015) used NSGA to optimize a plate-type evaporator for minimum cost and pressure drop. A more detailed overview of the optimization methods here mentioned can be found in Chapter 2.

1.3 Thermal energy storage technologies

In DG systems, the issue related to the fluctuation of renewable energy sources availability can be also overcome by system layout which includes a Thermal Energy Storage (TES). The basic idea behind a TES is to provide a buffer to balance the fluctuation and the mismatch between energy supply and demand of thermal energy (Nielsen 2003). A practical example can be TES application in solar energy systems. In such a plant there is the need for an effective means by which the excess heat collected during periods of bright sunshine can be stored and later released for utilization during the night or other periods (Sharma et. al 2009).

Classification of TES technologies is made based on the mechanism used by the medium in the tank to store the energy. There are three main classes of storage: (i) specific or sensible heat storage, (ii) latent heat storage, also called phase-change materials storage, and (iii) thermochemical heat storage.

In sensible heat storage heat is stored by raising the temperature of the heat storage medium (HSM) without the occurrence of phase change (Hasnain 1998). The total amount of the stored heat can be expressed as $Q = \int_{Ti}^{Tf} mCp\ dt$, where Cp is the specific heat of the medium and m its mass, T_i and T_f are respectively initially and final temperature states of the HSM (Avghad et al 2016). An efficient sensible heat storage requires, therefore, a medium with a high specific heat capacity that can reduce the costs of the system. Moreover, the HSM should have long-term stability in terms of thermal cycling and should be compatible with the container material in which storage takes place (Khare et al 2013). Different media can be used in sensible heat storage and they can be both liquid and solid. HSM liquids are plentiful and economically competitive. At low temperature (max 90 °C) water is one of the best storage medium since it has a higher specific heat (≈ 4.2 kJ/kg K) and low cost. It has also the advantage of being a liquid that can easily be pumped to transport

thermal energy. A water TES is often the logical choice for building heating or cooling (Frazzica et al 2016). However, due to its high vapor pressure water as heat storage material requires insulation and pressure withstanding container for operation at high temperature.

When it comes to higher temperature, synthetics oils, molten salts (MSs) or liquid metals are a viable solution as HSM. MSs are of particular interest in solar power systems as well as for non-solar applications. MSs are mainly nitrate salts since they show low corrosion range and show a high thermal stability. The two most used MS are Solar salt, that are a binary salt consisting of 60% of NaNO3 and 40% of KNO3, it melts at 221 °C and is kept liquid at 288 °C in an insulated storage tank; or HitecXL, a ternary salt consisting of 48% Ca(NO3)2, 7% NaNO3, and 45% of KNO3 with a melting point of 130 °C (Kuravi et al. 2013). They are liquid at atmospheric pressure. They can reach a temperature of 450-500°C, which is higher than the maximal temperature achievable with current high-temperature oil that is around 390°C, thereby increasing the potential cycle efficiency of a bottoming power-block. Moreover, MSs are cheaper and more environmentally safe than the other HSM. The major limit of the MS is its high freezing point. Freezing in synthetic oil currently occurs at about 15°C, whereas the ternary and binary molten salts freeze at about 120°C and 220°C, respectively (Kearney at al. 2003).

Solid material such as rocks or metal can be also suitable as HSM. They can store high or low-temperature heat since these materials will not freeze or boil. Moreover, solids do not leak from their container (Hasnain 1998).

Latent heat storage provides a high energy storage density and it stores heat as latent heat of fusion at a constant temperature corresponding to the phase transition temperature of the phase change materials (Agyenim et al. 2010). The latent heat storage technology depends on absorbing or releasing heat from the storage material, so-called phase change material (PCM), when it undergoes a phase change process from solid to solid, solid to liquid, liquid to gas or the opposite. The heat stored can be evaluated according to the following equation $Q = \int_{Ti}^{Tm} mCp\, dt + ma_m \Delta h_m + \int_{Tm}^{Tf} mCp\, dt$ where Cp is the specific heat of the HSM and m its mass, T is

temperature at the initial status T_i, final status T_f and melting status T_m, a_m represents the melted fraction of the material and Δh_m is the enthalpy of fusion (latent heat of fusion) (Mohamed et al 2017). Advantages of these storage systems are the reduction of the storage volume, due to the higher energy storage capacity of latent TES, that decreases the amount of HSM and the volume of the container itself, the possibility of recover the stored energy at almost constant temperature, and the ability of store a big amount of energy even if the difference of temperature between the source of heat and heat sink is low (Halawa et al 2005). The selection of a PCM is based on several characteristics of desirables for such application. Those materials should have a high latent heat of transition and a suitable phase-transformation temperature, high density, small volume change, and low vapor pressure; moreover, they should have a good chemical stability to avoid any degradation that can corrode the container and they should be not toxic or flammable (Pielichowska and Pielichowski 2014). Phase change materials generally are divided into organic materials (such as paraffin and alkanes) and inorganic phase change compounds, including salts, salt hydrates, metals, and alloys (Farid et al 2004).

Thermochemical thermal storage exploits chemical reactions to absorb energy that can be lately reversed (Dinçer and Rosen 2011). The heat intended to be stored is used to excite an endothermic chemical reaction. If this reaction is completely reversible, the thermal energy can be recovered completely by the reverse reaction. This mechanism has the advantages of a high storage energy densities, indefinitely long storage duration at near ambient temperature, and heat-pumping capability. The main limit of this solution is the development level of reversible thermochemical reaction, that is at a very early stage (Abedin and Rosen 2011).

Storage systems can be also classified according to two different concepts: active or passive. When the heat transfer into the HSM is done by forced convection, the TES is called active. An active TES can be also called direct when the same medium is used as HTF and HSM, or indirect where HTF and HSM are different. The active direct TES deals with the problem of the selection of the medium since it has to be at the same time a good HTF and HSM. On the other hand, active indirect TES are

often more expensive due to the need of an addition HE. One of the most used active direct systems is the two tanks direct system, which consists in a storage system where the HSM is directly stored in a hot tank, in order to use it during cloudy periods or nights and, when cooled , it is pumped to the other tank, cold tank, where it remains waiting to be heated one more time.

The passive TES is mainly used for solid storage systems but also in latent TES. This concept imposes that the HTF passes through the storage to charge and discharge the system, while the HSM does not circulate (Gil et al. 2010).

CHAPTER 2

THERMO-ECONOMIC ANALYSIS

In this chapter the general equation and the main indexes used to compute the economic analysis are listed and their meaning in investment appraisal is described.

2.1 Main financial appraisal indexes

Initial investment cost of a power plant is not negligible, particularly for renewable power plant where many components are not at a state-of-the-art stage concerning production. Moreover, income from selling of energy obtained by renewables are sometimes lower than the one obtained from traditional plant, due to the lower amount of energy that can be produced from green technologies.

In order to balance this gap, specific feed-in tariff has been introduced in many counties to encourage renewables plants installation. A feed-in tariff is a policy mechanism, consisting in a financial contribution per kWh of energy produced over a certain period, which varies according to the size or type of plant. This policy aiming at promoting the installation of renewable technologies by means of reduction of recovery time of the costs of the plant or initial capital investment and later increasing the profits.

One of the most crucial and complex stages in the capital budgeting decision process is the financial or economic evaluation of the investment proposals (Dayananda et al 2002). Anyway, the evaluation of the main financial indexes can give an indication of the profitability of the investment. In the following, indexes definition can be found.

Net Present Value

Net Present Value (NPV) approach consists in discounting all future cash flows resulting from the innovation project with a given discount rate and then summing them together. NPV is evaluated according the following equation (Khan 1999):

$$NPV = \sum_{t=0}^{n} \frac{NCF_t}{(1+r)^t}$$

where:

- NCF_t is net cash flow generated by innovation project in year t;
- r is the discount rate;
- n is lifespan of the project investment evaluated in years;
- t the index of the period of time considered as increment for life duration.

Future cash flow is discounted every year since it considers the money devaluation with time. Profitable projects NPV has to be a positive value. The final value can then be estimated either as zero (in the case of an innovation facing complete obsolescence), negative (in the case of an innovation involving rehabilitation or recycling costs, as, for example, in the energy sector) or as a proxy of future cash flow based on resale value, balance-sheet metrics or "perpetual" value (Žižlavský 2014).

Main advantages of NPV approach are (i) the association of a cash flow to an investment, rather than a time period or a time rate, (ii) the capability of consider project with different risk profiles, (iii) explicit arbitrary threshold, such as a minimum rate of return or a maximum pay-back time, are not involved (Gaily 2011). On the other hand, NPV limitations are the evaluation of the discounted rate and cash flow evaluation. The discount rate in the evaluation of innovation projects should be made of two elements: one related to general risk, the other the perceived risks (financial, technical and commercial) associated with the specific project (Doctor et al. 2001). Determination of the exact value of the cash flows to be discounted is required in NPV calculation for each time period considered in the evaluation. This value could be rather difficult, if not impossible, to determine for long-term project that appears to be discriminated by this approach.

Internal Rate of Return

Internal rate of return (IRR) is the discount rate when the NPV of a particular cash flows is exactly zero. The higher the IRR, the more growth potential a project has

(Belyadi 2017). In mutually exclusive projects, the project with higher IRR must be picked. Evaluation of the IRR is done using a similar equation as NPV except that the NPV is replaced by a zero:

$$0 = \sum_{t=0}^{n} \frac{NCF_t}{(1 + IRR)^t}$$

It is calculated manually by trial and error, or by a special routine in computerized spreadsheets.

Profitability Index

The profitability index (PI) is the ratio of discounted benefits over the discounted costs. It is also referred to as benefit-cost ratio, cost-benefit ratio, or even capital rationing. PI express the relationship between NPV and investment funds that generate NPV volume. It expresses investment analysis in relative terms, in the form of net benefit per unit of measurement relative to the cost of the investment (Gurau 2010).

PI can be expressed by the following equation:

$$PI = \frac{\sum_{t=1}^{n} CFD_t \cdot (1 + k)^{-t}}{I_o} = \frac{NPV + I_o}{I_o}$$

where:

- CFD_t is available cash flow in year t;
- I_o is the initial investment;
- n is the lifespan of the project investment evaluated in years;
- t is the index of the period of time considered as increment for life duration;
- k is the minimum acceptable rate of profitability.

In a decision process of a project investment, if the NPV of the project has a positive value, the project investment is considered profitable only if PI is higher than 1 (Glazebrook 1976).

Main advantages of PI use are that it considers the risk involved in future cash flows by exploitation of cost of capital and that it takes the time value of money into

consideration. Disadvantage of this method is the need of an estimate about the cost of capital to carry on the calculation.

Payback period and discounted Payback period

The payback (PB) is the evaluation of the return per year starting from the project begin until the accumulated returns are equal to the initial investment cost, so the investment is paid back. The PB period (PBP) is the time take to achieve the payback. It indicates how quickly the initial investment costs are recovered but it does not really measure investment profitability (Lefley 1996).

PBP methods disadvantages are that (i) it does not take any regard of returns after the payback period and, (ii) it ignores the timing of the returns. As regards of the first issue it is only in very limited circumstances that ignoring the returns after the payback period has some effect on the investment decision (Pike 1985). On the other hand, the second limit has been somehow addressed by the development of the discounted payback method.

The payback method introduced by Rappaport (1965) based on the discounted cash flow, which the opportunity investment rate is related to payback period measure. Actually, not even the discounted payback suggested by Rappaport considers the returns after the payback period, but it is an improved measure of the liquidity and project time risk respect to the conventional PB approach.

CHAPTER 3

SMALL-SCALE BIOMASS POWER PLANT IN DISTRIBUTED GENERATION FRAME

The aim of this work is to analyze systems that use biomass as the main renewables source in a cogenerative DG environment and evaluate how the efficiency or the profitability of such a system can be modified when they are coupled with other technologies, that can be either traditional or innovative.
In particular, analyzed cases can be divided into two branches:

- The first one considers a hybrid biomass-solar plant. It is composed of a biomass boiler, an externally fired gas turbine (EFGT), a concentrating solar panel (CSP) system, a TES, and an ORC; all organized in a modular layout. The profitability of this layout has been studied in different Mediterranean areas, along with the efficiency and effect of different organic fluid use in the ORC module.
- The second branch is focused on biomass boiler furnace technology coupled with different systems, such as steam Rankine Cycle, ORC or TES. The different proposed layouts have been analyzed according to thermo-economic factors. Finally, a optimization code has been developed that aims at finding the optimal operating condition to minimize the costs.

3.1 Hybrid Solar/biomass system

Hybrid energy systems incorporate a combination of one or several renewable energy sources such as solar photovoltaic, wind energy, micro-hydro and eventually some storage system as backup (Ashok 2007). The main advantage is to combine the inherent characteristics of different renewables to overcome their limits. Deshmukh and Deshmukh (2008) designed and evaluated the

performances of a hybrid photovoltaic/ wind hybrid system where solar and wind energy combination can attenuate fluctuations in power produced and significantly reduce energy storage requirements. A hybrid wind–fuel cell energy system has been simulated by Khan and Iqbal (2005) where load is supplied from the wind turbine with a fuel cell working in parallel. The simulation results showed that the voltage variation at the output was within the acceptable range and the proposed system has also the advantages of no need conventional battery storage.

In this work, biomass is combined with solar energy to increase solar plant's dispatchability and compensate lack of solar energy presence during night hours and unfavourable weather conditions.

3.1.1 Externally-fired gas turbine and Concentrated Solar Panel modules

CHP plant analysed here is a modular layout composed of independent Power blocks (Figure 3.1). Each block has its own function: gas turbine and ORC are responsible for electric power generation; thermal energy sources are the biomass furnace and CSP plant. TES store excess of heat that remains available in the event heat demand is higher than produced heat.

EFGT thermodynamic cycle is characterized by an inter-refrigerated compression (A-C) with an overall pressure ratio of 10. Turbine inlet temperature (TIT) has been fixed at 800°C to keep low the cost of the HE. Heat to the working fluid has been provided by a gas-gas High Temperature Heat Exchanger (HTHE) that transfers the heat of the flue gas exiting the biomass furnace to the compressed air (C-D). The air is then expanded in the turbine (D-E). All the thermodynamic points of the cycle are shown in Figure 4.4. The heat of the air exiting the turbine has a temperature sufficiently high (390°C) to be recovered and transmitted to the molten salts flowing in the

heat exchanger indicated as Heat Recovery Molten Salts Heat Exchanger (HRMSHE). Since the minimum temperature of the cold tank is 200 °C, sensible heat can be further recovered from the gas for cogeneration.

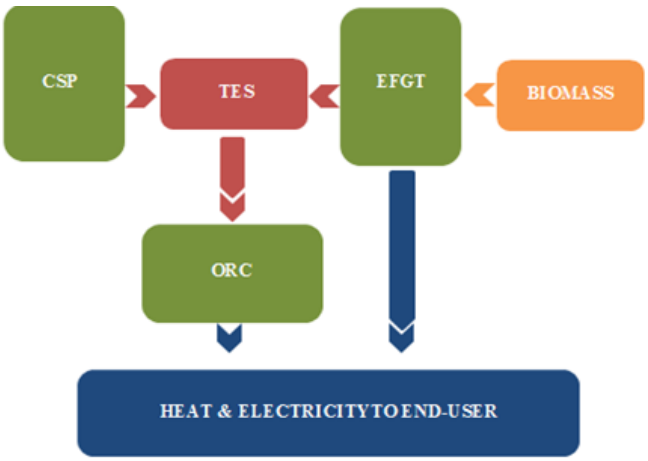

Figure 3. 1 Power blocks and energy flows through the proposed plant (Pantaleo et al. 2018)

CSP section is technologically composed by Parabolic trough collectors (PTCs). A PTC consists of an absorber made by a tube with a transparent cover and a parabolic reflector plate (see Figure 3.2). Absorber is the focus of the concentrator and converts received solar radiation into heat transferred to the working fluid.

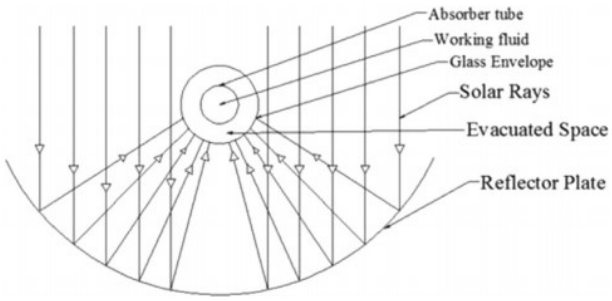

Figure 3. 2 Schematic diagram of Solar parabolic trough collector (Jebasingh and Herbert 2016)

In PTC the temperature of the focal line or absorber tube can be as high as 350–400 °C. The HTF can be of different types, such as water, air oil or some other mixture and flow along the absorber. The thermal energy is stored and became therefore immediately usable.

PTC technology considered in this study is based on the same solution used in the experimental facility built by ENEA (Italian agency for research and development involving nuclear and alternative energies) in a demonstration plant called “Archimede” in Sicily (Giannuzzi et al. 2007). The aim of that project was to produce electricity in a cogenerative layout with a steam turbine, therefore heat was required heat at high temperature. Molten salts (MSs) were selected as most suitable HTF for this application since they can reach a maximum temperature of around 500°C with low environmental risks (they are basically fertilizer (Falchetta and Maccari 2006)). A mixture of MSs composed of lithium, sodium and potassium nitrates is the HTF considered in the plant analyzed in this thesis. The same mixture of MSs flows in the PTCs and in a two-tank TES in a so-called “Direct Heating” configuration, because it requires no additional HE between the solar plant and the storage system. MSs flows in the PTCs also during the night to avoid an excessive cooling of the system. Temperatures of the hot and cold tanks of the storage have been chosen 370 °C and 200 °C respectively. The difference in temperature between the two tanks is the maim CSP design process parameter. It is made of one or more lines of collectors and the higher the difference in temperature between entering and exiting HTF the higher should be the number of collectors that compose the line. To increase to 170 °C a MSs flow rate of 6 kg/s, assuming a fluid velocity of 1.2 m/s, a line with an overall length of 506 m is required, which means each line is composed of 6 collectors of 96 m.

3.1.2 Organic Rankine Cycle optimization

The technology that can exploit with an acceptable efficiency a thermal source of 370 °C is ORC. As regards this module the total thermal input has been assumed of 2790 kW_t and, since the heat is available at a relatively high temperature, a recuperative configuration is chosen for the cycle.

Selection of the ORC parameters has a big impact on the overall ORC performance. To select the best performing ORC to integrate in this hybrid biomass/solar configuration, two different optimization steps have been performed. The first one is a single-objective (SO) optimization that aims at selecting the best performing organic fluid. The second-one is a multi-objective optimization (MO) where the best set of cycle parameters, such as evaporating pressure or pinch point temperature is evaluated. The research of the optimal solution has been performed by means of Genetic Algorithm (GA) in the first step and NSGA in the second one. Those algorithms are implemented in an in-house Python code (Bufi et al. 2017) where the complex thermodynamic behaviour of the organic fluid is described by multi-parameter equations of state (EOS) based on Helmholtz free-energy, as provided by the open-source library CoolProp (Bell et al. 2013). More details on the optimization algorithm can be found in Annex-I.

The two organic fluid selected to carry out the SO optimization are R113 and toluene. Both selected because of their stability in the considered temperature range (200-370°C) and their zero or near-zero ODP. Objective function of the SO optimization is the cycle thermal efficiency:

$$\eta_I = \frac{\dot{W}_{exp} - \dot{W}_{pump}}{\dot{Q}_{in}} \qquad (1)$$

Where:

- $\dot{W}_{exp}$ is the expander shaft power output, considering a mechanical efficiency equal to 0,96 and an isentropic efficiency 0,8;

- $\dot{W}_{pum}$ is the pump shaft power input, considering a mechanical efficiency equal to 0,96 and an isentropic efficiency 0,75;
- $\dot{Q}_{in}$ thermal power input from MSs.

Optimization parameters are:

- Evaporating pressure P_{ev} where subscript EV indicates evaporating status;
- Superheating $\Delta T_{TIT} = T_{TIT} - T_{ev}$ where T indicates the temperature;
- Pinch point Temperature at the Heat Recovery Vapour Generation that will be indicated as ΔT_{PP}.

To the optimization problems have been imposed the following constraints:

- $0.4P_c \leq P_{ev} \leq 0.9P_c$ where the subscript c indicates critical status;
- $\Delta T_{TIT} \leq (T_{hot\ tank} - T_{ev})$;
- $7K \leq \Delta T_{TIT} \leq 10K$;
- $5K \leq \Delta T_{min,RHE}$, where $\Delta T_{min,RHE}$ is the minimum difference temperature in the Recuperative Heat Exchanger.

Convergence of the SO optimization has been reached after 11 generations per fluid by imposing 200 individuals per generation. The results of the algorithm are listed in Table 1, where it is possible to see that the fluid with the higher thermal efficiency is the Toluene, whose corresponding ORC has an efficiency of 30.3 %; 5.6 percent points higher than R113.

Table 3.1 SO optimization results (Bufi et al. 2017)

Fluid	p_{ev} [bar]	ΔT_{TIT} [K]	η_I	η_{II}	UA [kW/K]
Toluene	21.27	51.45	0.303	0.643	125.93
R113	29.88	144.79	0.286	0.606	417.41

Toluene provides also an equivalent overall heat exchanger surface UA 3.3 time smaller than R113. From the results, it is possible to see the optimization action that aims at increase vaporization pressure and reduce pinch point temperature difference.

Once the working fluid is selected, the MO optimization process has been carried out in order to find the best solution for the following quantities:

- η_I;
- Exergy or second law efficiency

$$\eta_{II} = \frac{\dot{W}_{exp} - \dot{W}_{pump}}{\dot{Q}_{in}(1 - T_0/T_m)}$$

  where subscript 0 is related to the ambient condition and T_m is the log-mean temperature calculated between the inlet and outlet temperature of the MSs in the HRMSHE;
- UA.

Moreover, also the turbine size parameter, which is the ratio of turbine exit volumetric flow rate and enthalpy drop, the Toluene flow rate $\dot{m}_f$ and the expander volumetric ratio have been optimized.

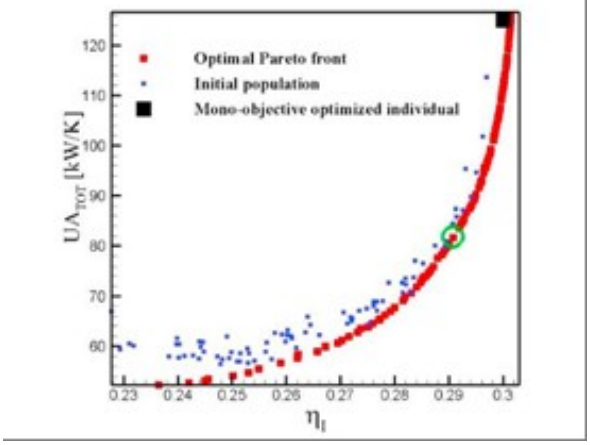

Figure 3. 3 Pareto front (red squares) of the optimal individuals at the MO optimization with Toluene. Initial population is indicated with blue squares (Bufi et al 2017)

The MO optimization results are grouped in a non-dominated Pareto front (in Figure 3.3) and the best solution can be chosen as a trade-off between UA and η_I reduction. After the MO optimization process, the optimal configuration of the cycle has a Pev= 25.21 bar and $\Delta T_{TIT} = 50.05$ and $\dot{m}_f = 4.4$ kg/s.

Exergy efficiency of the cycle η_{II} is equal to 61.4 %. Finally, UA=82.2 kW/K results to be reduced by 36% respect to the SO optimization value and the thermal efficiency lower of 1%. More detailed results can be found in the PAPER N.2, which has been written as parts of this thesis work and can be found in PART 2.

3.1.3 Energy analysis of the complete system configuration

The complete layout has finally a combined-cycle configuration. The topping cycle is a biomass-fired EFGT (Figure 3.4 a) and the bottoming one is an ORC, that recovers heats form the MS circuit (Figure 3.4 b).

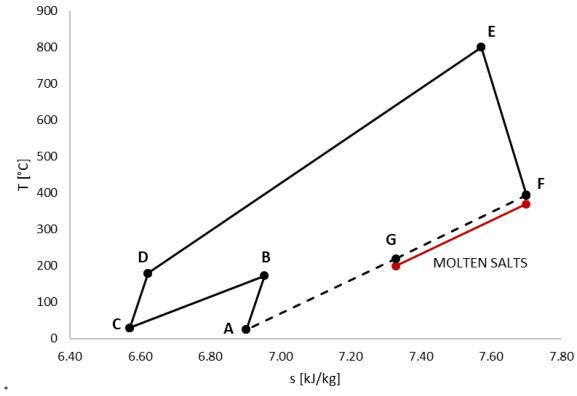

a)

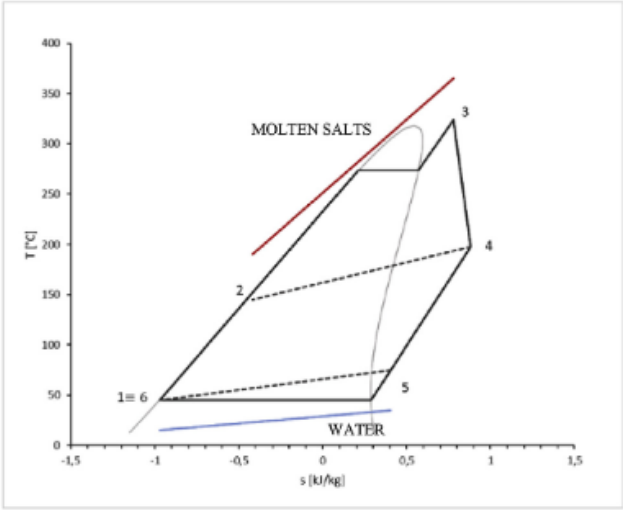

b)

Figure 3. 4 T-S diagram of topping EFGT (a) and bottoming ORC (b) (Pantaleo et al. 2018)

The red and the blue line in Figure 3.4 b are respectively the MSs flowing in the HRMSHE and the cooling water in the condenser. Once each power block of the layout has been described and defined, it is possible to depict how these blocks interact each-others in terms of energy fluxes. Biomass boiler supplies the heat yields by the biomass combustion to the EFGT, that produce electricity immediately available in the grid and heat that from the high-temperature exhaust gas is supplied through the HRMSH to the MSs.

According to this hypothesis, EFGT is in operation 24h per day. The ORC is designed to convert in electricity a thermal input of 2790 kW, which is the sum of the heat supplied by the EFGT equal to 1890 kW and the heat from the solar plant equal to 900 kW, hypothetically. Solar contribution is supplied directly from the solar field during the day hours and from the TES in the night. ORC work at 100% of load during the day or as long as the TES can supply energy; once the TES is empty the operational point of the ORC is 70% of the design point.

At the design point the thermal power generated by the solar field is calculated by the following equation:

$$\dot{Q}_{th,solar\_field} = \eta_{sol,PTC} \cdot A_c \cdot DNI$$

where $\eta_{sol,PTC}$=0.73 is the efficiency of the solar collectors, A_c=3230 m^2 is the total intercepting area of one collectors' line and DNI is the Direct Normal Irradiance of the solar field equal to 800 W/m^2. All those quantities are referred to the design point status and considering the solar field installed in Priolo Gargallo in Italy. Under such conditions the $\dot{Q}_{th,solar\_field}$ = 1885 kW per line of solar collectors, therefore it is reasonable to consider two different scenarios: the first one with a solar multiple (SM) equal to 2.1 with 1 line of solar collectors and the second scenario with 2 lines of solar collectors and so SM=4.2. SM is defined as the ratio of the thermal power generated by the solar field at the design point to the thermal power input of the power block that exploits this energy, in this layout the ORC. SM represents a measure of the excess thermal power produced by the solar field and that could be delivered to the TES. The energy balance of the whole plant is reported in the energy flow scheme in Figure 3.5, that is related to the case with SM 2.1. A detailed energy and exergy analysis of the system can be found in the PAPER

N.3, which has been written as parts of this thesis work and can be found in PART 2.

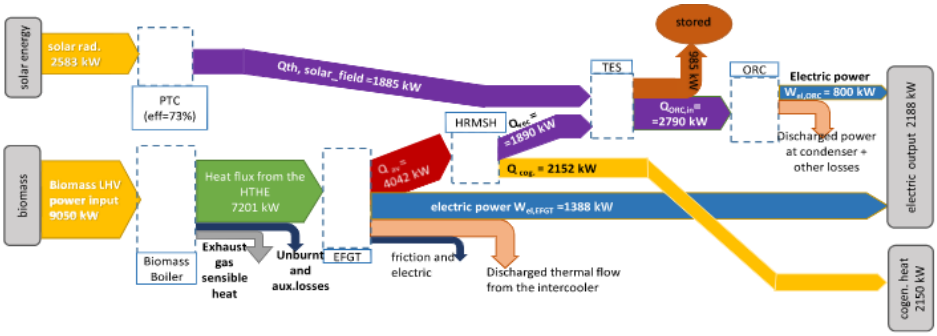

Figure 3. 5 Energy flows at the design point (Pantaleo et al.2018)

In addition to the two scenarios already mentioned cited in Priolo Gargallo considering SM =2.1 and SM =4.2, the study has been also carried out in other two different sites that are Marseilles in France and Rabat in Morocco to analyze the influence of the annual solar radiation on the energy plant production. From now on, the analysis is carried out on six scenarios summarized in Table 3.2.

Table 3.2 Acronyms of the examined cases (Pantaleo et al. 2018)

Solar Multiple (SM)	Priolo	Marseilles	Rabat
2.1	P1	M1	R1
4.2	P2	M2	R2

The DNI for each site has been evaluated by means of the software Meteonorm (Irradiation data web site).

Electricity production of the plant is expressed in equivalent operating hours using the following equation:

$$h_{eq} = \frac{AEP}{\dot{W}_{el,tot}}$$

where the annual energy production (AEP) is then calculated assuming baseload operation for the biomass EFGT and the ORC for 8040 h, and the solar energy production is evaluated based on the TES capacity and the value of SM of the solar field. $\dot{W}_{el,tot}$ is the sum of the electric power produced by both EFGT and ORC.

3.1.4 Thermal Energy Storage capacity selection

TES is a component that has a large effect on the overall plant efficiency since it affects the h_{eq}, the amount of solar energy dissipated and the ORC electricity production. Moreover, its capacity influences the economic profitability of the plant since the bigger the TES is, the higher the investment cost is. TES capacity is therefore selected by the research of the value that can minimize the LEC.

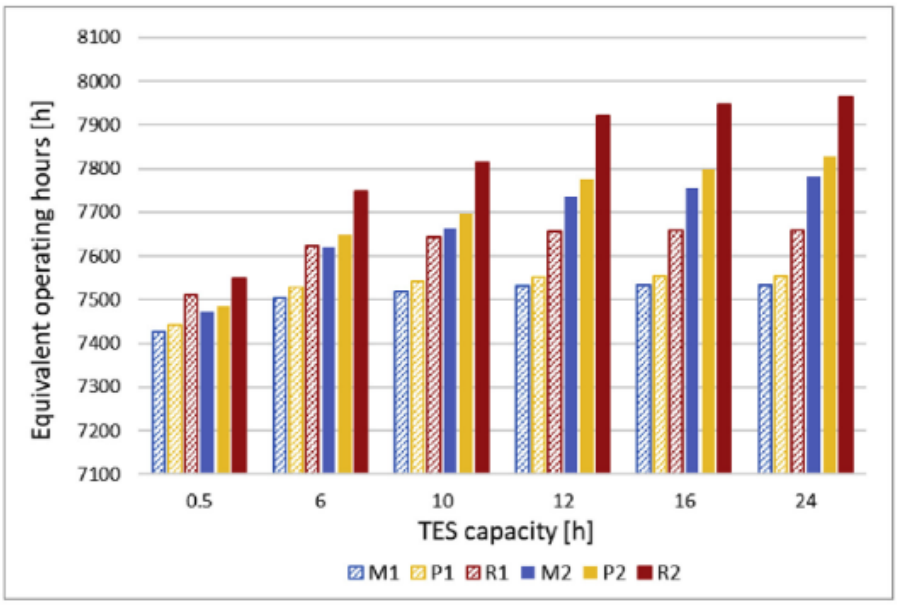

Figure 3. 6 Equivalent operating hours of the solar section at different TES capacity (Pantaleo et al 2018)

It has been considered a TES with a capacity that varies from 0.5 hours (h) to 24 h. Variation of the h_{eq} as a function of the TES capacity is shown in Figure 3.6 where it is possible to see that the higher the TES capacity is, the higher the h_{eq} is. On the other hand, the advantages of a TES capacity higher than 12 h especially in the three scenarios with a SM=2.1 is not remarkable.

The influence of the TES capacity on the ORC annual electricity generated is shown in Figure 3.7. From the graph, it is or can be seen that in the scenarios P1, M1, and R1 the electricity production increases for TES capacity lower than 8 h, with a gain of 5% if the TES capacity varies from 6h to 8h. A negligible variation in the energy production can be observed for TES capacity higher than 8 h.

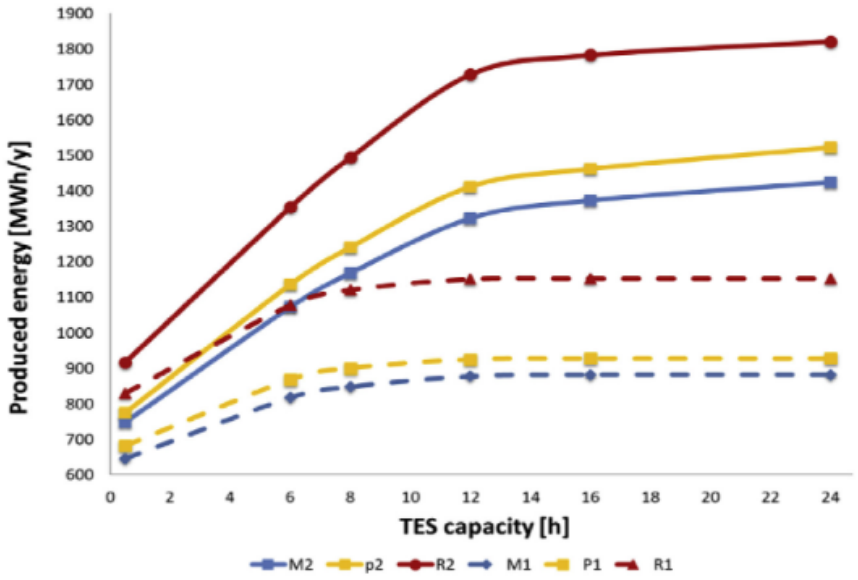

Figure 3. 7 Annual electricity produced by the ORC as a function of TES capacity (Pantaleo et al. 2018)

A similar behavior can be seen in the three sites if a SM=4.2 is taken into account. Under this hypothesis, the ORC electricity production increases for

a TES capacity lower or equal to 12 h. Selection of a TES with a capacity higher than 12 h has no remarkable advantages in terms of energy production. The LCE of the hybrid plant is then evaluated according to:

$$LCE = \frac{f_a \cdot (I_{EFGT} + I_{CSP} + I_{TES} + I_{ORC} + I_{EBI}) + C_{O\&M} + C_B}{E_G},$$

where:

- I represents the turnkey costs and it has been considered for each component;
- I_{EBI} is the cost related to the engineering building and installation;
- $C_{O\&M}\ and\ C_B$ are the costs of operation and maintenance of the plant and biomass costs respectively;
- E_G is the total produced electricity;
- $f_a = \frac{r}{r-\left(\frac{1}{1+r}\right)^l}$ is the annuity factor, function of the discount rate r and the economic lifetime l.

A complete thermo-economic assessment of the plant can be found in PAPER N.3 in PART 2.

The variation of the LCE value calculated as a function of the TES capacity is shown in Figure n. 3.8 where the results of all scenarios are plotted.

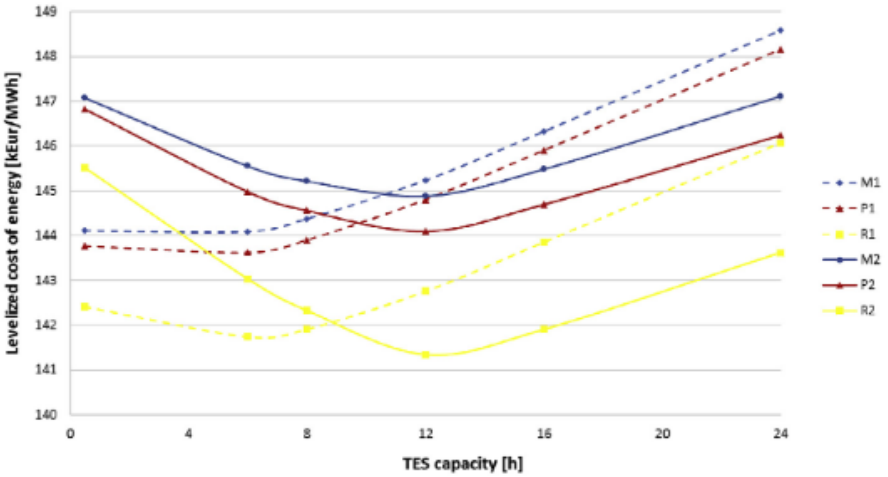

Figure 3. 8 LCE as function of the TES capacity in all analyzed scenarios (Pantaleo et al. 2018)

The minimum value of LCE is reached for a TES capacity of 6h in the scenarios P1, M1, and R1, while the optimal TES capacity is 12h in the scenarios P2, M2 and R2. These results can be explained by the limited advantages obtained by a bigger TES in terms of energy production or energy dissipation respect to the higher initial investment costs, due to the higher TES capacity.

3.1.5 Economic appraisal and profitability results

The profitability assessment has been performed assuming a TES with a capacity respectively of 6 and 12 h for the scenarios with 1 and 2 lines of collectors, which minimize the LCE. Moreover, the results have been compared to some previous studies done by the same authors on a similar EFGT turbine fuelled only by biomass (Camporeale et al. 2015) and a similar hybrid solar/biomass system with a different layout (Pantaleo et al. 2017).
In Figure 3.9 the LCE of the analyzed hybrid plant biomass EFGT with CSP is plotted as a function of the biomass costs. This last configuration presents an LCE lower than in Pantaleo et al. (2017), (see Figure 4.9), because the

reduced conversion efficiency respect to the configuration is balanced by the lower solar section size and costs.

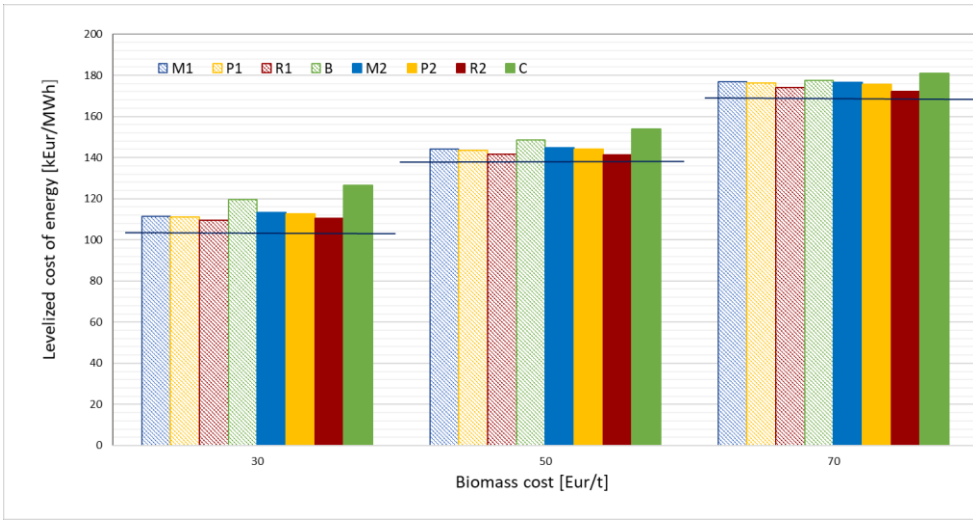

Figure 3. 9 LCE as a function of biomass cost. Case B and C are related to the system configurations in Pantaleo et al. (2017). The horizontal line represents the scenario in Camporeale et al. (2015) of only biomass

Rabat proves to be the location with the lowest LCE, due to the highest solar energy radiation and system producibility. On the other side, all hybrid configurations present an LCE higher than the one of only biomass fuel suggested by Camporeale et al. (2015). For the only biomass scenario indeed, LCE values range between 100 and 170 Eur/MWh at biomass fuel costs that vary from 30 to 70 Eur/t. For the hybrid layout proposed best location of Rabat has LCE values range between 110 and 174 Eur/MWh, in Priolo Gargallo and Marseille LCE values are comparable and the minimum LCE value is 111 Eur/MWh while the maximum 176 Eur/MWh. From the obtained results it is possible to state that the proposed CSP hybridization with specific subsidies can be competitive with other renewable energy sources.

NPV and IRR values have been also calculated for all the six scenarios of the proposed hybrid plant and compared to the cases in Camporeale et al. (2015) and Pantaleo et al. (2017). The results of these two values as function of the

biomass cost are shown in Figure 3.10 a) and b) respectively. NPV and IRR maximum values are 14,000 kEur and 25%, both related to Rabat at higher solar field size; the minimum values are -600 kEur and 3.7% correspond to Marseille with the lower solar field size. The hybridization of the biomass EFGT with CSP increases the global electricity efficiency, due to the solar energy input, but reduces both NPV and IRR in all the scenarios respect to the only biomass configuration. The reason of the lower profitability of the hybrid system is that the current investment costs of the PTCs with MSs as HTF are very high and these higher costs are not compensated by the increased global energy efficiency of the solar input, and by the higher electricity selling price of the solar-based fraction with respect to biomass-based one. Only the scenario R2 shows a higher NPV of the only biomass case and also the highest IRR when biomass cost is equal to 70 Eur/t.

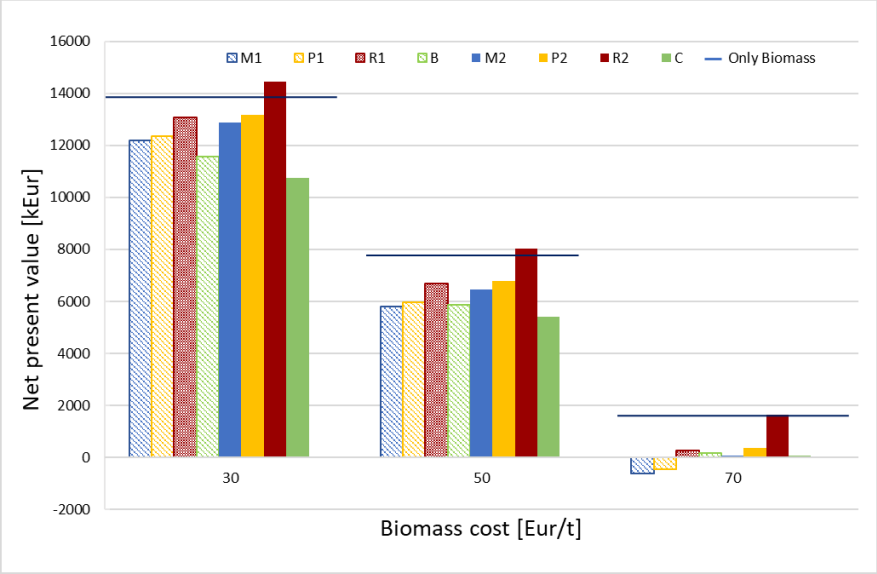

a)

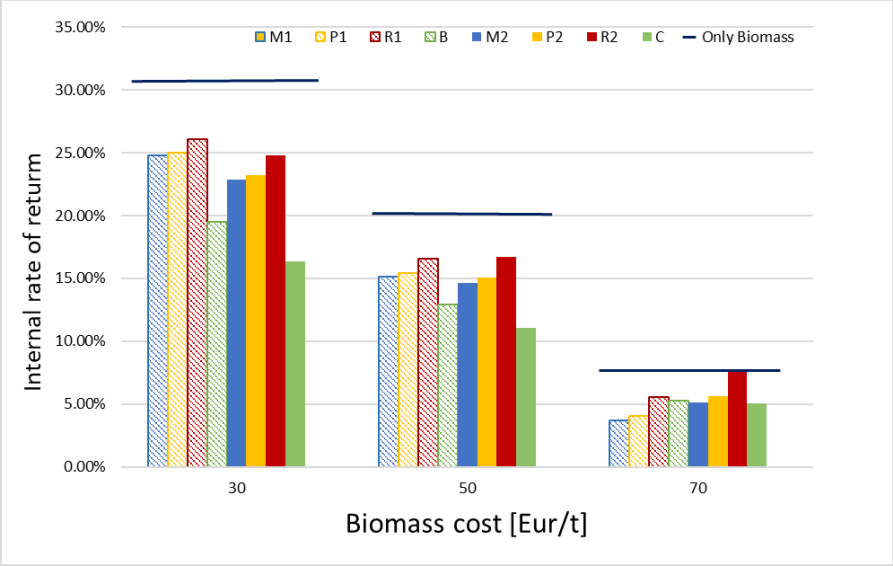

b)

Figure 3. 10 a) NPV and b) IRR as a function of biomass cost for the different scenarios. Case B and C are related to the system configurations in Pantaleo et al. (2017). The horizontal line represents the scenario in Camporeale et al. (2015) of only biomass

On the other hand, for a biomass cost of 70 Eur/t, the plant configuration in locations as Marseilles or Priolo Gargallo present negative NPV, except for the two collectors line scenario.

An interesting option can be considering the use of the medium-high temperature heat still present in this hybrid system for cogeneration purposes. This heat can be, for instance supplied by the exhaust gas of the EFGT, that leaves the cold tank at a temperature of around 200°C.

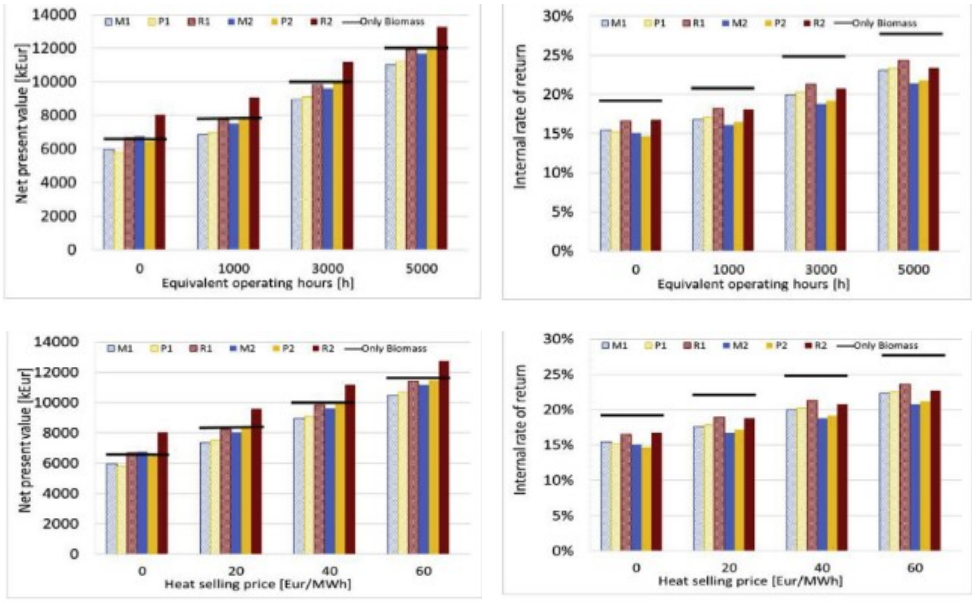

Figure 3. 11 NPV and IRR as a function of the equivalent operating hours and heat selling price under cogeneration hypothesis (Pantaleo et al. 2018)

With the assumption of matching the heat demand by producing hot water at 70-90°C and selling the thermal energy at 40Eur/MWh (top graphs in Figure 3.11), NPV of sites as Priolo Gargallo or Marseille are comparable to the only biomass case, if a solar field with SM=4.2 is considered. Equivalent operating hours in cogeneration mode have been varied in the range of 0-5000 h/year. A similar analysis has been carried out fixing 3000 equivalent hours/year in CHP mode operation and varying of thermal energy selling price from 0 to 60 Eur/MWh (down graphs in Figure 3.11).

3.1.6 Conclusions

The first branch of this study was focused on the thermodynamic and economic analysis of a hybrid (solar-biomass) combined-cycle system composed of an externally fired gas-turbine (EFGT) fuelled by biomass (woodchips) and a bottoming organic Rankine cycle (ORC) plant. The thermodynamic modeling was performed assuming two CSP sizes and in

three different sites, Priolo Gargallo, Rabat and Marseilles, in order to analyze the effect of the different DNI.

ORC and TES sections have been considered as crucial elements of the analyzed configuration. Organic fluid of the ORC and parameters such as evaporating pressure and turbine inlet temperature have been selected with a dedicated optimization code, based on NSGA algorithm, in order to maximize the thermal efficiency of the plant and minimize the heat exchanger surface area, that is directly related to the plant price. The resulting cycle was, therefore, the cycle that has the lowest impact on the LCE of the overall system, due to the relatively lower investment costs and higher energy conversion capability. The importance of TES selection is due to its direct effect on the LCE because of the high cost, but also to its indirect effect since it limits the electricity produced by the ORC. A trade-off choice has been done and two different TES capacity values have been selected for the two different CSP sizes.

The results obtained from the thermo-economic analysis showed that the global conversion efficiency is higher when using CSP integration and the reports a higher investment NPV when integrating solar energy, due to the increased electricity generation and higher solar-based electricity selling price. A comparison has been also done with a previously proposed solar-biomass hybrid solution with a higher temperature (550 °C) of the CSP working fluid and direct solar energy input to the topping EFGT. Results demonstrate a higher profitability of the hybrid-system configuration due to the higher flexibility of the proposed layout respect to the previous one. The profitability of the system can be even higher if specific subsides for hybrid systems are settled by government. An advantage of this configuration is the availability of high-grade heat for cogeneration from the topping EFGT plant

that can improve the profitability of the overall system when a suitable heat demand is available.

3.2 Biomass-fired combined heat and power systems

Small-scale biomass-fired CHP plants are a common choice when it comes to DG framework since they are well-proved and commercially available solutions, able to supply energy without remarkable fluctuations if the biomass is correctly managed.

Albeit a biomass furnace can be individually installed as heat generation system for commercial or residential applications, normally this solution has limited profitability due to the inherent limitations of such a boiler. A biomass furnace is indeed not able to follow the fluctuation of the end-user heat demand and it is often oversized in order to meet the heat demand peak. An oversized furnace runs the risk of operating for a high number of hours at part-load and so with a lower conversion efficiency, a higher biomass consumption and emissions respect to design point.

A solution that helps to overcome these limits can be placed between the boiler and the end-user a TES, that can be of help in correcting the mismatch between the supply and the heat demand of energy. Moreover, the biomass boiler can also be coupled with a steam turbine or an ORC. This layout made the system also able to generate electricity that can be directly supplied to the end-user or sold to the grid and therefore increases the overall profitability of the system.

In this section, two different biomass-fired layouts are described and for each of them, the effect of TES and bottoming cycle integration is analyzed. The aim is to quantify the benefits of such configurations and understanding their application limits.

3.2.1 Layout 1

The first layout considered is a combined cycle composed of a steam turbine (ST) as topping cycle and a bottoming ORC that can convert part of the heat from the ST in useful work. Heat is supplied to the system by means of a moving grate biomass furnace. Between the biomass boiler section and ST topping cycle, there is an intermediate two-tanks MSs TES circuit. Temperature of the hot and cold tanks are respectively 450°C and 200°C. A sketch of the system layout can be found in Figure 3.12.

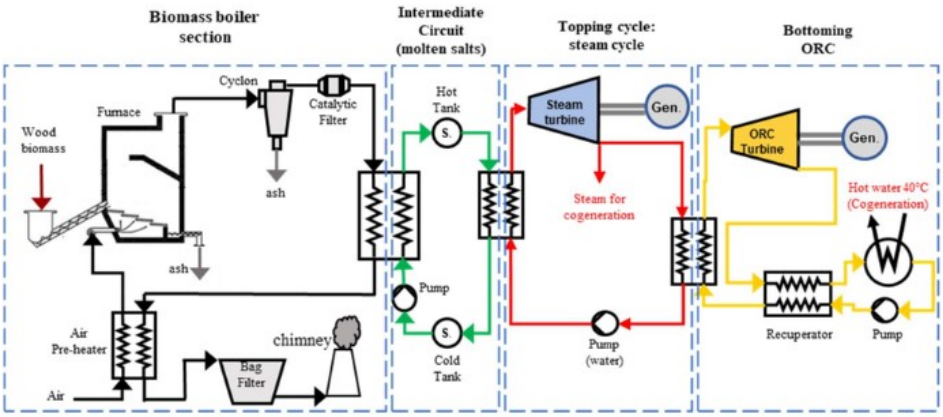

Figure 3. 12 System configuration layout (Sorrentino et al. 2018)

The steam inlet conditions to the ST are 220 °C and 20 bar, and at an outlet temperature of 150 °C the steam is conveyed to the evaporator of the ORC plant. The ORC section has a recuperative configuration and a temperature of 45 °C has been assumed as condensation temperature. The water exiting the condenser still has a temperature suitable for low-temperature heat demand such as residential end-users. The low steam temperature at the turbine outlet narrows the field of organic fluid selection and made refrigerants almost the only suitable working fluids for this ORC application. Pentafluoropropane (R245fa) has been selected as working fluid due to its thermodynamic

properties compatible with the heat source. Moreover, it is a “dry fluid”, not subjected to greenhouse gas emission regulations as it does not damage the ozone layer, and is non-flammable, non-toxic, and has satisfactory thermal stability (Kang 2012). The layout so far described is indicated in the following analysis as CASE A.

Other two separated cases have been considered and compared to CASE A:

- CASE B: system layout composed by the biomass boiler coupled only to the ST through the MSs tank;
- CASE C: where the bottoming cycle is made up of the ORC that receives heat directly from the TES section, therefore at a higher temperature than the ORC in CASE A (450 °C). Under this hypothesis, it is reasonable to consider Toluene as working fluid.

Thermodynamic simulations have been carried out by means of the software Cycle-Tempo® for both the ST and ORC sections and for the complete CASE A. Cycle-Tempo® is a flow sheeting program used to evaluate and optimize energy conversion systems, developed at the Delft University of Technology. The first and second law of thermodynamics are the basis of the calculation procedure. Irreversibilities have to be specified by the user even if the program can provide default values for specific apparatuses (Woudstra et al. 2010). It is also possible to carry out multi-parameter optimization of the implemented system and the calculated results can be shown in various thermodynamic diagrams, such as T-s diagram or T-Q diagram. Further information on the software can be found in the Cycle-Tempo® website.

Further input parameters are as follows: biomass boiler efficiency = 88%; mechanical/isoentropic efficiency ST and ORC Turbine = 90/75%; electric

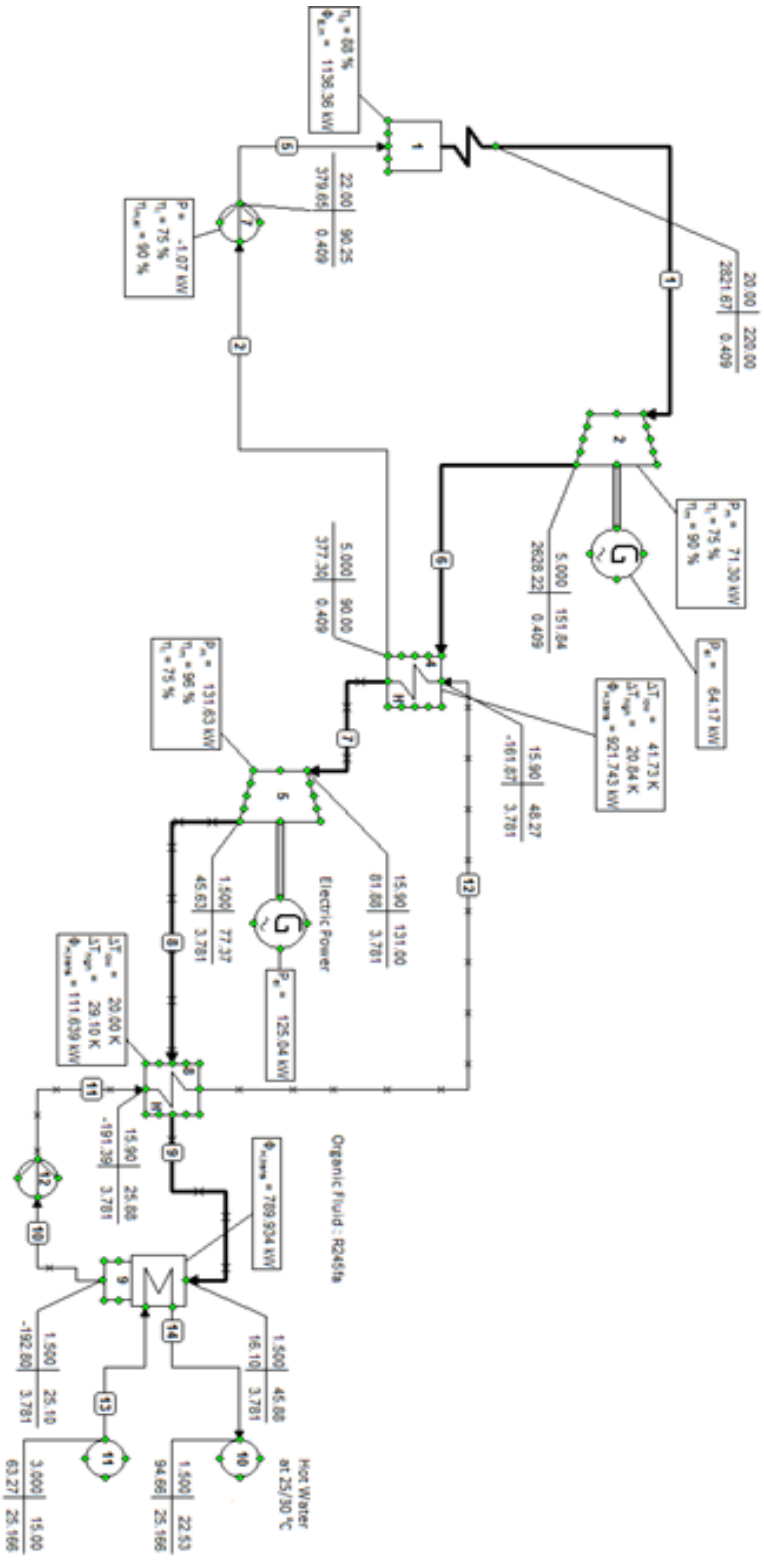
Electric Power
Organic Fluid : R245fa
Hot Water at 25/30 °C

Figure 3. 13 Cycle-Tempo layout for CASE B (top) and CASE C (down)

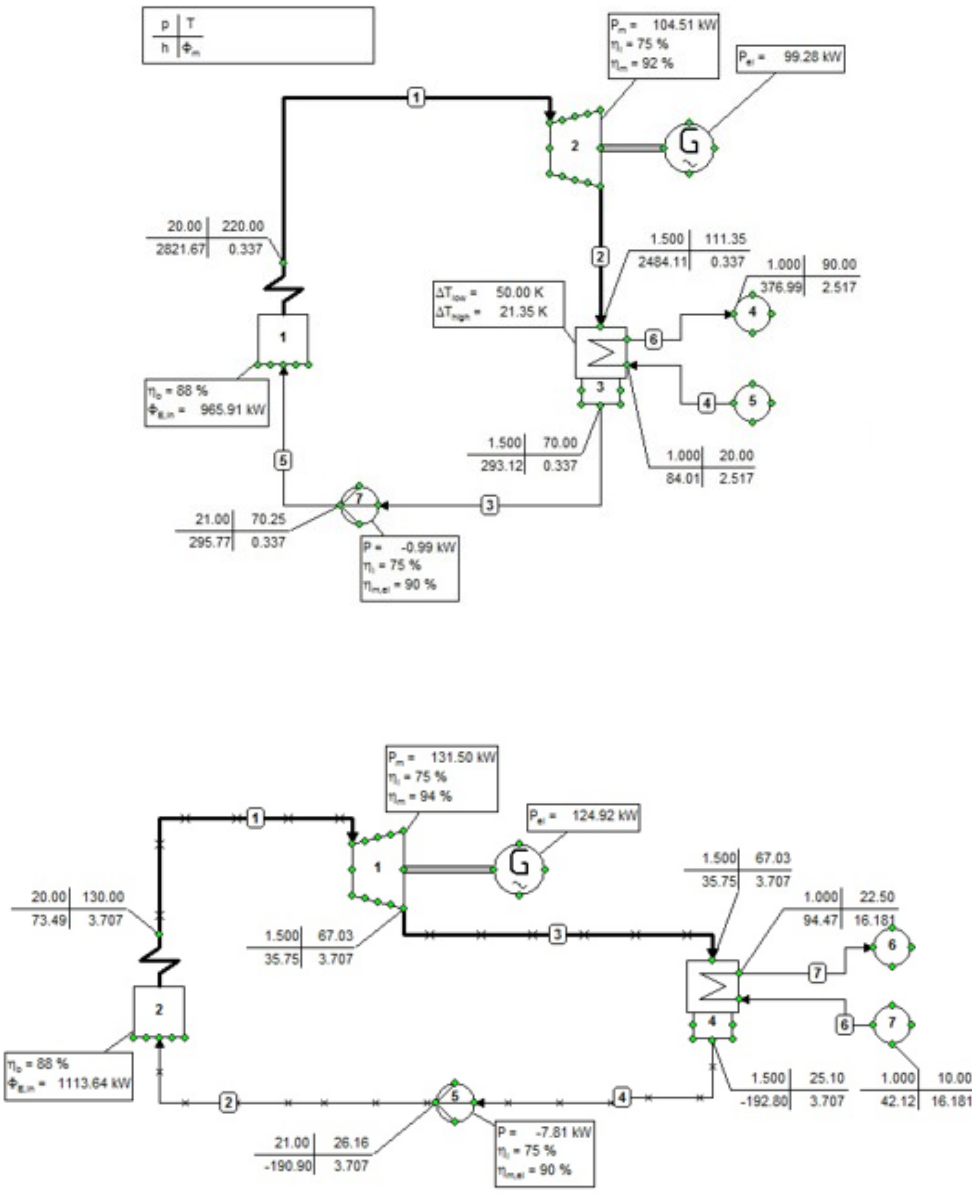

Figure 3. 14 Cycle-Tempo layout for CASE B (top) and CASE C (down)

genset efficiency =92%; ST and ORC Turbine nominal power (case A) = 70 and 120 kWe respectively). In Figures 3.13 and 3.14 it can be seen how each layout has been implemented in Cycle-Tempo® and the thermodynamics results obtained after the simulation for each cycle point. CASE A results have been validated by means of the data supplied by Ingeco (Ingeco project website) where a simulation of a similar plant can be found.

Thermo-economic assessment

Thermo-economic assessment has been done on three cases described in the previous section considering them in three different applications: (i) industrial, (t) tertiary and (r) residential end-users. Together with CASES A, B and C a third case, CASE D has been also analyzed; that has the same configuration of A but includes the option to switch on or off the bottoming ORC on the basis of the heat demand available.

Plant has been considering operating at baseload operation mode and operating hours have been assumed equal to 7,500. Heat demand has been assumed of 4,000/1,800/1,200 hours/year at temperature of 110/90/35 °C, respectively for industrial/tertiary/residential consumers.

Investment and operational costs of the plant have been taken from data estimated directly from the manufacturers. As regards biomass, the following assumptions have been done: LHV= 4.18 kWh/kg; biomass cost of 80 Eur/t, and biomass ash and discharged cost has been settled as 70 Eur/t of ash. Feed-in tariff for biomass electricity has been assumed of 287 Eur/MWh and heat selling price has been considered 60/80/100 Eur/MWh respectively for industrial, tertiary and residential end-users.

Further details on the analyzed plant and on its thermo-economic assessment can be found in PAPER N.4 in PART 2 of this thesis work.

Results and conclusions

The global conversion efficiency has been evaluated as the sum of useful heat and electricity generated divided by the biomass energy input. Results for each case are shown in Figure 3.15. The highest conversion efficiency is reached by CASES B and D in industrial applications due to the high heat demand rate. CASE D proves to be more performing thanks to its flexibility in switching on or off the ORC.

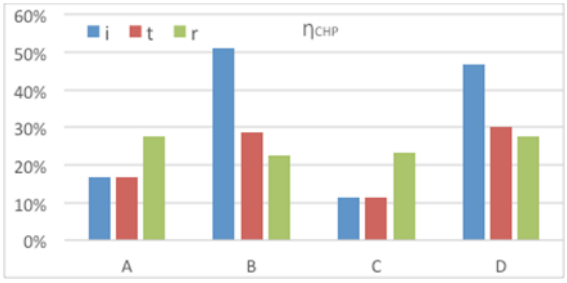

Figure 3. 15 Conversion efficiency for CHP cases A to D when industrial (i), tertiary (t) and residential (r) are considered (Sorrentino et al. 2018)

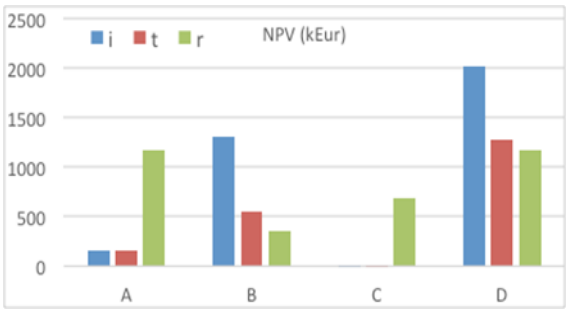

a)

The same conclusions can be drawn for the tertiary end-user segment since the global energy efficiency is lower in comparison to the industrial end-user typology because of the reduced heat demand.

CASE C shows its highest profitability only under the

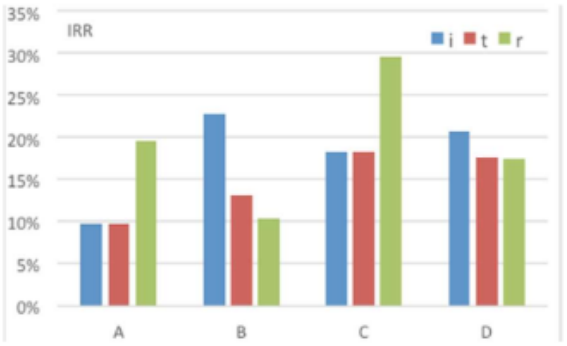

b)

Figure 3. 16 a) NPV and b) IRR of the cases A to D when industrial (i), tertiary (t) and residential (r) are considered (Sorrentino et al.2018)

hypothesis of residential application, where the cogeneration temperature can be suitable for cogeneration purposes at 35 °C. Anyway, this value still remains quite low if compared to the usual CHP one.

The same consideration can be done if IRR and NPV of the different cases are considered and their values are plotted in Figures 3.16 (a) and (b). CASE D proves to be the configuration with the highest NPV, followed by the CASE B that shows also the highest IRR for industrial end-users.

This study proved that the end-user and its energy demand profile is a key factor to select the optimal CHP configuration. In fact, stand-alone ORC system has been proven to be profitable only for low-temperature cogeneration purpose the conversion efficiency reach a promising value of 18%. TES has a positive effect in this case due to the higher temperature of the available heat that can be obtained by the use of MSs as intermediate circuit. The lower upfront costs of a simpler configuration, such as in CASE B, results in a more profitable system when it comes to industrial application. Finally increasing the flexibility of the plant, for instance allowing to turn on/off a module when necessary, can make a big difference in the system profitability as proved by the comparison of the CASE A and CASE D results.

3.2.2 Layout 2

Allowing flexible operating conditions in a CHP plant can increase the profitability of the same plant configuration, as shown in the analysis done in chapter 4.2.1. In the same study has been also highlighted that according to the end-user characteristics is also important keeping investment costs low, if the conversion efficiency of the plant cannot compensate them. On the other hand, all the analysis so far carried out proved that coupling a biomass boiler with a TES and/or with an ORC plant in a CHP system can remarkably increase systems performance and profitability.

In 2011 UK government introduced the Renewable Heat Incentive (RHI), a payment system similar to the feed-in tariff system for generation of heat from renewable energy sources (Renewable heat incentive website). This system pushed several domestic and non-domestic users to meet their heat demand exploiting thermal energy produced by alternative sources. Thanks to these incentives many end-users of the food retail sectors installed biomass boilers to satisfy their heat demand, aiming at reducing carbon footprint from retail activities and thus mitigates the future impacts of climate change, also motivated by the introduction of the non-domestic RHI.

In these applications, normally, moving grate furnaces fed by wood pellets are installed and they produce no pressurized hot water that can reach a maximum temperature of 95°C. Boilers are often sized to meet the peak of the thermal heat demand, this means their operating load is for most of the time lower than nominal conditions, leading to low efficiency and high emissions during operation. This initial configuration has been then here modified in order to overcome these well-known limitations.

In the configuration analysed here, a two-tank MSs TES is directly coupled to the original biomass boiler while a bottoming ORC system receives heat

from the TES and supply the required heat to the end-users (as shown in Figure 3.17).

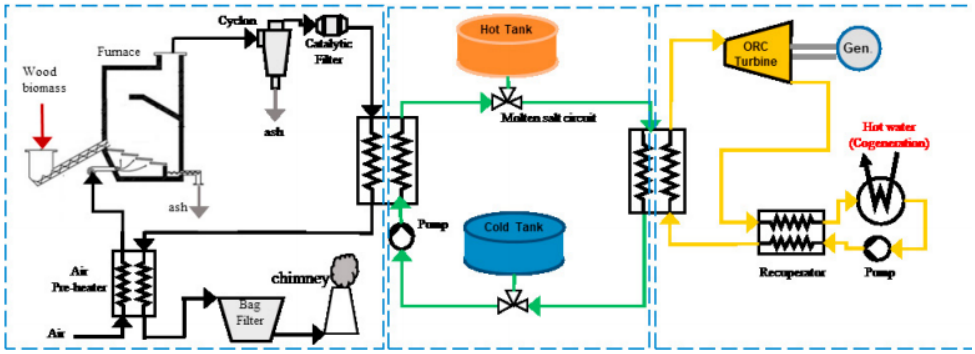

Figure 3. 17 Layout of the modular CHP plant (Sorrentino et al. 2018)

In this new configuration, ORC thermal source characteristic has been kept equal to the previously analyzed configuration, where the hot-tank temperature equals 450 °C, while a temperature of 200°C has been chosen for the cold tank to avoid excess work for the circulating pump. Toulene has been selected as organic fluid, according to the same considerations previously done. For this application ORC should work in heating load-following mode, which means condensing temperature must be higher (85°C) reducing electric cycle efficiency, which results equal to 18.8 %.

Thermal energy storage: sizing and operating conditions selection

Heat demand data of a generic store were available and have been used as samples for winter, summer or mid-season heat demands (see Figure 3.18). This information has been used as input data to size the TES.

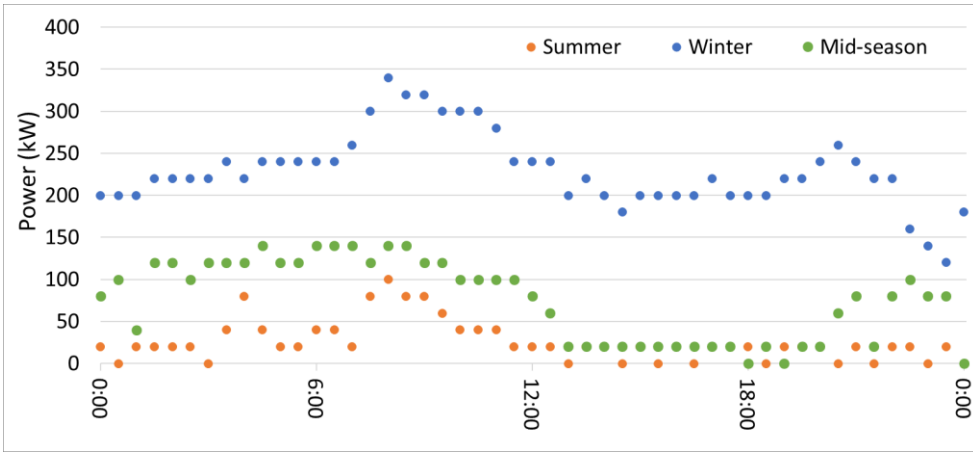

Figure 3. 18 Heat demands patterns of a store in a random Winter, Summer or mid-season day (Sorrentino et. al 2018)

Sizing process has been done taking into account wintertime, where the power demand reaches its peak, equal to 350 kW. Using the results of the thermodynamic analysis done on the ORC, a thermal input Q_1 of 455 kW is required by the ORC, in order to satisfy this demand. Thus, the size of the ORC, W_{el}, selected for this application results of 85 kW.

Biomass boiler has been sized in order to satisfy the average ORC heat demand of 317 kW, therefore a furnace of 350 kW has been chosen.

Assuming a furnace operation in baseload conditions, the cumulative heat sent to the TES at time t $E(t)$ gives

$$E(t) = \int_0^t (Q_{prod} - Q_{req})dt$$

where:

- Q_{prod} is the thermal power produced by the biomass boiler;
- Q_{req} is the thermal power required by the ORC.

This integral has been evaluated in the range 0< t< T =24h and TES size has been computed as

$$V_{TES} = max\ (E) - min(E) \qquad 1)$$

The TES capacity, obtained from this simplified procedure is 550 kWh, as shown in Figure 3.19.

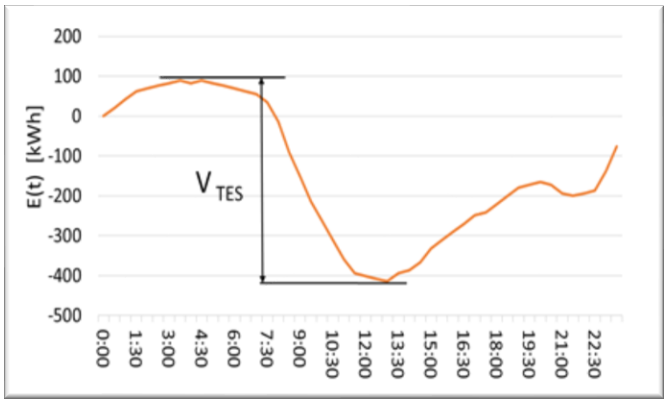

Figure 3. 19 Hourly energy stored in the TES (Sorrentino et al. 2018)

Once each layout component has been sized, it is possible to select the operating strategy of the system related to summer and mid-season conditions.

This optimization procedure has been done by means of a trial and error strategy. Crucial in this calculations was imposing technical operational limitations concerning the biomass furnace. Calculations have been done under the following hypotheses:

- the furnace should be turned off at part load lower than 20%;
- between two ignition cycles, a time interval of at least one hour should be considered.

As regards part load performances of the ORC the model developed by Wang et al. (2016) has been considered. Low of variation of the boiler's efficiency as function of the load has been given by the boiler's manufacturer.

The best performing operation mode in the two considered cases is shown graphically in Figure 3.20 a) considering summer heat demand and b) in mid-season conditions.

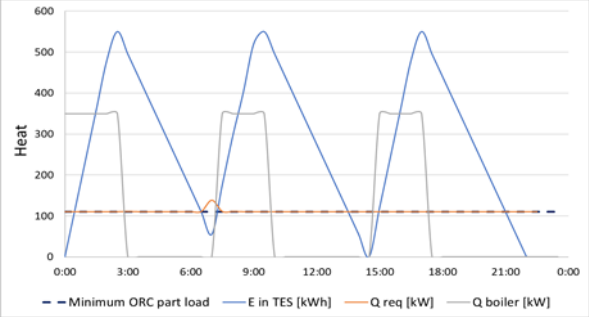

a)

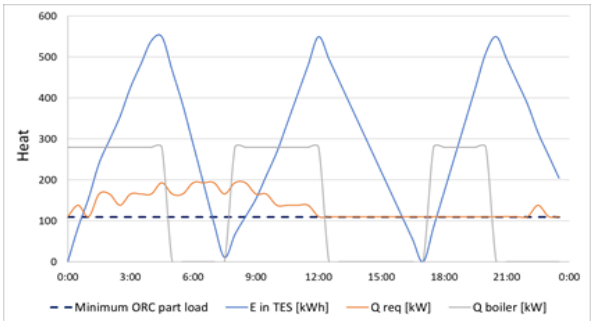

b)

Figure 3. 20 Dynamic behavior of the biomass boiler thermal power output (Qboiler), thermal demand (Qreq) and energy stored in the TES (E), following the operating strategy selected in summer (a) and in a mid-season (b)

During summer, the ORC works the whole day constantly at minimum part load, see Figure 3.20 (a). Under these conditions the boiler is switched on at 100% of part load, supplying heat the required heat to the store and the remaining heat is sent to the TES. Once the TES is full, biomass boiler is switched off and heat demand is satisfied through the TES. Biomass boiler works then for 7 h per day at maximum load during an average summer day. In mid-season, ORC requires more heat in the first half of the day, Figure 3.20 b), thus the time interval between two furnace ignitions is smaller than the one required after midday. TES integration allows, to switch off the furnace for several hours especially in the afternoon when the heat required is lower. Boiler operates at high part load, around 80%, for 13 h per day.

Techno-economic assessment

Finally, after components and operation mode condition selection, the quantification of the advantages and the evaluation of the limits of this configuration can be carry on.

To do so, the following cases have been considered:

- CASE 1: represents the layout in the previous part of this section 4.2.2described. This configuration is composed by a biomass boiler of 350 kWt connected to a TES having a capacity of 550 kWh and an ORC of 85 kWe. The operating conditions of this case have been selected by means of the above calculations;
- CASE 2: where a conventional biomass boiler of 520 kWt is installed, and the heat demand is satisfied by the hot water produced by the biomass boiler. This case represents the initial configuration.

For the sake of completeness further two cases have been considered:

- CASE 3: a boiler with the same size of CASE 2 is here coupled to an ORC of 85 kWe, that supplies heat to the store through the condenser. This case has no TES and MSs circuit is used only as HTF to supply heat to the ORC;
- CASE 4: biomass boiler and TES as in CASE 1 but no ORC is coupled to the TES. The biomass boiler follows the heat demand of the store, but the TES compensates the fluctuations.

To estimate the biomass consumption, full load and part load efficiencies of the MS boiler have been assumed equal to that of the conventional biomass boiler installed in store. The technical operating limit of 20% of part load has been considered also in CASE 2, 3 and 4. The energy production has been computed under the hypothesis that the biomass boiler and the ORC operate

following the thermal load in CASE 2 and 3, while the same operating condition of CASE 1 has been considered for CASE 4.
In CASES 1 and 3 system operates as CHP and the equivalent operating hours for electricity production, assuming a thermal load following operating mode, have been estimated as 1,864 per year. To carry on the analysis one typical day in each season has been assumed, hence the number of days considered are 75/76/161 respectively in winter, summer and mid-seasons.
Further details on the analyzed plant and on hypothesis and methodology used can be found in PAPER N.5 in PART 2 of this thesis work.

Results and conclusion

In the financial appraisal the levelized cost of heat for CASE 1 and 4 is evaluated and results equal to 38 Eur/MWh, while it is equal to 52 Eur/MWh for CASE 2 and 3. The reduction in the levelized cost of heat is due to the TES implementation, that allows turning off the biomass boiler at low demand. The energy dissipated is indeed in CASE 2 and 3 18 % of the total energy produced by the biomass boiler, whereas is the 9% in CASE 1 and 4.

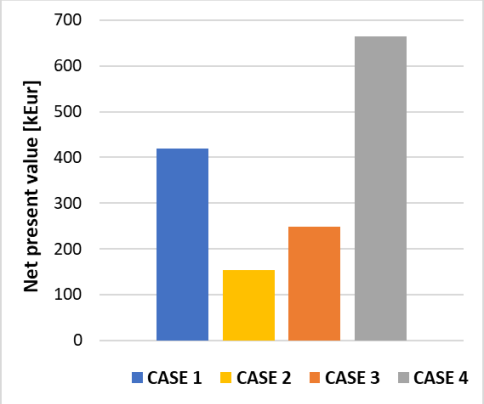

Figure 3. 21 Net Present Value (Sorrentino et al. 2018)

The minimum of net present value minimum is reached in CASE 2, as shown in Figure 3.21. This is due to the higher biomass consumption of the boiler in summer and mid-season, where the low part-load leads to low efficiency values. This layout is never used in practice and the peak demand is normally satisfied by a back-up gas boiler.

CASE 3 has a low NPV because of the low number of operating hours that do not compensate the high initial investment cost. In fact, choosing a heat load-following operation limits ORC electricity production and make unprofitable the ORC investment.

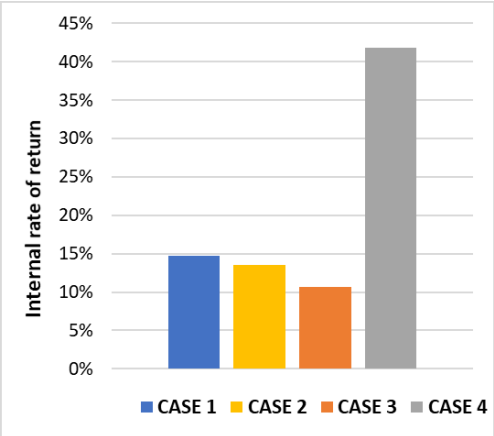

a)

The internal rate of return (IRR) in Figure 3.22 (a) and the Profitability Index of Figure 3.22 (b) confirm the considerations done for the NPV: in a thermal load following mode, considering the low amount of electricity produced, coupling an ORC to a biomass boiler does not increase

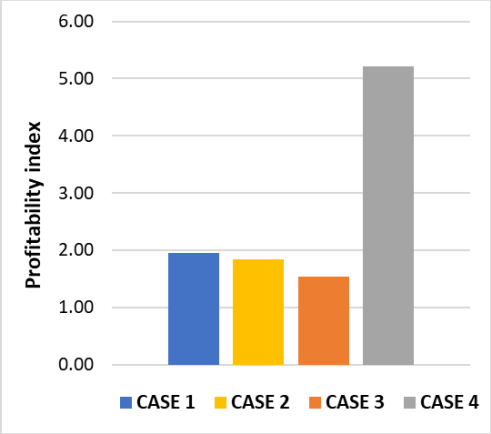

b)

Figure 3. 22 Internal Rate of Return (a) and Profitability index (b) (Sorrentino et al. 2018)

the investment profitability. On the other hand, considering a TES in biomass boiler/ORC layout can decrease the IRR compared to the baseload case, CASE 2. The profitability index of the CASE 1 is also more profitable than CASE 3, since this allows higher global conversion efficiency due to the peak shaving effect of the thermal storage buffer.

The main conclusions obtainable from this analysis are:

- Coupling a TES to a biomass boiler has a positive effect on the boiler performances in thermal-load following mode, since it reduces the boiler operating hours at part-load and, in any case, it increases the part-load. That helps the boiler to operate with higher efficiency and to reduce biomass consumption and emissions;
- Profitability of ORC installation in a CHP plant result extremely reduced when it operates only in load following mode and to produce mainly heat for cogeneration purposes. ORC investment became more profitable when it operates on baseload condition and maximizing the electricity generation.

Finally allowing flexibility of the plant operating mode can generally increase profitability of a CHP plant in DG, especially if the thermal demand is satisfied by a TES and therefore a small ORC can be implemented in the system to supply the electricity required by the end-user.

CHAPTER 4

CONCLUSIONS

A concluding summary is proposed in this chapter as an overview of the main results reported in this thesis. Some outlines for the future are reported together with possible development of this work.

4.1 Conclusions

Modular power plants in distributed generation approach have been considered in this thesis. These plants are made by independent blocks, such as biomass boiler or Organic Rankine cycle for power production and thermal energy storage, to increase the availability of the energy produced by renewables and to allow a smoother operation of the topping system, due to the decoupling of energy production and demand. In particular, the focus of this thesis has been the biomass-fuelled systems integrated in combined heat and power generation plants. Performances of these plants have been computed and profitability analysis of different configurations have been carried on. All the cases analysed in this thesis can be classified based on the renewable source they exploit in hybrid or biomass CHP.

A hybrid solar-biomass layout has been firstly proposed. It is composed by a biomass externally fired gas-turbine (EFGT) and a solar plant as topping cycle and an organic Rankine cycle (ORC) as bottoming cycle. A two-tanks thermal energy storage (TES) with molten salts was integrated to supply the heat produced by the EFGT and the solar plant to the ORC. Thermo-economic assessment of the hybrid layout has been computed in three different Mediterranean areas, Priolo Gargallo (Italy), Marseille (France), and Rabat (Morocco). Results are then compared to a similar hybrid solar-biomass plant with a different layout configuration and to a combined EFGT and ORC plant fed only by biomass. The analysis demonstrates the advantages of solar integration in biomass plant, due to the higher selling-price of solar-based electricity that increases profitability of the investment. These advantages are even higher if installation of this system is done in areas where direct normal irradiance value is

higher (e.g. Rabat), increasing energy conversion efficiency of the plant. In this configuration, high-temperature heat (at around 200 °C) is available for cogenerations purpose, making the system more profitable if there is a compatible heat demand. Finally, settling a specific subsides for power generation from this type of system can balance the higher initial investment costs reducing payback time of the investment.

Several layouts based on biomass boiler technology have been then proposed and compared to understand the effect of each integrated module. ORC and TES have been coupled to the biomass boiler steam Rankine cycle and a thermo-economic analysis of each layout has been performed. Obtained results have been then compared and the following conclusions can be listed:

- TES implementation has in most of the case a positive effect on the system performance and increases profitability of the investment. It increases the average value of the boiler part-load, too, and helps in reducing the amount of partial-load operating hours. This leads to reduction of biomass consumption and boiler emissions since the boiler can work at higher load with higher efficiency. Excess of heat produced is not dissipated but stored; it can be supplied to end-user with time delay on request by the TES, allowing eventually to turn off the boiler;
- End-user characteristics are a crucial factor in modular distributed generation plant selection. Stand-alone ORC profitability is reduced when used for cogeneration purpose, especially in high temperature application and in thermal following mode. On the other hand, consider low-temperature heat production in ORC application can increase investment profitability. In case of high temperature heat demand a TES or a steam turbine proved to be a best performing choice. Industrial applications favour simple plant configuration with lower initial investment costs;
- Allowing flexible mode operation of a combined heat and power plant leads to reduced operational costs and higher conversion efficiency. In fact, having the chance to turn on or off the biomass boiler when heat demand is low reduce biomass consumption and energy dissipation, while satisfying electric demand by means of a

working ORC and turning it off when the demand of the end-user is low permits the selection of a smaller ORC, reducing investment costs of the complete layout. Implementation of a TES is crucial if flexible operating mode of the system shall be permitted.

4.2 Outlook

A techno-economic analysis on unconventional boiler with molten salts as heat transfer fluid should be the natural next step of this work, in order to analyse the feasibility of this boiler integration and the effect of such a technical modification on the system performance and investment profitability. Moreover, a future analysis can be the evaluation of the effect of implementing modules that allows also cold in the layout, such as chiller, in a trigeneration configuration. Simulations with a system working 24/7 shall be carry out.

Due to the number of parameters involved and technical limitations of each system component, selection of the optimal size of the plant element is a challenging task, along with choice of operating mode of the modules. The future steps of this research will focus on developing an optimization code, that helps in the automatic selection of system operating mode, and component, based on the objective function chosen by the decision maker. The selection should be done considering end-user demand characteristics and key techno-economic factors such as solar irradiance and collector efficiency, biomass availability, and supply costs. Moreover, a key research question arises from the need to assess off-design operation, part-load, and dynamic performance of the system components (EFGT, CSP and ORC) and of the whole-system.

ANNEX-I

GENETIC ALGORITHM IN POWER PLANT OPTIMIZATION PROCESSES

The aim of this chapter is to give an overview of the optimization methods applied to renewable power plants. In particular, it has been briefly defined what optimization is and are listed the main optimization methods. Then, a summary of genetic algorithm (GA) and non-dominated sorting genetic algorithm (NSGA) has been given. Advantages and main limits of the most important algorithms used are here described. A literature review of these methods applied to renewable systems is finally given.

Optimization definition and main methods

Optimization is the area of study where the input values of a function, that minimize or maximize this function, have to be found (Pardalos 2002). These values are called optimal solution of the optimization problems.

A general optimization problem can be written mathematically as:

$$\text{Minimize/maximize } f_i(x) \tag{1}$$

subject to:

$$Ax \leq b \tag{2}$$

$$x \geq 0 \tag{3}$$

Where $f_i \in \mathcal{R}^n$, $b \in \mathcal{R}^m$, $A \in \mathcal{R}^{m \times n}$ and the inequalities expressed in eq. 2 and eq.3 are to be interpreted componentwise. The function to be minimized is called objective function, represented by eq. 1.; while eq.2 and eq. 3 represent the constrains of the problem.

Most of the time, optimum mathematical solution does not coincide with the optimum problem solution because the inherent problem characteristics impose constrain to the solutions field of existence, making often the optimum mathematical solution unfeasible. Optimization problems are classified as mono-objective or multi-objective depending on the number of functions that have to be optimized.

Traditional methods to find the optimum of a problem are Linear-Programming, Lagrangian relaxation, quadratic programming, etc. but their implementation require computational times that are too high for practical purpose. Have been then developed heuristic and meta-heuristic algorithm that are able to find the optimum faster and in a more efficient way. These algorithms are divided in two categories called trajectory methods and population-based methods (Baños et al. 2011). Trajectory methods are extensions of iterative procedures. In this type of methods, a single solution is used during the research process and the solution is found using incorporated techniques that enable the algorithm to escape from local optima. The outcome is a single optimized solution. Hill climbling and simulated annealing can be included in trajectory algorithms. The second type of meta-heuristic algorithms are called Population-based since they use a population of solutions as starting point, which evolve during a given number of iterations. Outcome is a population of solutions that is reached when the stop condition is fulfilled. The main population-based meta-heuristics include genetic algorithms (GA) and evolutionary algorithms (Gendreau and Potvin 2010). All the so far mentioned optimization methods are used to solve mono-objective problems.

In real application, optimization problems are often made by more than one objective functions, that are in conflict and have to be optimized simultaneously. The methods to solve multi-objectives problems are aggregate weight functions algorithms and Pareto-based methods. The aggregate weight functions combine the objectives functions of the problem in one function, assigning to each function a relative importance called weight (Izui et al 2015). The main disadvantages of this method are the assignment of the weight to each function and the solution itself, that is a single solution

not easily convertible as solution for several functions. Pareto-based methods go beyond these limits due to their capability to solve a set of equations and give as solution a set of non-dominated solutions from which the decision maker can select the optimum for the project. Two solutions are defined non-dominated (or indifferent) when each of them is not better nor worse than the other one (Goldberg 1989). Multi-objective algorithms can be also trajectory and population-based and among them we include methods such as multi-objective simulated annealing and non-dominated sorting genetic algorithm (NSGA).

Genetic algorithm and non-dominated sorting genetic algorithm

GA is an optimization algorithm biologically inspired (Holland 1992). Unlike trajectory methods that evaluate and improve a single solution, GA calculations start from a set of solution, called population, that is normally randomly selected and improved iteratively. The solution that compose the population is called individual or genes and are organized in group or chromosome, called string. To each string is assigned a fitness value, that is a numerical measure of the accuracy of the solution respect to the objective function. The fitness function gives, based on the measured performance, the chance of reproductive opportunities.

The next generation is computed applying the operation of selection, crossover and mutation to the string with the higher fitness value. Selection process made a copy of the string in proportion to their fitness and placed in an intermediate generation and can be compared to natural selection process. Crossover operation recombine two strings producing two completely new strings, that are inserted in the next generation. Crossover point of the parent string is chosen randomly. Mutation modifies a string generating a new individual or a new set of individuals in a given string. This operation prevents an early convergence of the algorithm and, producing inhomogeneity within the population, ensures convergence to a global optimum.

Mutation can be viewed as a way out of getting stuck in local minima and is often performed after crossover has been applied (Mayer-Baese and Schmid 2014).
Iteration process is stopped when a stopping criterion is reached. Stopping criterion is defined by GA user and can be based or on the number of iterations that should not exceeds a specified value, or on the improvement for the best function value that is less than a fixed value for the last n-consecutive iterations (Arora 2012).
Solution obtained by performing the GA algorithm is for single objective optimization problems. Being a population-based approach, GA are well suited to solve multi-objective optimization problems. A generic single-objective GA can be modified to find a set of multiple non-dominated solutions in a single run (Konak et al 2006). The set of optimal solution obtained by multi-objective GA are organized in a Pareto front optimal solution. All the solution in a Pareto front are non-dominated and on such a non-dominating sorting procedure is based Nondominated Sorting Genetic Algorithm NSGA (Srinivas and Deb 1994).

Application to renewable plants

Renewable energies sources are the best solution to slow down climate change and protect environment. The main limits of renewables technologies are their lower efficiency and higher costs if compared with traditional energy conversion systems. Optimization algorithms are proving to be a powerful tool for solving complex problems related to renewables application, such us system sizing or parameters selection. Application of optimization algorithm to a renewable system can increase its efficiency and therefore its profitability and it exists a wide literature on these applications.
In many parts of the world, direct solar radiation is one of the best prospective sources of energy. The main limit of power generation from solar energy is the intermittent nature of such a system but implementation of a TES is an effective solution for ensuring continuous power flow. Selection of the TES has to be done in order to keep investment and operational costs acceptable. Kalogirou (2004) proposed a solution to the the problem of maximizing the economic benefits of a

solar-energy system by means of artificial neural networks and GA. Artificial neural networks learnt the correlation of collector area and storage-tank size on the auxiliary energy required by the system from which life-cycle savings can be estimated, while GA is then employed to estimate the optimum size of these two parameters for maximizing life-cycle savings.

As regards power production from wind, critical problems are optimal turbine design and wind farm layout selection. Benini and Toffolo (2002) presented a multi-objective evolutionary algorithm for the optimization of the geometrical parameters of the rotor configuration of stall-regulated horizontal-axis wind turbines with the aim of achieving the best trade-off performance between the total energy production per area of wind park and cost. The best performing layout of a wind farm is selected by determining the optimum position of wind turbines within the farm. Grady et al. (2005) developed a GA to determine the optimal placement of wind turbines for maximum production capacity while limiting the number of turbines installed and the acreage of land occupied by each wind farm.

Sustainability of biomass power plant is assessed according to indicators such as efficiency, greenhouse gas emissions, land use, water and so on. To obtain the optimal location of a biomass-fuelled systems, Reche et al. (2008) applied particle swarm optimization method and with the obtained results the compute the maximization of the profitability index of the system by mean of GA. An optimization method for multi-biomass energy conversion applications was presented by Rentizelas et al. (2009). In this paper technical, regulatory, social and logical constraints were considered. An analysis on economic and environmental performance of a large number of agricultural biogas plants was performed by Madler et al. (2009), where the multi-criteria study aimed at finding the most efficient one.

In the last decades, interest in integration of different renewable energy sources is increased and new optimization problems have been then defined. A first problem is the selection of the renewables to integrate in the plant in order to maximize the energy generated and minimize the combined lack of energy and the costs. Moura

and Almeida (2010) developed a multi-objective model that, using historic data for the wind, solar and hydro availability and energy consumption, enables the optimization of the renewable mix, ensuring a minimum level of intermittence, a minimum non-guaranteed peak load share (both in summer and in winter) and a minimum global cost. Also crucial is the selection of the size of the systems that have to be implemented and, eventually of the storage. GA has been employed by Lagorse et al. (2009) for optimizing a hybrid system coupling a photovoltaic, a battery and a fuel cell for street lighting systems. Eke et al. (2005) presented an optimization method for designing a wind-photovoltaic hybrid system to cover the electricity consumption considering the monthly average solar irradiation and wind speed data. Moreover, Ould et al. (2010) selected the size a hybrid solar–wind-battery system using multi-objective GA in order to minimize the annualized cost system and the loss of power supply probability.

BIBLIOGRAPHY

Abedin A. H., Rosen M. A, (2011) *A critical review of Thermochemical Energy Storage System,* The Open Renewable Energy Journal, 4: 42-46.

Ackermann, T., Andersson, G., & Söder, L. (2001) *Distributed generation: a definition.* Electric Power Systems Research. 57(3), 195–204.

Agyenim, F., Hewitt, N., Eames, P., & Smyth, M. (2010). *A review of materials, heat transfer and phase change problem formulation for latent heat thermal energy storage systems (LHTESS)*. Renewable and Sustainable Energy Reviews, 14(2), 615–628.

Ahmad, A. A., Zawawi, N. A., Kasim, F. H., Inayat, A., & Khasri, A. (2016). *Assessing the gasification performance of biomass: A review on biomass gasification process conditions, optimization and economic evaluation.* Renewable and Sustainable Energy Reviews, 53, 1333–1347.

APO Asian Productivity Organization. *Reusing biomass waste in industrial boilers for energy recovery*. http://www.apo-tokyo.org/ biomassboiler/D0 online-resources.htm; 2010.

Arora, J. S. (2012). *Genetic Algorithms for Optimum Design*. Introduction to Optimum Design, 643–655.

Ashok, S. (2007). *Optimised model for community-based hybrid energy system*. Renewable Energy, 32(7), 1155–1164.

ASHRAE, 2013, ANSI/ASHRAE Standard 34-2013, *Designation and Safety Classification of Refrigerants*, ASHRAE, Atlanta, USA

Avghad S. N., Keche A. J., Kousel A., (2016) *Thermal Energy Storage: A Review.* IOSR Journal of Mechanical and Civil Engineering (IOSR-JMCE) e-ISSN: 2278-1684, p-ISSN: 2320-334X, Volume 13, Issue 3 Ver. II (May- Jun. 2016), PP 72-77

Atul Sharma, V.V. Tyagi , C.R. Chen , D. Buddhi (2009), *Review on thermal energy storage with phase change materials and applications*, Renewable and Sustainable Energy Reviews 13; 318–345;

Badr, O., Probert, S. D., & O'Callaghan, P. W. (1985). *Selecting a working fluid for a Rankine-cycle engine*. Applied Energy, 21(1), 1–42.

Balat, M., Balat, M., Kırtay, E., & Balat, H. (2009). *Main routes for the thermo-conversion of biomass into fuels and chemicals. Part 1: Pyrolysis systems*. Energy Conversion and Management, 50(12), 3147–3157.

Balat, H., & Kırtay, E. (2010). *Hydrogen from biomass – Present scenario and prospects*. International Journal of Hydrogen Energy, 35(14), 7416–7426.

Baños, R., Manzano-Agugliaro, F., Montoya, F. G., Gil, C., Alcayde, A., & Gómez, J. (2011). *Optimization methods applied to renewable and sustainable energy: A review.* Renewable and Sustainable Energy Reviews, 15(4), 1753–1766.

Bao, J., & Zhao, L. (2013). *A review of working fluid and expander selections for organic Rankine cycle*. Renewable and Sustainable Energy Reviews, 24, 325–342.

Bahrami, M., Hamidi, A. A., & Porkhial, S. (2013). *Investigation of the effect of organic working fluids on thermodynamic performance of combined cycle Stirling-ORC*. International Journal of Energy and Environmental Engineering, 4(1), 12.

Bartocci, P., Bidini, G., Laranci, P., Zampilli, M., D'Amico, M., & Fantozzi, F. (2018). *Environmental Impact on the Life Cycle for Turbine Based Biomass CHP Plants.* Volume 3: Coal, Biomass, and Alternative Fuels; Cycle Innovations; Electric Power; Industrial and Cogeneration; Organic Rankine Cycle Power Systems.

Belyadi, H., Fathi, E., & Belyadi, F. (2017). *Economic Evaluation. Hydraulic Fracturing in Unconventional Reservoirs*, 325–392.

Bell, I.H., Quoilin, S., Wronski, J., Lemort, V., (2013), *Coolprop: An open-source reference-quality thermophysical property library*. In: ASME ORC 2nd International Seminar on ORC Power Systems.

Benini E, Toffolo A., (2002), *Optimal design of horizontal-axis wind turbines using blade-element theory and evolutionary computation*. Journal of Solar Energy Engineering;124(4):357–63.

Boschiero, M., Cherubini, F., Nati, C., & Zerbe, S. (2016). *Life cycle assessment of bioenergy production from orchards woody residues in Northern Italy.* Journal of Cleaner Production, 112, 2569–2580.

Bridgwater, A. V. (1996). *Production of high grade fuels and chemicals from catalytic pyrolysis of biomass.* Catalysis Today, 29(1-4), 285–295.

Bufi E. A., Camporeale S. M., Cinnella P., (2017), *Robust optimization of an Organic Rankine Cycle for heavy duty engine waste heat recovery,* Energy Procedia 129, 66-73.

Caputo, A. C., Palumbo, M., Pelagagge, P. M., & Scacchia, F. (2005). *Economics of biomass energy utilization in combustion and gasification plants: effects of logistic variables.* Biomass and Bioenergy, 28(1), 35–51.

Camporeale S. M., Pantaleo A. M, Ciliberti P., Fortunato B., (2015), *Cycle configuration analysis and techno-economic sensitivity of biomass externally fired gas turbine with bottoming ORC,* Energy conversion Management 105: 1239-1250.

Chen H, Goswami DY, Stefanakos EK (2010). *A review of thermodynamic cycles and working fluids for the conversion of low-grade heat*. Renewable and Sustainable Energy Reviews 2010;14(9):3059–67.

Cherubini, F., & Strømman, A. H. (2011). *Life cycle assessment of bioenergy systems: State of the art and future challenges.* Bioresource Technology, 102(2), 437–451.

Cycle-Tempo® website: *http://www.asimptote.nl/software/cycle-tempo/*

COGEN Europe (The European Association for the Promotion of Cogeneration, www.cogen.org). The European educational tool on cogeneration, 2nd ed. December 2001.

Cortright, R. D., Davda, R. R., & Dumesic, J. A. (2002). *Hydrogen from catalytic reforming of biomass-derived hydrocarbons in liquid wate*r. Nature, 418(6901), 964–967.

Dai, Y., Wang, J., & Gao, L. (2009). *Parametric optimization and comparative study of organic Rankine cycle (ORC) for low grade waste heat recovery*. Energy Conversion and Management, 50(3), 576–582.

Dayananda D., Irons R., Harrison S., Herbohn J., Rowland P., (2002), *Capital Budgeting. Financial appraisal of investment Projects*, Cambridge University Press

Das D, Veziroglu TN. *Hydrogen production by biological processes: a survey of literature.* Int J Hydrogen Energ 2001; 26:13e28

Desai, N. B., & Bandyopadhyay, S. (2009). *Process integration of organic Rankine cycle*. Energy, 34(10), 1674–1686.

Deshmukh, M. K., & Deshmukh, S. S. (2008). *Modeling of hybrid renewable energy systems*. Renewable and Sustainable Energy Reviews, 12(1), 235–249.

Demirbas, A. (2004). *Combustion characteristics of different biomass fuels.* Progress in Energy and Combustion Science, 30(2), 219–230.

Dinçer I., Rosen M. A., (2011), *Thermal Energy Storage (TES) Methods*. Thermal Energy Storage, 83–190.

Doctor, R.N., Newton, D.P., & Pearson, A. (2001). *Managing uncertainty in research and development.* Technovation, 79-90.

Ebrahimi, K., Jones, G. F., & Fleischer, A. S. (2017). *The viability of ultra-low temperature waste heat recovery using organic Rankine cycle in dual loop data center applications*. Applied Thermal Engineering, 126, 393–406.

El-Khattam, W., & Salama, M. M.. (2004). *Distributed generation technologies, definiytions and benefits.* Electric Power Systems Research, 71(2), 119–128.

Eke R, Kara O, Ulgen K., (2005), *Optimization of a wind/PV hybrid power generation system*. International Journal of Green Energy; 2(1):57–66.

Falchetta M., Maccari A., (2006), *Calore ad alta temperatura dal sole per produrre elettricità e idrogeno",* Le Scienze, N.459

Farid MM, Khudhair AM, Razack SAK, Al-Hallaj S. *A review on phase change energy storage: materials and applications*. Energy Convers Manag 2004;45(9):1597–615.

Frazzica, A., Manzan, M., Sapienza, A., Freni, A., Toniato, G., & Restuccia, G. (2016). *Experimental testing of a hybrid sensible-latent heat storage system for domestic hot water applications*. Applied Energy, 183, 1157–1167.

Gailly, B. (2011). *Developing innovative organizations: a roadmap to boost your innovation potential*. Houndmills, Basingstoke, Hampshire: Palgrave Macmillan

Gendreau M, Potvin J-Y., (2010), *Handbook of metaheuristics*. International series in operations research and management science. Springer.

Giannuzzi, G. M., Majorana, C. E., Miliozzi, A., Salomoni, V. A., & Nicolini, D. (2007). *Structural Design Criteria for Steel Components of Parabolic-Trough Solar Concentrators*. Journal of Solar Energy Engineering, 129(4), 382.

Gil, A., Medrano, M., Martorell, I., Lázaro, A., Dolado, P., Zalba, B., & Cabeza, L. F. (2010). *State of the art on high temperature thermal energy storage for power generation. Part 1—Concepts, materials and modellization*. Renewable and Sustainable Energy Reviews, 14(1), 31–55.

Glazebrook k.D., (1976), *A profitability index for alternative research projects*, Omega, Vol. 4, No.1, pp. 79-83.

Grady SA, Hussaini MY, Abdullah MM., (2005), *Placement of wind turbines using genetic algorithms*. Renewable Energy; 30(12):259–70

Gupta, A., & Verma, J. P. (2015). *Sustainable bio-ethanol production from agro-residues: A review*. Renewable and Sustainable Energy Reviews, 41, 550–567.

Gurau M. A., (2012), *the use of profitability index in economic evaluation of industrial investment projects.* Proceedings in Manufacturing Systems, Volume 7, Issue 1.

Halawa E, Bruno F, Saman W., (2005), *Numerical analysis of a PCM thermal storage system with varying wall temperature.* Energy Convers Manag;46(15):2592–604.

Hajabdollahi, Z., Hajabdollahi, F., Tehrani, M., & Hajabdollahi, H. (2013). *Thermo-economic environmental optimization of Organic Rankine Cycle for diesel waste heat recovery.* Energy, 63, 142–151.

Halim, R., Rupasinghe, T. W. T., Tull, D. L., & Webley, P. A. (2013). *Mechanical cell disruption for lipid extraction from microalgal biomass.* Bioresource Technology, 140, 53–63.

Hasnain, S. M. (1998). *Review on sustainable thermal energy storage technologies, Part I: heat storage materials and techniques*. Energy Conversion and Management, 39(11), 1127–1138.

Holland JH., (1992) *Adaptation in nature and artificial systems: an introductory analysis with applications to biology, control and artificial intelligence.* Massachusetts: MIT Press.

Huang, Y., Wang, Y. D., Chen, H., Zhang, X., Mondol, J., Shah, N., & Hewitt, N. J. (2017). *Performance analysis of biofuel fired trigeneration systems with energy storage for remote households.* Applied Energy, 186, 530–538.

Hung, T. C., Shai, T. Y., & Wang, S. K. (1997). *A review of organic Rankine cycles (ORCs) for the recovery of low-grade waste heat.* Energy, 22(7), 661–667.

Ibrahim, H., ilinca, A., & Perron, J. (2008). *Energy storage systems Characteristics and comparisons. Renewable and Sustainable Energy Reviews, 12(5), 1221–1250.*

IEA, 2002. *Distributed Generation in Liberalised Electricity Markets, Paris*, p. 128.

Imran, M., Usman, M., Park, B.-S., Kim, H.-J., & Lee, D.-H. (2015). *Multi-objective optimization of evaporator of organic Rankine cycle (ORC) for low temperature geothermal heat source*. Applied Thermal Engineering, 80, 1–9.

Ingeco project website: http://www.verticale.net/sistemi-di-cogenerazione-a-ciclo-Combinato.

Irradiation data web site: http://www.meteororm.com.

Izui K., Yamada T., Nishiwaki S. Tanaka K., (2015), *Multiobjective optimization using an aggregative gradient-based method*, Structural and Multidisciplinary Optimization, 51(1), 173-182.

Jacquet, N., Maniet, G., Vanderghem, C., Delvigne, F., & Richel, A. (2015). *Application of Steam Explosion as Pretreatment on Lignocellulosic Material: A Review*. Industrial & Engineering Chemistry Research, 54(10), 2593–2598.

Jebasingh, V. K., & Herbert, G. M. J. (2016). *A review of solar parabolic trough collector.* Renewable and Sustainable Energy Reviews, 54, 1085–1091.

Jørgensen K. *Biomass combustion technology* at B&W Vølund A/S, /www.volund.dkS. Lecture presented on 14.05.2007 in Aalborg University.

Kang, S.H. (2012). *Design and experimental study of ORC (organic Rankine cycle) and radial turbine using R245fa working fluid*, Energy 41, 514-524.

Kalogirou SA., (2004), *Optimization of solar systems using artificial neural-networks and genetic algorithms*. Applied Energy;77(4):383–405.

Karellas S., Schuster A. (2008). *Supercritical Fluid Parameters in Organic Rankine Cycle Application.* Int. J. of Thermodynamics ISSN 1301-9724 Vol. 11 (No. 3), pp. 101-108.

Karmee, S. K. (2016). *Liquid biofuels from food waste: Current trends, prospect and limitation.* Renewable and Sustainable Energy Reviews, 53, 945–953.

Kearney, D., Herrmann, U., Nava, P., Kelly, B., Mahoney, R., Pacheco, J., Cable R., Potrovitza N., Blake D., Price, H. (2003). *Assessment of a Molten Salt Heat Transfer Fluid in a Parabolic Trough Solar Field*. Journal of Solar Energy Engineering, 125(2), 170.

Khan, M.Y. (1999). *Theory & Problems in Financial Management*. Boston: McGraw Hill Higher Education.

Khan, M. J., & Iqbal, M. T. (2005). *Dynamic modelling and simulation of a small wind–fuel cell hybrid energy system.* Renewable Energy, 30(3), 421–439.

Khare, S., Dell'Amico, M., Knight, C., & McGarry, S. (2013*). Selection of materials for high temperature sensible energy storage*. Solar Energy Materials and Solar Cells, 115, 114–122.

Kyoungsoo Ro, Saifur Rahman, *Two-loop controller for maximizing performance of a grid-connected photovoltaic-fuel cell hybrid power plant*. IEEE Transactions on Energy Conversion, 13(3), 276–281.

Knothe, G. (2008). *"Designer" Biodiesel: Optimizing Fatty Ester Composition to Improve Fuel Propertie.* Energy & Fuels, 22(2), 1358–1364**.** JRAIA international symposium 2012.

Konak, A., Coit, D. W., & Smith, A. E. (2006). *Multi-objective optimization using genetic algorithms: A tutorial*. Reliability Engineering & System Safety, 91(9), 992–1007.

Kontomaris, K. (2012). *A zero-odp, low gwp working fluid for high temperature heating and power generation from low temperature heat: dr-2.*

Koroneos, C., Spachos, T., & Moussiopoulos, N. (2003). *Exergy analysis of renewable energy sources.* Renewable Energy, 28(2), 295–310.

Küçük, M. M., & Demirbaş, A. (1997). *Biomass conversion processes. Energy Conversion and Management*, 38(2), 151–165.

Kumar, A.; Jones, D.D.; Hanna, M.A (2009). *Thermochemical biomass gasification: A review of the current status of the technology*. Energies, 2, 556–581

Kuravi, S., Trahan, J., Goswami, D. Y., Rahman, M. M., & Stefanakos, E. K. (2013). *Thermal energy storage technologies and systems for concentrating solar power plants.* Progress in Energy and Combustion Science, 39(4), 285–319.

Lagorse J, Paire D, Miraoui A., (2009), *Sizing optimization of a stand-alone street lighting system powered by a hybrid system using fuel cell. PV and battery.* Renewable Energy; 34(3):683–91.

Lam PS, Sokhansanj S, Bi X, Lim CJ, Melin S (2011) *Energy input and quality of pellets made from steamexploded Douglas fir (Pseudotsuga menziesii).* Energy and Fuels 25(4):1521-1528.

Lang, W., Colonna, P., & Almbauer, R. (2013). *Assessment of Waste Heat Recovery. From a Heavy-Duty Truck Engine by Means of an ORC Turbogenerator.* Journal of Engineering for Gas Turbines and Power, 135(4), 042313.

Lefley, F. (1996). *The payback method of investment appraisal: A review and synthesis*. International Journal of Production Economics, 44(3), 207–224.

Lin, Y., & Tanaka, S. (2005). *Ethanol fermentation from biomass resources: current state and prospects.* Applied Microbiology and Biotechnology, 69(6), 627–642.

Linke, P., Papadopoulos, A., & Seferlis, P. (2015). *Systematic Methods for Working Fluid Selection and the Design, Integration and Control of Organic Rankine Cycles—A Review*. Energies, 8(6), 4755–4801.

Macchi E., Astolfi M.. *Organic Rankine Cycle (ORC) Power Systems Technologies and Applications.* Woodhead Publishing, 2017.

Madhawa Hettiarachchi, H. D., Golubovic, M., Worek, W. M., & Ikegami, Y. (2007). *Optimum design criteria for an Organic Rankine cycle using low-temperature geothermal heat sources*. Energy, 32(9), 1698–1706**.**

Madlener R, Antunes CH, Dias LC., (2009), *Assessing the performance of biogas plants with multi-criteria and data envelopment analysis*. European Journal of Operational Research;197(3):1084–94.

Maschio, G., Koufopanos, C., & Lucchesi, A. (1992). *Pyrolysis, a promising route for biomass utilization*. Bioresource Technology, 42(3), 219–231.

Meher, L., Vidyasagar, D., & Naik, S. (2006). *Technical aspects of biodiesel production by transesterification—a review.* Renewable and Sustainable Energy Reviews, 10(3), 248–268.

Meyer-Baese, A., & Schmid, V. (2014). *Genetic Algorithms. Pattern Recognition and Signal Analysis in Medical Imaging*, 135–149.

McKendry, P. (2002). *Energy production from biomass (part 2): conversion technologies.* Bioresource Technology, 83(1), 47–54.

Mohamed, S. A., Al-Sulaiman, F. A., Ibrahim, N. I., Zahir, M. H., Al-Ahmed, A., Saidur, R., Yılbaş B. S., Sahin, A. Z. (2017). *A review on current status and challenges of inorganic phase change materials for thermal energy storage systems*. Renewable and Sustainable Energy Reviews, 70, 1072–1089.

Molino, A.; Iovane, P.; Donatelli, A.; Braccio, G.; Chianese, S.; Musmarra, D. (2013) *Steam gasification of refuse-derived fuel in a rotary kiln pilot plant: Experimental tests*. Chem. Eng. Trans., 32, 337–342.

Molino, A.; Chianese, S.; Musmarra, D. (2016) *Biomass gasification technology: The state of the art overview*. J. Energy Chem., 25, 10–25

Molino, A., Larocca, V., Chianese, S., & Musmarra, D. (2018). *Biofuels Production by Biomass Gasification: A Review*. Energies, 11(4), 811.

Moura PS, De Almeida AT., (2010), *Multi-objective optimization of a mixed renewable system with demand-side management*. Renewable and Sustainable Energy Reviews;14(5):1461–8

Muralikrishna, I. V., & Manickam, V. (2017). Life Cycle Assessment. Environmental Management, 57–75.

Nielsen K., (2003), *Thermal Energy Storage A State-of-the-Art*, A report within the research program Smart Energy-Efficient Buildings at NTNU and SINTEF 2002-2006

Nussbaumer, T. (2003*). Combustion and Co-combustion of Biomass: Fundamentals, Technologies, and Primary Measures for Emission Reduction*. Energy & Fuels, 17(6), 1510–1521.

OECD, 1991 *Estimation of greenhouse gas emissions and sinks.* Final Report from the OECD experts meeting, 18–21 February 1991, OECD, Paris.

Ould B, Sambou V, Ndiaye PA, Kébé CMF, Ndongo M., (2010), *Optimal design of a hybrid solar-wind-battery system using the minimization of the annualized cost system and the minimization of the loss of power supply probability (LPSP).* Renewable Energy ;35(10):2388–90.

Overend RP, Chornet E (1987) *Fractionation of lignocellulosics by steam-aqueous pretreatments*. Philosophical Transaction of the Royal Society A 321(1561):523-536.

Pantaleo A. M., Camporeale S. M, Miliozzi A., Russo V., Shah N., Markides C. N., (2017), *Novel hybrid CSP-biomass CHP for flexible generation: Thermo-economic analysis and profitability assessment,* Appl. Energy 204, 994-e1006.

Pantaleo A. M., Camporeale S. M, Sorrentino A., Miliozzi A., Shah N., Markides C. N., (2018) *Hybrid solar-biomass combined Brayton/organic Rankine-cycle plants integrated with thermal storage: Techno-economic feasibility in selected Mediterranean areas*. Renewable Energy.

Pardalos P.M., Resende M. G. C., (2002), *Handbook of applied optimization,* Oxford University Press.

Parthasarathy, P.; Narayanan, K.S. *Hydrogen production from steam gasification of biomass: Influence of process parameters on hydrogen yield—A review*. Renew. Energy 2014, 66, 570–579.

Pasetti, M., Invernizzi, C. M., & Iora, P. (2014). *Thermal stability of working fluids for organic Rankine cycles: An improved survey method and experimental results for cyclopentane, isopentane and n -butane*. Applied Thermal Engineering, 73(1), 764–774.

Patel, P. S., & Doyle, E. F. (1976). *Compounding the Truck Diesel Engine with an Organic Rankine-Cycle System*. SAE Technical Paper Series.

Patel A.G., Maheshwari N.K., Vijayan P.K., Sinha R.K.. (2005) *A study on sulfur-iodine (S-I) thermochemical water splitting process for hydrogen production from nuclear heat*, in: processing of Sixteenth Annual Conference of Indian Nuclear Society, Science behind Nuclear Technology, Mumbai, India, November 15e18.

Patel, M., Zhang, X., & Kumar, A. (2016). *Techno-economic and life cycle assessment on lignocellulosic biomass thermochemical conversion technologies: A review*. Renewable and Sustainable Energy Reviews, 53, 1486–1499.

Pérez-Navarro, A., Alfonso, D., Álvarez, C., Ibáñez, F., Sánchez, C., & Segura, I. (2010). *Hybrid biomass-wind power plant for reliable energy generation.* Renewable Energy, 35(7), 1436–1443.

Pepermans G., Driesen J., Haeseldonckx D., Belmans R., D'haeseleer W., *Distributed generation: definition, benefits and issues*, Energy Policy 33 (2005) 787–798.

Petrou, E. C., & Pappis, C. P. (2009). Biofuels: A Survey on Pros and Cons. Energy & Fuels, 23(2), 1055–1066.

Pielichowska, K., & Pielichowski, K. (2014). *Phase change materials for thermal energy storage. Progress in Materials Science, 65, 67–123.*

Pike, R.H., (1985). *Disenchantment with DCF promotes IRR. Certified Accountant*. July: 14-17.

Quoilin, S., Declaye, S., Tchanche, B. F., & Lemort, V. (2011). *Thermo-economic optimization of waste heat recovery Organic Rankine Cycles.* Applied Thermal Engineering, 31(14-15), 2885–2893.

Rappaport. A., (1965). *The discounted payback period*. Mgmt. Services. July/August: 30-36.

Reche P, Jurado F, Ruiz N, García S, Gómez M. (2008) *Particle swarm optimization for biomass-fuelled systems with technical constraints.* Engineering Applications of Artificial Intelligence;21(8):1389–96.

Renewable heat incentive website: *https://www.gov.uk/non-domestic-renewable-heat-incentive*.

Rentizelas AA, Tatsiopoulos IP, Tolis A., (2009), *An optimization model for multi-biomass tri-generation energy supply.* Biomass and Bioenergy;33(2):223–33.

Rosendahl L., (2013), Biomass *combustion science, technology and engineering,* Woodhead Publishing.

Sansaniwal, S.K.; Rosen, M.A.; Tyagi, S.K. *Global challenges in the sustainable development of biomass gasification: An overview*. Renew. Sustain. Energy Rev. 2017, 80, 23–43.

Schuster, A., Karellas, S., Kakaras, E., & Spliethoff, H. (2009). *Energetic and economic investigation of Organic Rankine Cycle applications.* Applied Thermal Engineering, 29(8-9), 1809–1817.

Sercan Teleke, Mesut E. Baran, Subhashish Bhattacharya, and Alex Q. *Huang, Rule-Based Control of Battery Energy Storage for Dispatching Intermittent Renewable Sources.* IEEE transactions on sustainable energy, vol. 1, no. 3, October 2010.

Sikarwar, V.S.; Zhao, M.; Clough, P.; Yao, J.; Zhong, X.; Memon, M.Z.; Shah, N.; Anthony, E.J.; Fennell, P.S. *An overview of advances in biomass gasification*. Energy Environ. Sci. 2016, 9, 2939–2977.

Srinivas N, Deb K., (1994), Multiobjective optimization using nondominated sorting in genetic algorithms. J Evol Comput; 2(3):221–48.

Sharma, A., Pareek, V., & Zhang, D. (2015). *Biomass pyrolysis—A review of modelling, process parameters and catalytic studies*. Renewable and Sustainable Energy Reviews, 50, 1081–1096.

Sorrentino, A., Pantaleo, A. M., Markides, C. N., Braccio, G., Fanelli, E., & Camporeale, S. M. (2018). *Energy performance and profitability of biomass boilers in commercial sector: the case study in the UK*. Energy Procedia, 148, 639–646.

Stelte W. (2013). *Steam explosion for biomass pre-treatment*. Danish Technological Institute, Energy & Climate, Center for Renewable Energy and Transport, Section for Biomass.

Swami SM, Chaudhari V, Kim DS, Sim SJ, Abraham MA (2008). *Production of hydrogen from glucose as a biomass simulant: integrated biological and thermochemical approach*. Ind Eng Chem Res; 47:3645e51.

Subramanian AK, Marwaha Y., (2006), *Use of bagasse and other biomass fuels in high pressure travelling grate boilers.* Int Sugar J; 108:6–9.

Sun, Y., & Cheng, J. (2002). *Hydrolysis of lignocellulosic materials for ethanol production: a review.* Bioresource Technology, 83(1), 1–11.

Tabatabaie, S. M. H., & Murthy, G. S. (2016). *Effect of geographical location and stochastic weather variation on life cycle assessment of biodiesel production from camelina in the north western USA.* The International Journal of Life Cycle Assessment, 22(6), 867–882.

Tagliaferri, C., Evangelisti, S., Clift, R., & Lettieri, P. (2018). *Life cycle assessment of a biomass CHP plant in UK: The Heathrow energy centre case.* Chemical Engineering Research and Design, 133, 210–221.

Taylan, O., Kaya, D., Bakhsh, A. A., & Demirbas, A. (2017). *Bioenergy life cycle assessment and management in energy generation.* Energy Exploration & Exploitation, 36(1), 166–181.

Van der Lans RP, Pedersen LT, Jensen A, Glarborg P, Dam-Johansen K. (2000) *Modelling and experiments of straw combustion in a grate furnace*. Biomass Bioenergy; 19:199–208.

Vankeirsbilck, I.; Vanslambrouck, B.; Gusev, S.; De Paepe, M., (2011) *Organic Rankine cycle as efficient alternative to steam cycle for small scale power generation*. HEFAT2011 8 th International Conference on Heat Transfer, Fluid Mechanics and Thermodynamics

Wang, Z. Q., Zhou, N. J., Guo, J., & Wang, X. Y. (2012). *Fluid selection and parametric optimization of organic Rankine cycle using low temperature waste heat*. Energy, 40(1), 107–115.

Wang, J., Yan, Z., Wang, M., Li, M., & Dai, Y. (2013). *Multi-objective optimization of an organic Rankine cycle (ORC) for low grade waste heat recovery using evolutionary algorithm.* Energy Conversion and Management, 71, 146–158.

Werther J, Saenger M, Hartge EU, Ogada T, Siagi Z. (2000) *Combustion of agricultural residues*. Progr Energy Combust Sci; 26:1–27.

Woudstra N., Woudstra T., Pirone A., van der Stelt T., (2010), *Thermodynamic evaluation of combined cycle plants*, Energy Convers Manage

Wu, D. W., & Wang, R. Z. (2006). *Combined cooling, heating and power: A review.* Progress in Energy and Combustion Science, 32(5-6), 459–495.

Xi, H., Li, M.-J., Xu, C., & He, Y.-L. (2013). *Parametric optimization of regenerative organic Rankine cycle (ORC) for low grade waste heat recovery using genetic algorithm*. Energy, 58, 473–482.

Yin, C., Rosendahl, L. A., & Kær, S. K. (2008). *Grate-firing of biomass for heat and power production*. Progress in Energy and Combustion Science, 34(6), 725–754.

Žižlavský, O. (2014). *Net Present Value Approach: Method for Economic Assessment of Innovation Projects*. Procedia - Social and Behavioral Sciences, 156, 506–512.

(2009) *Thermochemical Conversion Processes*. In: Biofuels. Green Energy and Technology. Springer, London

PART II

PAPER 1

Solar/biomass hybrid cycles with thermal storage and bottoming ORC: System integration and economic analysis

Antonio M Pantaleo[1,4,5]1, Sergio M Camporeale[2], Arianna Sorrentino[2], Adio Miliozzi[3], Nilay Shah[4], Christos N Markides[4,5]

1. *Dipartimento DISAAT, Università degli Studi di Bari, Via Amendola 165/A 70125 Bari, Italy*
2. *Department, Polytechnic University of Bari, Via Orabona 4, 70125 Bari, Italy*
3. *Energy Technologies Department, ENEA, Casaccia Research Centre, Via Anguillarese, 301. 00123 S.M. di Galeria, Rome, Italy*
4. *Centre for Process Systems Engineering (CPSE), Imperial College London, South Kensington Campus, SW7 2AZ, London, UK*
5. *Clean Energy Processes (CEP) Laboratory, Imperial College London, South Kensington Campus, SW7 2AZ, London, UK*

Division of work among authors

Thermodynamic calculations have been done by Arianna Sorrentino (AS) in collaboration with Sergio M. Camporeale (SC). Adio Miliozzi (AM) was responsible for dimensioning and calculation of the solar plant. Antonio M. Pantaleo (AP) carried out the economical appraisal. The paper was written by AP with the help of AS. Comments and supervision were provided by SC, Nilay Shah and Christos N. Markides.

Abstract

This paper focuses on the thermodynamic modelling and thermo-economic assessment of a novel arrangement of a combined cycle composed of an externally fired gas turbine (EFGT) and a bottoming organic Rankine cycle (ORC). The main novelty is that the heat of the exhaust gas exiting from the gas turbine is recovered in a thermal energy storage from which heat is extracted to feed a bottoming ORC. The thermal storage can receive heat also from parabolic-trough concentrators (PTCs) with molten salts as heat-transfer fluid (HTF). The presence of the thermal storage between topping and bottoming cycle facilitates a flexible operation of the system, and in particular allows to compensate solar energy input fluctuations, increase capacity factor, increase the dispatchability of the renewable energy generated and potentially operate in load following mode. A thermal energy storage (TES) with two molten salt tanks (one cold and one hot) is chosen since it is able to operate in the temperature range useful to recover heat from the exhaust gas of the EFGT and supply heat to the ORC. The heat of the gas turbine exhaust gas that cannot be recovered in the TES can be delivered to thermal users for cogeneration.

The selected bottoming ORC is a superheated recuperative cycle suitable to recover heat in the temperature range of the TES with good cycle efficiency. On the basis of the results of the thermodynamic simulations, upfront and operational costs assessments and subsidized energy framework (feed-in tariffs for renewable electricity), the global energy conversion efficiency and investment profitability are estimated.

Keywords: CHP, cogeneration, biomass, gate cycle, concentrating solar, ORC, combined cycle, bottoming cycle

1. Introduction

The European Commission is introducing new and ambitious targets for the penetration of renewable energy (27% of internal energy consumption), energy efficiency (reduction of 25% of energy consumption) and the reduction of greenhouse gas emissions (40% relative to 2005 levels) by 2030. These targets can be pursued by distributed heat and power generation, where renewable energy sources integrated with suitable energy storage systems can provide efficiently heat and electric power close to the end users. Concentrating solar power (CSP) and biomass-fired combined heat and power (CHP) plants can contribute towards all of these goals. CSP technologies generate electricity by concentrating the incident solar radiation onto a small area, where a heat transfer fluid (HTF) is heated. This thermal energy is then transferred by the HTF to a power generating system to drive a thermodynamic energy- conversion cycle. The integration of thermal energy storage (TES) can make CSP dispatchable and facilitate the overall energy conversion process. Nevertheless, solar energy is inherently intermittent such that even with TES the capacity factor of solar power plants is limited and often needs to be integrated by fossil boilers. Biomass can be an interesting alternative to fossil fuels to compensate the lack of solar energy: however, the thermal inertia of the furnace makes this technology well suited for base load operation but not for fluctuating operation to meet variable requests of heat and electricity from end users. TES can compensate the input and output energy fluctuations and overcome the individual drawbacks of solar and biomass as primary energy resources and allows such plants to achieve either base load or flexible operation [1][2].

The performance of a variety of system configurations of such hybrid plants under a variable solar input has been investigated in literature [3][4]. Some solar-biomass hybrid configurations are based on parabolic-trough collectors (PTCs), backup boilers and Rankine cycles [5][6], on the substitution of steam bleed regeneration with water preheating by solar energy [7] or on Fresnel collectors [8] to achieve higher temperatures. Some applications consider the use of solar

towers or solar dishes and compressed air as HTF [9]. None of the previous research has addressed the integration of parabolic-trough CSP and molten salt TES with biomass combustion in externally fired gas turbines (EFGT). The use of biomass has been widely investigated in the literature as it provides added socio- economic and environmental benefits [10]; in small-to-medium scale CHP plants this includes dual-fuelling of biomass and natural gas in externally/internally fired gas turbines [11][12][13]. The influence of part load efficiencies on optimal EFGT operation was investigated in [14], while the improved energy performance and profitability of employing a bottoming ORC has been investigated in different energy-demand segments [15][16]. The literature on ORC systems and working fluid selection is also extensive [17][18][19]. In particular, a combined cycle with a 1.3 MW biomass EFGT topping cycle and 0.7 MW bottoming ORC plant was proposed in [20].

In the present paper, which goes beyond the work proposed in Ref.[20][21], the heat and power generation system is composed by independent "power blocks", which are the generation sections (gas turbine and ORC), the thermal energy sources (biomass furnace and CSP plant), the TES and the thermal end users. The TES can compensate the solar input fluctuations and needs to be optimized to minimize exergy losses when heat is recovered from the topping cycle and from CSP to be transferred to the bottoming ORC. The technologies adopted for the TES and the ORC to meet these goals are described in the next paragraph.

2. Technology description and thermodynamic analysis

The main power blocks that compose the power plant are depicted in Fig 1. A detailed thermodynamic analysis of the EFGT is described in Ref. [20], while a similar EFGT-ORC combined cycle coupled to a CSP section is proposed in [21]. However, in the last configuration, the solar input is used to feed the topping gas turbine in combination to biomass fuel. The overall cycle pressure ratio of the EFGT is 12 and the TIT is 800 °C, which allows a low cost for the heat exchanger material (steel). Combustion air in the biomass furnace is taken from the ambient for a more flexible regulation, since the circuit of the working

air flowing into the turbine and the circuit of the combustion air flowing into the furnace are decoupled. The rated LHV input produced by the biomass combustion is 9050 kW, the net electric power output is 1388 kW while the available heat flow at the turbine exit is equal to 4093 kWt at 390°C. Therefore, the temperature of the Hot Tank of the TES has been accommodated to 370°C. The available heat of the air exiting the turbine is firstly recovered in the heat exchanger HRMSH (Heat Recovery Molten Salts Heater) where molten salts coming from the Cold Tank are heated up to 370°C and conveyed to the Hot Tank. The Cold Tank temperature, as explained in the following, has been assumed of 200°C.

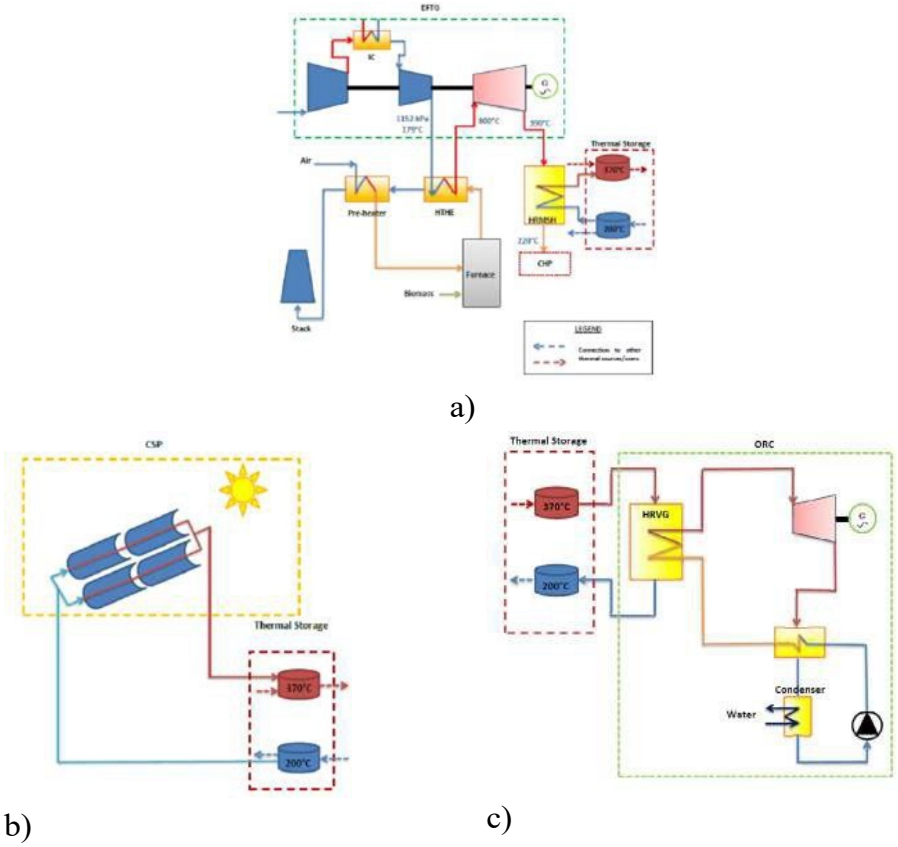

Fig 1. Plant layout of the power blocks that compose the plant. (a) EFGT; (b) CSP (c) ORC.

Therefore, at rated operating conditions, considering a unitary value of heat capacity ratio between air flow and molten salts flow, and assuming ΔT of 20°

at both the hot and the cold ends of the HRMSH, the thermal flow that can be recovered in the HRMSH is 1890 kW from the biomass EFGT. Under such conditions air has still a temperature of 220°C and its sensible heat can be further recovered for cogeneration. The required area of the solar field is evaluated assuming a standard direct normal irradiance (DNI) of 800 W/m2. The solar-collector section is based on ENEA technology of PTCs [22] [23][24][25] as from figure 2(b). Although this technology allows for temperature up to ~550 °C, in this work a lower temperature of about 370°C is considered in order to meet the temperature of the Hot Tank of the thermal storage. The CSP consists of a line with six collectors connected in series. This length, about 600 meters, is necessary to allow the Heat Transfer Fluid (HTF) to increase its temperature of 170°C (from 200°C to 370°C) under normal operating conditions of flow and irradiation. The solar collector field is sized to supply 900 kWt that is the 33% of the total rated thermal input to the ORC plant. The TES section is a two-tank molten-salt system, where the temperature difference between the two tanks is moderately higher than conventional systems that use oil as HTF (170 °C instead of 100 °C) and therefore allows for a lower volume of the two tanks [26]. A mixture of molten salts (lithium, sodium and potassium nitrates) is chosen for both the HTF and the TES medium. These salts freeze at about 120°C and are liquid at temperatures higher than 200 °C [26]. For this reason, a temperature of 200°C is assumed for the cold tank. The molten salts flow in the solar field during normal operation but also at night, recycled from the cold tank. The system's heat losses are generally limited, and the fluid will cool only a few degrees. In the event of a lack of heating from the sun, the temperature can be restored using some heaters inside the two tanks. The technical specifications of the solar field under two different scenarios of the TES capacity are reported in Table 1, where the solar multiple represents the ratio of the solar-field thermal energy output to the total thermal energy demand (at design point conditions) from the bottoming ORC cycle. The required ground area is estimated assuming a distance between collector lines of 2.5 times the PTC aperture size. In the first considered scenario

one collector line was adopted and the amount of energy stored in the TES allows 6 hours of further production (SM 1.96). In the second case, two lines have been adopted and the amount of energy available in the TES allows 18 hours of further production (SM 3.9). The TES capacity is sized to account only for the fluctuations of the thermal input coming from the solar section. The EFGT input heat to the TES feeds directly the ORC, with the assumed baseload operation, hence it does not imply a TES sizing.

In this paper, the Hottel model is adopted for evaluating the average monthly reduction coefficient of the direct normal irradiance DNI, (kWh/m^2 month). The site of Priolo Gargallo (Siracusa, Italy, Latitude 37°08'04", Longitude 15°03'00", 30 m a.s.l., solar collector positioning N-S) has been selected, resulting in a DNI of 2,256 kWh/m^{2}yr and an effective radiance of 1,760 kWh/m^{2}yr. Adopting the methodology proposed in Ref.[27], the useful solar thermal power output is 3,978 and 7,956 MWh/yr for the two assumed CSP sizes (Cases B and C in Table 3, respectively).

Solar field characteristics		
Case study	**B**	**C**
Intercepting area (m^2)	3,228	6,457
Required ground area (m^2)	8,071	16,142
Thermal power output (MW)	1.808	3.616
Solar thermal power available for TES (MW)	0.887	2.6956
Design TES capacity (MWh)	5.178	16.02
Design TES discharge hours	5.48	16.96

Table 1. Design characteristics of the solar field and the thermal storage

The bottoming ORC recovers heat from molten salts flowing from the Hot Tank to the Cold Tank of the TES, with the adoption of a Heat Recovery Vapour Generator (HRVG) (Figure 2c). Since the heat is available at high temperature (from 370 to 200 °C) a recuperative configuration is chosen for the cycle. In particular, the cycle contains a pump (6-1) that supplies the fluid to the recuperator (1-2). The recuperator pre-heats the working fluid using the thermal

energy from the turbine outlet. The HRVG produces the evaporation of the organic fluid up to the requested condition of the turbine inlet (2-3), by recovering the heat from the molten salts. Then, the vapour flows in the turbine (3-4) connected to the electric generator. At the exit of the turbine, the organic fluid goes to the hot side of the recuperator (4-5) where it is cooled before entering the condenser. Finally, the condenser closes the cycle (5- 6). Considering the operating temperature range of the molten salts, toluene is a suitable working fluid for the ORC cycle since it shows a relatively high critical temperature. Subcritical cycles are firstly examined, considering both saturated and superheated cycles. The T-s diagrams of a saturated cycle and a superheated one, having the same evaporation pressure, are shown in Figures 3(a) and 3(b), respectively. In both figures, the lines representing molten salts flowing in the HRVG and cooling water flowing in the condenser are indicated. The comparison of the two cycles in Figure 2, shows that the saturated cycle is characterized by higher temperature difference between hot and cold side along the HRVG and by lower heat recovered in the recuperator. As a consequence, the heat exchange surfaces of both the HRVG and the recuperator are much lower for the saturated with respect to the superheated cycle. The ORC cycle is sized assuming Toluene working fluid with components efficiencies as reported in [25], condenser temperature of 40°C, $\text{Ä}T_{min}$ in the RHE of 25°C and ÄTmin in the HRVG of 20°C. Under such hypotheses, the efficiency of the ORC cycle increases with the evaporation pressure; however, over 10 bar, the increase is low. The cycle efficiency also increases with superheating. Therefore, the plant performance have been evaluated considering an evaporation pressure of 10 bar and a superheated vapor temperature of 350°C. The total amount of the thermal input to the ORC cycle has been estimated assuming that, at rated operating conditions, 70% of the thermal input comes from the EFGT and 30% from the solar field. In particular, it is supposed that the heat flow of 1,890 kWt recovered at rated power by molten salts in the HRMSH is entirely transferred to the organic fluid in the HRVG. The thermal input to the ORC cycle is then integrated

by the solar contribution of 900 kWt. Definitely, the total input to the ORC is 2790 kW and the electric power is 800 kWe.

3. Annual Energy Production

The annual energy output is estimated considering the two sizes of the TES (cases B and C) and compared to a plant without solar field (100% biomass fuel) as already examined in [20] (case A). The EFGT is supposed to be operated at baseload for all the time. The ORC plant, instead, is operated at baseload in case A while, in the cases B and C, the ORC is operated at full load when receiving heat from the EFGT and either CSP or TES. Instead the ORC is operated at 70% of full load when the stored thermal energy is over, and it receives heat only from the EFGT.

Case study	**A**	**B**	**C**
Biomass furnace (kW_t)	9,050	9,050	9,050
Biomass input (t/yr)	25,694	25,694	25,694
Topping EFGT net electric power (kW)	1,388	1,388	1,388
Bottoming ORC net electric power (kW)	700	800	800
Electric efficiency gas turbine	15.3%	15.3%	15.3%
Electric efficiency of the ORC (1)	21.5%	29%	29%
Solar share (solar/total energy input yearly basis)	0	6.9%	13.3%
Net electric generation (MWh/yr)	16,786	16,710	17,223
Equivalent operating hours (hr/yr)	8,039	7,568	7,805

(1). Ratio of electric power output and thermal power transmitted in the HRVG.
Case A: 100% biomass input; Cases B and C: CSP with different TES capacity

Table 2. Description of the three case studies considered in the present work

Part load efficiency reduction is neglected in this preliminary analysis. The rated electric power of the combined cycle in case A (only biomass fuel, Lower Heating Value: LHV=9050 kJ/kg) is 2,088 kWe (with bottoming ORC of 700 kW) while in case B and C (biomass + solar input as from table 3) the combined cycle net power output is 2,188 kWe (bottoming ORC of 800 kW).

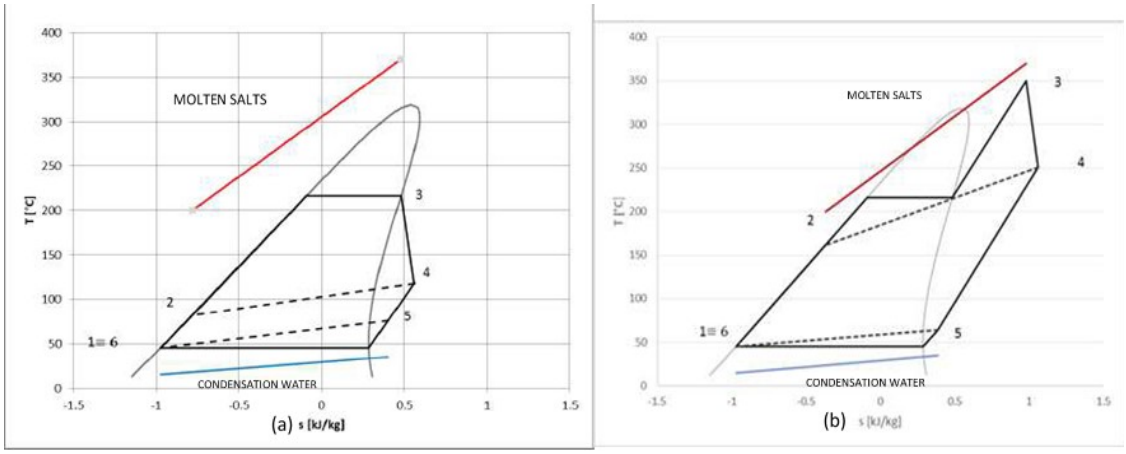

Figure 2. T-s chart for a saturated cycle (a) and a superheated one (b), fed by molten salts flowing from the Hot tank to the cold one.

The electric auxiliary consumption is 6%, and the thermal power output for CHP is of 963 kWt at 104 °C and 2106 kWt at 220 °C respectively for the case A and cases B and C. The modelling results report a net electric efficiency (electricity/input biomass energy at nominal solar energy input) of 23% for the 100% biomass. The energy generated is reported in Table 3. In all cases, the biomass energy input and the power output from the EFGT are the same.

4. Thermo-economic assumptions

A profitability assessment of the hybrid CSP-biomass combined EFGT-ORC CHP plant is proposed in this section. For each case study, a sensitivity analysis to the heat demand intensities and the biomass purchase price are considered. A basic strategy is assumed here of electricity fed into the grid, given that renewable CHP plants are eligible for feed-in tariffs in the Italian energy market. The financial appraisal of the investment is carried out assuming the following hypotheses: (i) 20 years of operating life and feed-in tariff duration for renewable electricity; no ‘re-powering’ throughout the 20 years; zero decommissioning costs, straight line depreciation of capital costs over 20 years; (ii) maintenance costs, fuel supply costs, electricity and heat selling prices held constant (in real

2017 values); (iii) cost of capital (net of inflation) equal to 5%, corporation tax neglected, no capital investments subsidies. Electricity is sold to the grid at the feed-in electricity price available in the Italian energy market [28], which is 180 and 296 Eur/MWh respectively for biomass electricity and CSP electricity [28]. The electricity generation is calculated at 8,040 operating hours per year. The further revenues from sales of cogenerated heat at high temperature (1890 kWt at 220°C) are here not considered, however they represent a significant increase of revenue in case of onsite heat demand availability. The turnkey costs are estimated by means of interviews and data collection from manufacturers of the selected technologies, as described in [20]. For the CSP section, PTCs and TES costs were derived from NREL cost figures [29], according to the lessons learnt from ENEA/Enel Archimede project [30]. In particular, unitary PTC costs of 250 Eur/m^2 and TES costs of 20 kEur/MWh are assumed. The Capex cost are assumed respectively 4,700 – 5,984 and 7,031 kEur for cases A, B and C, with specific investment costs respectively of 2.26, 2.51 and 2.95 kEur/kWe. The annual O&M costs are assumed 3.5% of the turnkey cost, biomass cost is 50 Eur/t and the ash discharge are accounted for assuming unitary cost of 70 Eur/t ash. Personnel costs are 268 kEur/yr [20].

5. Thermo-economic analysis results

Figure 3 reports on the energy performance (global electric efficiency and solar share) and Levelized Cost of Energy (LCE) at different biomass supply costs (in the case of electricity-only production) for the proposed case studies. The global electric efficiency is evaluated as the ratio between the annual electric energy production and the annual LHV energy input from biomass combustion. A comparison with the hybrid solar/biomass system configuration proposed in [21] where the solar input from the same typology of PTCs and TES is provided to the topping gas turbine at 550 °C reducing the biomass consumption, is also shown in Figure 3. The global electricity efficiency is the ratio of electricity annual sales and biomass energy input, while the solar share is the percentage of solar energy input on a yearly basis. The Net Present Value (NPV) and Internal

Rate of Return (IRR) as a function of the biomass supply cost, for electricity-only scenario, are reported in Figure 4.

The proposed hybridization of the biomass EFGT with CSP (Case B and C) presents comparable global electric efficiency (in comparison to only biomass - case A), while the LCE increases.

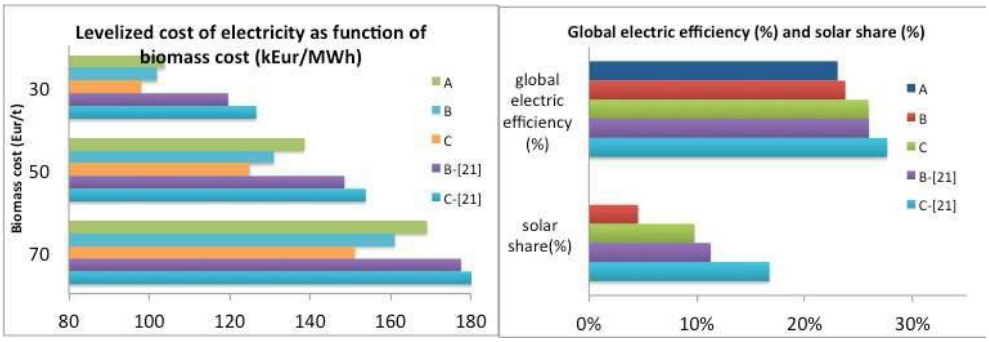

Figure 3. LCE as a function of the biomass purchase price (left) and energy balances as resulting from thermodynamic modelling (right) for Cases A, B and C and Cases B and C of ref [21]

In fact, the solar input increases the electricity generated via the bottoming ORC at fixed biomass supply cost but also increases the investment costs. Moreover, the trade-off between higher revenues from solar-based electricity and increased investment costs for the CSP and TES sections increases the NPV and IRR when the solar hybridization is considered, and this is more evident at low biomass supply costs. Moreover, increasing the size of CSP and TES (from case B to C) is beneficial for global energy efficiency balances, as expected, but also for investment profitability, due to the relatively low cost of the molten salt storage (in the proposed temperature range), in comparison to the increased revenues from solar electricity feed-in tariffs. These considerations are different from what reported in [21], where a different solar- biomass hybridization system was proposed. In that case, despite the higher solar share and electric efficiency, the LCE results higher and NPV, IRR are lower than in this configuration.

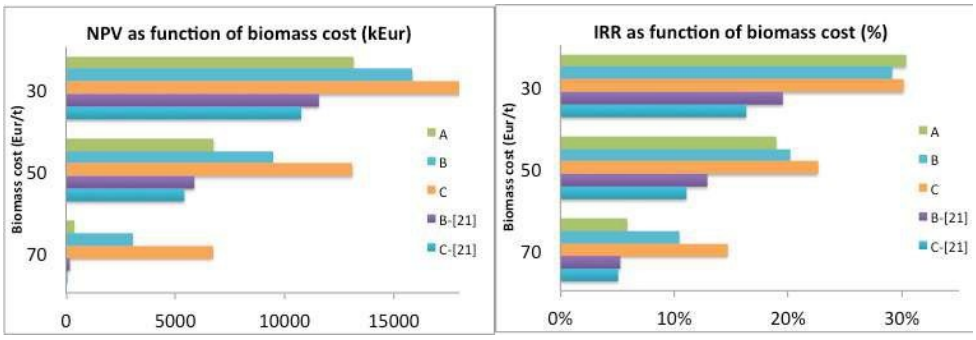

Figure 4. NPV (left) and IRR (right) for Cases A to C and Cases B and C of ref [21], as a function of biomass supply cost for electricity- only scenario

6. Conclusions

A thermodynamic and economic analysis has been performed on a hybrid (solar-biomass) combined cycle composed of an externally fired gas-turbine (EFGT) and a bottoming organic Rankine cycle (ORC) integrated by a linear parabolic trough collector field with molten salts as the heat transfer fluid. In order to improve the flexibility of the plant, a thermal storage recovers excess heat from the gas turbine and the solar field and transfers it to the ORC cycle and thermal end users, when requested. The thermal input of the gas turbine is about 9 MW, with a power output of 1.3 MW, while the bottoming organic Rankine cycle has electric output of 700 or 800 kW with or without the solar hybridization configuration. The thermodynamic modelling has been performed assuming two CSP sizes, and the energy performance results report higher global conversion efficiencies when using CSP integration and the thermo-economic analysis reports a higher NPV of the investment when integrating solar energy, due to the increased electric generation and higher value of solar-based electricity.. A comparison with a previously proposed solar/biomass hybridization with higher temperature (550°C) of CSP working fluid and direct solar energy input to the topping gas turbine demonstrates the higher profitability of this system configuration. Another advantage of this configuration, not been highlighted in this economic analysis, is the availability of high-grade heat for cogeneration

from the bottoming ORC, that could make the difference when a proper heat demand is available.

References

[1] Liu, M., Steven Tay, N. H., Bell, S., Belusko, M., Jacob, R., Will, G., … Bruno, F. (2016). Review on concentrating solar power plants and new developments in high temperature thermal energy storage technologies. Renewable and Sustainable Energy Reviews, 53, 1411–1432.

[2] Anuradha Mishra M, Chakravarty N, Kaushika N. Thermal optimization of solar biomass hybrid cogeneration plants. J Sci Ind Res 2006;65(4):355–63.

[3] Srinivas, T., & Reddy, B. V. (2014). Hybrid solar-biomass power plant without energy storage. Case Studies in Thermal Engineering, 2, 75–81.

[4] Vidal, M., & Martin, M. (2015). Optimal coupling of a biomass based polygeneration system with a concentrated solar power facility for the constant production of electricity over a year. Computers and Chemical Engineering, 72, 273–283.

[5] Pérez Á, Torres N. Solar parabolic trough e biomass hybrid plants: a cost efficient concept suitable for places in low irradiation conditions. In: Solar-PACES conference 2010.

[6] Schnatbaum L. Biomass utilization for Co firing in parabolic trough power plants. In: SolarPACES conference 2009.

[7] Amoresano, A., Langella, G., & Sabino, S. (2015). Optimization of solar integration in biomass fuelled steam plants. Energy Procedia, 81, 390–398.

[8] Peterseim JH, Tadros A, White S, Hellwig U, Klostermann F. Concentrated solar power/energy from waste hybrid plants e creating synergies. In: SolarPACES conference 2012.

[9] European Concentrated Solar Thermal Road-Mapping (2005), SES6-CT-2003-502578, DLR http://www.promes.cnrs.fr/uploads/pdfs/ecostar/ECOSTAR.Roadmap.pdf

[10] Pantaleo, a., Pellerano, a., & Carone, M. T. (2009). Potentials and feasibility assessment of small scale CHP plants fired by energy crops in Puglia region (Italy). Biosystems Engineering, 102(3), 345–359. doi:10.1016/j.biosystemseng.2008.12.002

[11] Riccio, G., & Chiaramonti, D. (2009). Design and simulation of a small polygeneration plant cofiring biomass and natural gas in a dual combustion micro gas turbine (BIO_MGT). Biomass and Bioenergy, 33(11), 1520–1531.

[12] Pantaleo, A. M., Camporeale, S. M., & Shah, N. (2013). Thermo-economic assessment of externally fired micro-gas turbine fired by natural gas and biomass : Applications in Italy. Energy Conversion and Management, 75, 202–213.

[13] Pantaleo, A. M., Camporeale, S., & Shah, N. (2014). Natural gas–biomass dual fuelled microturbines: Comparison of operating strategies in the Italian residential sector. Applied Thermal Engineering, 71(2), 686–696.

[14] Camporeale S, Turi F, Torresi M, Fortunato B, Pantaleo A, Pellerano A (2015) Part load performances and operating strategies of a natural gas-biomass dual fuelled microturbine for CHP operation, Journal for Engineering for Gas Turbines and Power, 137(12)

[15] Barsali S; Giglioli R; Ludovici G; Poli D. (2011). A micro combined cycle plant for power generation from solid biomass: coupling EFMGT and ORC. In 19th European Biomass Conference. Berlin: ETA-WIP,

[16] Bagdanavicius, A., Sansom, R., Jenkins, N., & Strbac, G. (2012). Economic and exergoeconomic analysis of micro GT and ORC cogeneration systems. In ECOS 2012 (pp. 1–11).
[17] OA Oyewunmi, AI Taleb, AJ Haslam, CN Markides (2014). An assessment of working-fluid mixtures using SAFT-VR Mie for use in organic Rankine cycle systems for waste-heat recovery, Computational Thermal Sciences 6 (4) 301-316.
[18] OA Oyewunmi, AI Taleb, AJ Haslam, CN Markides (2016). On the use of SAFT-VR Mie for assessing large-glide fluorocarbon working-fluid mixtures in organic Rankine cycles, Applied Energy 163, 263-282. doi:10.1016/j.apenergy.2015.10.040
[19] OA Oyewunmi and CN Markides (2016). Thermo-Economic and Heat Transfer Optimization of Working-Fluid Mixtures in a Low- Temperature Organic Rankine Cycle System, Energies 9 (6), 448:1-21;
[20] Camporeale S, Pantaleo A, Ciliberti P, Fortunato B, Cycle configuration analysis and techno-economic sensitivity of biomass externally fired gas turbine with bottoming ORC, Energy Conversion and Management 105 (2015) 1239–1250
[21] A. Pantaleo, S. Canporeale, A. Miliozzi, V. Russo, C. Markides, N. Shah Novel hybrid CSP-biomass CHP for flexible generation:Thermo-economic analysis and profitability assessment, (2017) Applied Energy, in press; DOI 10.1016/j.apenergy.2017.05.019
[22] ENEA Working Group. Solar thermal energy production: guidelines and future programmes of ENEA. ENEA Report. Available at http://www.solaritaly.enea.it/Documentazione/Documentazione.php; 2001.
[23] Technology Roadmap. Concentrating Solar Power, International Energy Agency, 2010
[24] Giannuzzi, G.M.; Majorana, C.E.; Miliozzi, A.; Salomoni, V.A.L.; Nicolini, D. (2007), Structural design criteria for steel components of parabolic-trough solar concentrators. Journal of Solar Energy Engineering, Vol. 129, 382-390.
[25] V.A. Salomoni, C.E. Majorana, G.M. Giannuzzi, A. Miliozzi, D. Nicolini (2010), New Trends in Designing Parabolic trough Solar Concentrators and Heat Storage Concrete Systems in Solar Power Plants, Solar Energy, Radu D Rugescu (Ed.), ISBN: 978-953-307- 052-0, InTech.
[26] Herrmann, U.; Kelly, B.; Price, H. (2004). Two-tank molten salt storage for parabolic trough solar power plants. Energy, Vol. 29, No. 5-6, 883-893.
[27] V. Russo , CSP Plant Thermal-hydraulic Simulation, Energy Procedia, Volume 49, 2014, Pages 1533-1542, Proceedings of the SolarPACES 2013 International Conference
[28] Italian Ministry of Economic Development, Incentives for energy from electric not-photovoltaic renewable sources, Legislative decrees of 07.06.2016
[29] Turchi, C., “Parabolic Trough Reference Plant for Cost Modeling with the Solar Advisor Model (SAM),” Technical Report, NREL/TP 550-47605, July 2010.
[30] Archimede solar power plant, https://en.wikipedia.org/wiki/Archimede_solar_power_plant

PAPER 2

Parametric multi-objective optimization of an Organic Rankine Cycle with thermal energy storage for distributed generation

Elio Antonio Bufi[a], Sergio Camporeale[a],*, Francesco Fornarelli[a], Bernardo Fortunato[a], Antonio Marco Pantaleo[b], Arianna Sorrentino[a], Marco Torresi[a]

[a]*Department DMMM, Polytechnic University of Bari, Via Orabona 4, 70125 Bari, Italy*
[b]*Department of Agro-environmental sciences, University of BariVia Amendola 165/A, 70125 Bari, Italy*

Division of work among authors

Thermodynamic calculations have been done by Arianna Sorrentino (AS) in collaboration with Sergio M. Camporeale (SC). Elio Bufi (EB) was responsible for optimization algorithm of the ORC in cooperation with AS. Antonio M. Pantaleo (AP) carried out the economical appraisal. The paper was written by EB with the help of AS. Comments and supervision were provided by SC, Francesco Fornarelli, Bernardo Fortunato and Marco Torresi

Abstract

This paper focuses on the thermodynamic modelling and parametric optimization of an Organic Rankine Cycle (ORC) which recovers the heat stored in a thermal energy storage (TES). A TES with two molten-salt tanks (one cold and one hot) is selected since it is able to operate in the temperature range useful to recover heat from different sources such as exhaust gas of Externally Fired Gas Turbine (EFGT) or Concentrating Solar Power (CSP) plant, operating in a network for Distributed Generation (DG). The thermal storage facilitates a flexible operation of the power system operating in the network of DG, and in particular allows to compensate the energy fluctuations of heat and power demand, increase the capacity factor of the connected plants, increase the dispatchability of the renewable energy generated and potentially operate in load following mode. The selected ORC is a regenerative cycle with the adoption of a Heat Recovery Vapour Generator (HRVG) that recovers heat from molten salts flowing from the Hot Tank to the Cold Tank of the TES. By considering the properties of molten salt mixtures, a ternary mixture able to operate between 200 and 400 °C is selected. The main ORC parameters, namely the evaporating pressure/temperature and the evaporator/condenser pinch point temperature differences, are selected as variables for the thermodynamic ORC optimization. An automatic optimization procedure is set up by means of a genetic algorithm (GA) coupled with an in-house code for the ORC calculation. Firstly, a mono-objective optimization is carried out for two working fluids of interest (Toluene and R113) by maximization of the cycle thermal efficiency. Afterwards, a multi-objective optimization is carried out for the fluid with the best performance by means of a Non-dominated Sorting Genetic Algorithm (NSGA) in order to evaluate the cycle parameters which maximize the thermal efficiency and minimise the heat exchanger surface areas. Toluene results able to give the best trade- off between efficiency and heat exchanger dimensions for the present application, showing that by with respect to the best efficiency point, the heat exchange area can be reduced by 36% with only a penalty of 1% for the efficiency.

Keywords: ORC; Organic Rankine Cycle, thermal energy storage, molten salts, optimization; genetic algorithm, distributed generation

1. Introduction

Due to the current environmental needs, the European Commission has set for 2030 new targets aiming at improving the energy efficiency and reducing the greenhouse gas emissions [1]. In order to achieve these targets, the spreading of renewable energy plays a central role, together with the continuous improving of component efficiency [2]. The intermittency characteristic of renewable sources (such as solar, wind) introduces the need of managing the energy production by means of energy storage devices. Thus, in the last years the development of TES coupled with CSP represents a key topic in the scientific community [3], [4]. Indeed, CSP with TES devices are suitable to be integrated in distributed generation (DG) networks composed by different power blocks that can supply heat, power or both, as described in Figure 1. In this paper, the CSP plant is supposed to be integrated by an Externally Fired Gas Turbine (EFGT) fed by biomass. A potential candidate for recover energy from the thermal energy storage and convert it in electric energy is the ORC technology (Figure 2). To convert most efficiently the thermal input of the TES in electric power, we assume that the ORC generates only electric power. However, note that all the methodologies applied to this system can be easily extended to a different configuration that includes also heat generation.

In ORC applications, the choice of the cycle parameters is of importance for improving the thermal efficiency and the exploitation of the thermal source. On the other hand, the expander and heat exchanger sizes influence the overall cost of the plant and a trade-off study for increasing efficiency and minimizing costs should be carried out. In this framework, the multi-objective optimization has gained interest as an efficient tool able to evaluate the best parameter configuration in the assigned design limits.

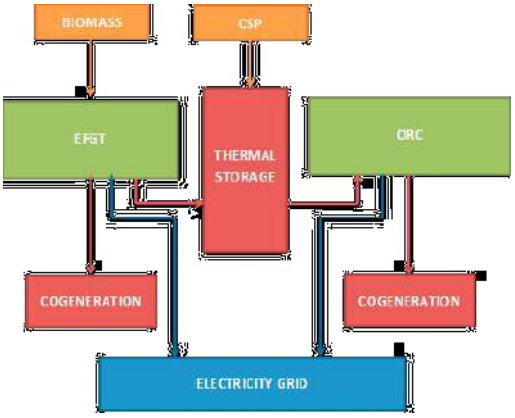

Figure 1 - Power blocks of the distributed heat and power plant

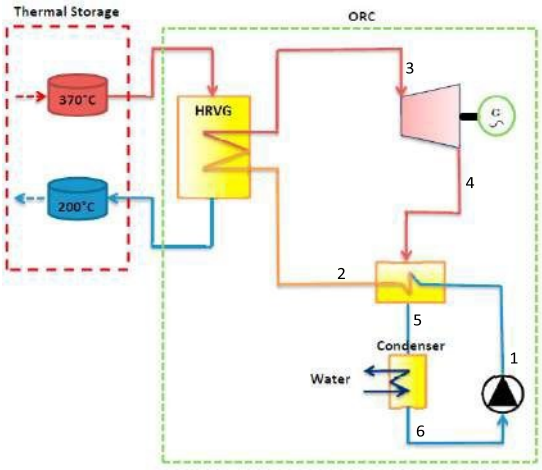

Figure 2 - ORC plant connected to TES

Especially, the Non-dominated Sorting Genetic Algorithm (NSGA) [5] has been implemented in several thermo-economic analysis and parameter selection for ORC applications. Muhammad et al. [6] performed a multi-objective optimization of an ORC evaporator for low temperature geothermal heat source by minimizing the costs and the pressure drop. Aiming to improve the performance of the HRVG, numerical simulation of the flow through the banks can give a significant contribution [7]. The primary geometrical parameters of evaporator were selected as decision variables which included length, width and plate spacing. Muhammad et al. [8] showed the results of a thermo-economic optimization for a regenerative ORC for waste heat recovery applications. Maximum thermal efficiency and minimum specific investment cost were selected as objective functions and relative increase in thermal efficiency and cost were analyzed. In the mono-objective optimization framework, Wang et al. [9] applied a genetic algorithm to improve the system performance of an ORC for different working fluids, whereas Xi et al. [10] examined the performances of three different cycle configurations with six working fluids by using exergy efficiency as the objective function to maximize.

The paper is organised as follows: Chapter 2 describes the technologies adopted for the plant, including EFGT, solar plant and thermal storage and gives the

thermodynamic analysis of the regenerative ORC plant assumed as reference first solution. Then, in Chapter 3, a preliminary mono-objective optimization by means of a genetic algorithm is carried out for the ORC plant, considering two fluids of interest: toluene and R113. By maximizing the thermal efficiency, the best set of cycle parameters (i.e. evaporation pressure, superheating and pinch point temperature difference in the evaporator) is evaluated. In Chapter 4, the fluid that shows the best efficiency is selected to perform a multi-objective optimization with NSGA in order to maximize the thermal efficiency and minimize the total surface area of the heat exchangers. An in-house code has been developed to calculate the regenerative ORC performance by implementing the CoolProp [11] libraries for the fluid properties calculation.

2. Technology description and hypotheses for the thermodynamic analysis

The detailed thermodynamic analysis of the EFGT is described in Ref. [12] and [13]. The EFGT is fed by biomass which produces a thermal input of 9050kWt at the rated LHV and produces a net electric power output of 1388kW while the available heat flow at the turbine exit is equal to 4093 kWt at 390°C. Therefore, the temperature of the Hot Tank of the TES has been accommodated to 370°C. The amount of thermal energy that can be recovered is 1890 kWt. The sensible heat can be further recovered for cogeneration, since the exiting air has still a temperature of 220°C.

The solar collector field is sized to supply 900 kWt and is based on ENEA technology of parabolic-trough concentrators (PTCs)[16][17][18][19].

Table 1 Basic calculation hypotheses for the ORC plant

Description	Value
Pump Isentropic Efficiency	0.75
Pump Mechanical Efficiency	0.96
Turbine Isentropic Efficiency	0.80
Turbine Mechanical Efficiency	0.96
Condenser temperature	40°C

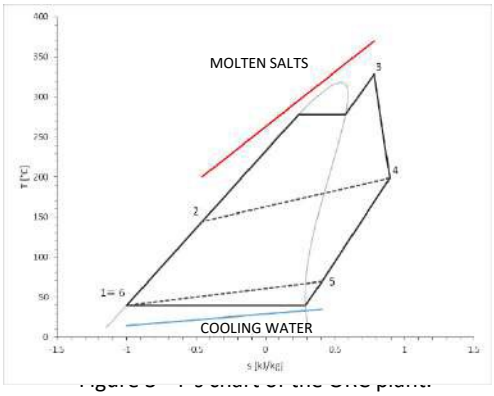

Although this technology allows for temperature up to about 550 °C, in this work a lower temperature of about 390°C is considered in order to meet the temperature of the Hot Tank of the thermal storage. Further details of the plant can be found in Ref. [20] The molten-salts mixture selected for the storage is composed by lithium salts, sodium and potassium nitrates. This mixture freezes at about 120°C and is liquid at temperatures higher than 200 °C [14]. For this reason, a temperature of 200°C is assumed for the cold tank. Under such hypotheses, the temperature difference between the two tanks is moderately higher than conventional systems that use oil as HTF (170°C instead of 100°C) and therefore allows for a lower volume for the two tanks [15].

The general calculation hypotheses for the ORC plant are summarized in Table 1. The total thermal input to the ORC has been assumed of 2790 kWt. The thermal power input is transferred to the organic fluid in the HRVG from the two-tank molten-salt system in the range 370-200°C. Since heat is available at high temperature, a recuperative configuration is chosen for the cycle. A T-s diagram of the cycle is shown in Figure 3, where the red and the blue lines indicate the molten salts flowing in the HRVG and cooling water in the condenser, respectively. In the following Chapter, a mono-objective parametric optimization is carried out in order to find the best plant efficiency point.

3. Mono-objective parametric optimization strategy with different working fluids

The working fluids of interest for ORC applications are characterized by heavy molecules, high thermal capacity and low boiling point. Thus, the thermodynamic behavior is quite complex and can be accurately described only by equations that account for real fluid effects. In this paper, two organic fluids have been chosen: toluene and R113. The main physical properties are listed in Table 2 in terms of molecular weight M, critical pressure and temperature (pc, Tc), ozone depletion potential (ODP) and global warming potential (GWP). The R113 is a refrigerant well known for its good performances in waste heat recovery [21], whereas toluene meets environmental and safety requirements. Besides, both fluids are chemically stable in

the range of temperature considered in this work, as shown by the maximum allowable temperature before decomposition Tmax (see Table 2).

Table 2. Working fluids physical properties

Fluid	M [kg/kmol]	p_c [bar]	T_c [K]	T_{max} [K]	ODP	GWP
Toluene	92.14	41.26	591.75	700	0	0
R113	187.38	33.92	487.21	787.5	0.9	6130

The parametric optimization of the ORC and the evaluation of the optimal set of the parameters of interest is performed in two steps by following the genetic (GA) and the Non-dominated Sorting Genetic (NSGA) algorithms for mono- and multi-objective optimization, respectively. In general, the genetic optimizations start from initial population, through genetic operator such as stochastic selection, mutation, crossover and evolve the population by selecting and combining the best individuals by following pre-defined selection criteria. During this process, the optimization parameters are varied until the global optimal value of the objective is found [4].

The mono-objective optimization by means of the genetic algorithm (GA) of the regenerative ORC is carried out with Toluene and R113 in order to maximize only the cycle thermal efficiency

$$\eta_I = \frac{\dot{W}_{exp} - \dot{W}_{pump}}{\dot{Q}_{in}} \quad (1)$$

where $\dot{W}_{exp}$ and $\dot{W}_{pump}$ are the expander shaft output power and pump input power, respectively, taking into account the isentropic and mechanical efficiencies defined in Table 1, while $\dot{Q}_{in}$ is the thermal input flow provided by the molten salts.

The fluid that provides the best performance, after the mono-objective optimization, is selected to perform the multi- objective optimization by means of the NSGA by maximizing $\eta_I$and minimizing $(UA)_{TOT} = (UA)_{HRVG}+(UA)_{RHE} = \dot{Q}_{in}/\Delta T_{lm,HRVG} + \dot{Q}_{in}/\Delta T_{lm,RHE}$, where U and A are the thermal conductivity and surface area of the heat exchangers, respectively, and ΔT_{lm} the log mean temperature difference for the HRVG and RHE.

The optimization parameters are: the evaporation pressure p_{ev}, superheating $\Delta T_{TIT} = T_{TIT} - T_{ev}$ (where T_{TIT} is the turbine inlet temperature), and pinch point temperature difference for the HRVG, ΔT_{pp} .

The search for the optimal parameter set is carried out with the following constraints: $0.4p_c \leq p_{ev} \leq 0.9p_c$, $0 \leq \Delta T_{TIT} \leq T_{hot\,tank} - T_{ev}$, $7K \leq T_{pp} \leq 10K$, $\Delta T_{min,RHE} \leq 5K$. Along with the best values of thermal efficiency and equivalent overall heat exchanger surface areas UA, other quantities of interest are evaluated:

- the exergy (second law) efficiency

$$\eta_{II} = \frac{\dot{W}_{exp} - \dot{W}_{pump}}{\dot{Q}_{in}(1 - T_0/T_m)} \tag{2}$$

where T_0 is the ambient temperature and T_m is the log-mean temperature given by

$$T_m = \left(T_{salt,in} - T_{salt,out}\right)/ln\left(T_{salt,in}/T_{salt,out}\right)$$

with $T_{salt,in}$ and $T_{salt,out}$ the inlet and outlet molten salt temperature, respectively;

- turbine size parameter $SP = \dot{V}_{out}{}^{0.5}/\Delta h^{0.25}$ (where $\dot{V}_{out}$, Δh are the turbine exit volumetric flow rate and enthalpy drop, respectively);
- fluid mass-flow rate $\dot{m}_f$;
- expander volumetric expansion ratio $V_r = \dot{V}_{out}/\dot{V}_{in}$ between the outlet and inlet volumetric flow.

The mono-objective optimization results are listed in Table 3 for the different working fluids. Convergence has been reached after 11 generations for each fluid, by considering a population of 200 individuals for each generation. It can be noticed that the optimization action, for maximizing the thermal efficiency, is devoted to increase the evaporation pressure and decrease the pinch point temperature difference in order to better exploit the thermal source. The best performance for the present application is provided by the toluene, with a maximum thermal and exergy efficiency of 30.3% and 64.3%, respectively. The R113 provides a thermal efficiency lower than toluene by 5.6 percent points, whereas (UA)TOT is 3.3 times higher. This result is explained by the temperature-heat power diagram in Figure 4. The R113 fluid is characterized by a lower critical temperature than toluene, then a longer path for superheating is required, thus resulting in a higher superheater exchange area.

The electric generator losses are not considered in this analysis: depending on the technology they can be estimated equal to 5% of the turbine shaft power output; further energy losses are due to the electric consumption of auxiliary devices needed, e.g., for molten salts circulation, cooling water, evaporation tower, etc.; such losses can be roughly assumed equal to about 6% of the produced electric power.

Table 3. Mono-objective optimization results for the fluids of interest.

Fluid	p_{ev}	ΔT_{III}	ΔT_p	η_I	η_{II}	SP	V_r	$\dot{m}_f$	UA
	[bar]	[K]	[K]			[m]		$[kg/s]$	[kW/K]
Toluene	21.27	51.45	7.06	0.303	0.643	0.205	220.16	4.73	125.93
R113	29.88	144.79	7.04	0.286	0.606	0.108	31.04	13.04	417.41

For these reasons, in the following, the toluene is selected and analyzed for the multi-objective optimization.

4. Results

In Figure 5, the multi-objective optimization results are shown as non-dominated individuals on the Pareto front. Convergence has been checked on the euclidean distance between the centroids of two successive Pareto fronts, and reached after 100 generations with 200 individuals for each generation. The multi-objective optimization provides a trade-off between the cycle efficiency η_I and overall heat exchanger cost. Indeed, without considering constraints about the surface areas, the mono-objective optimization evaluated the best parameter set for the highest efficiency but, on the other hand, (UA)TOT resulted very high, as shown in Figure 5 by the black square.

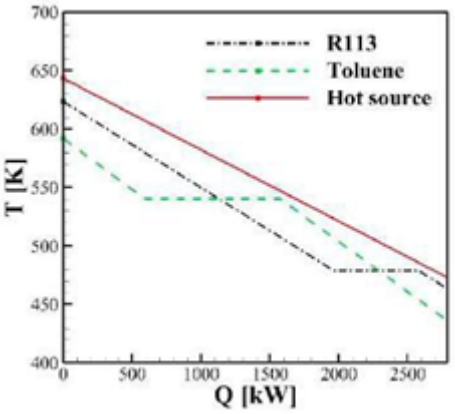

Figure 4. Temperature-Heat power diagram of the heat exchange in the HRVG for Toluene and R113 in the configuration optimized by mono-objective optimization (see Table 3).

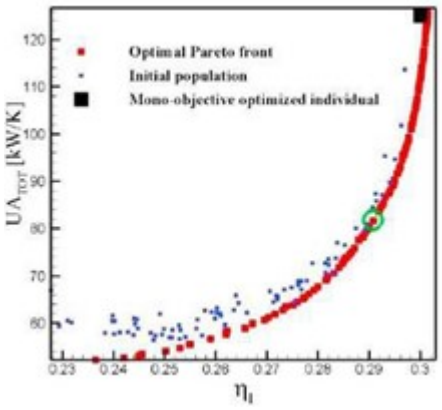

Figure 5. Pareto front (red squares) of the optimal individuals at convergence for the multi-objective optimization (fluid: Toluene). The initial population is marked with blue squares.

A compromise solution could be selected on the Pareto front (green circle in Figure 5) where the efficiency is only 1% lower than the mono- objective optimal individual, but $(UA)_{TOT}$ is reduced by 36%. Starting from this optimal configuration, it is possible to perform a sensitive analysis considering the parameter set of the multi-objective analysis shown in Table 4. In this paper, the effects of the evaporating pressure pev and and ΔT_{pp} on η_I and $(UA)_{TOT}$ are examined. Figure 5 shows that around the selected value pev =25.21 bar, efficiency η_I and $(UA)_{TOT}$ remain about constant. The increase of pev over 29 bar produces an increase of the thermal efficiency whereas (UA)REC increases very rapidly. For pev >32 bar (grey band), the value of ΔT_{rec} is lower than the value of 5K assumed as constraint in the optimisation search and for pev >35 bar there are no solutions since $(UA)_{REC}$ goes to infinity.

Fluid	p_{ev}	ΔT_{III}	ΔT_p	η_I	η_{II}	SP	V_r	$\dot{m}_f$	UA
	[bar]	[K]	[K]			[m]		[kg/s]	[kW/K]
Toluene	25.21	50.05	8.36	0.292	0.614	0.197	256.17	4.4	82.2

Table 4. Multi-objective optimization results for Toluene at the center of the Pareto front (green circle in Figure 4).

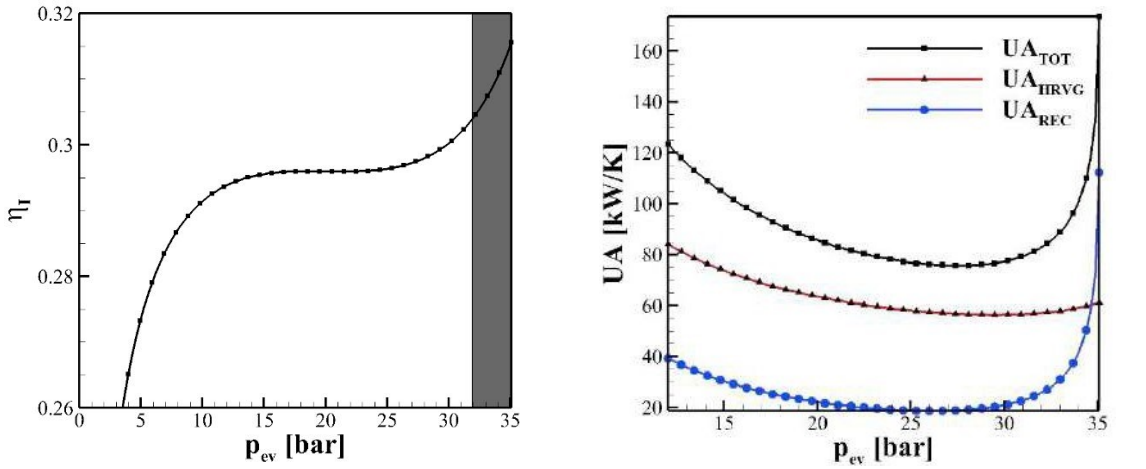

(a) (b)

Figure 6. Influence of the evaporating pressure on the thermal efficiency and total equivalent heat exchange areas

Figure 6 shows the effect of the pinch point temperature difference ΔTpp in the HRVG that has a key role on the ORC cost since it influences the heat exchanger size. By increasing ΔT_{pp} in the range 7-10 K there is a decrease of $(UA)_{TOT}$ up to 20%, with a decrease of thermal efficiency by 1%. For higher values of ΔT_{pp} the loss of efficiency is too high with a lower rate of decrease of $(UA)_{TOT}$.

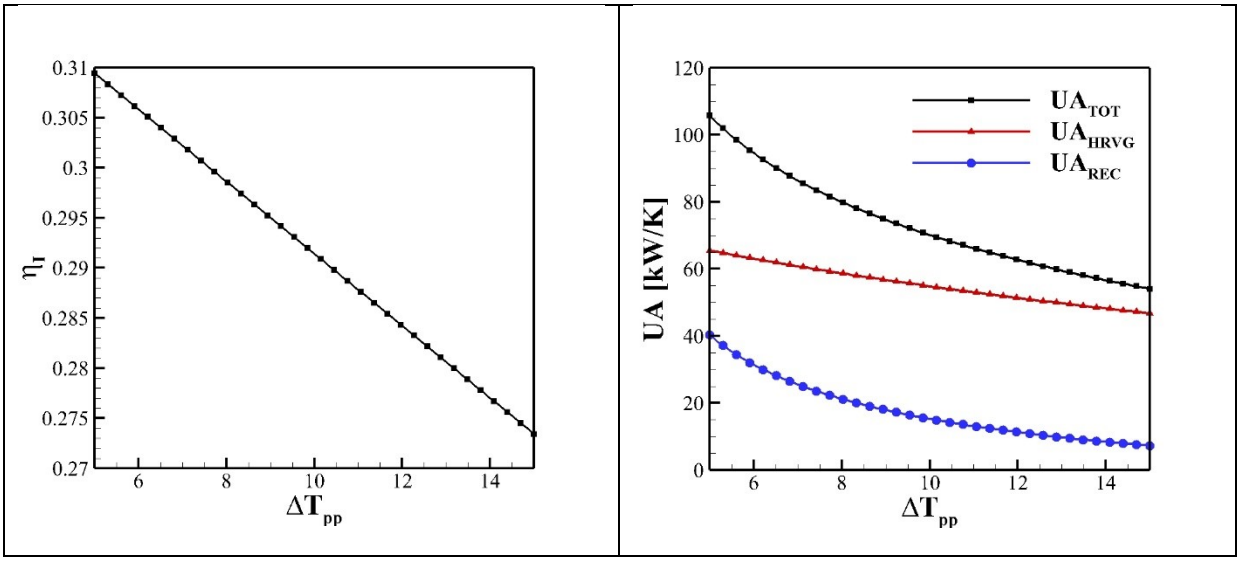

Figure 7. Influence of the pinch point temperature difference in the HRVG on the thermal efficiency and total equivalent heat exchange areas.

5. Conclusions

In this paper, a thermodynamic analysis, a mono-objective and multi-objective optimization have been performed on an Organic Rankine cycle (ORC) for Distributed Generation. The ORC plant is supposed to operate as power conversion unit of the energy stored in a two-tanks thermal energy storage, which operates in a range of temperatures from 200°C up to 350°C recovering heat from an Externally Fired Gas Turbine exhaust gas and a solar field.

The mono-objective optimization aimed to maximize the thermal efficiency by varying the evaporating pressure, pinch point temperature difference and the turbine inlet temperature. It has been done for two different organic fluids, Toluene and R113, and the results showed that the most performing fluid is Toluene with a maximum thermal efficiency η_I =30.3%. The multi-objective optimization by means of NSGA has been carried out for the Toluene, by maximizing η_I and minimizing the sum of $(UA)_{HRVG}$ and $(UA)_{RHE}$, showing that by reducing of 1% the efficiency the $(UA)_{TOT}$ is reduced by 36%.

Reference

[1] European Commission web site: http://ec.europa.eu/clima/news/articles/news_2014102401_en.htm accessed Nov 2014.

[2] Camporeale, S.M., Fortunato, B "Performance of a mixed gas-steam cycle power plant obtained upgrading an aero-derivative gas turbine" (1998) Energy Conversion and Management, 39 (16-18), pp. 1683-1692.

[3] Fornarelli, F., Camporeale, S.M., Fortunato, B., Torresi, M., Oresta, P., Magliocchetti, L., Miliozzi, A., Santo, G. "CFD analysis of melting process in a shell-and-tube latent heat storage for concentrated solar power plants",Applied Energy, 164 (2016), 711-722.

[4] Anuradha Mishra M, Chakravarty N, Kaushika N. Thermal optimization of solar biomass hybrid cogeneration plants. J Sci Ind Res 2006;65(4):355–63

[5] Deb, Kalyanmoy, et al. "A fast and elitist multiobjective genetic algorithm: NSGA-II." IEEE transactions on evolutionary computation 6.2 (2002): 182-197.

[6] Imran, Muhammad, et al. "Multi-objective optimization of evaporator of organic Rankine cycle (ORC) for low temperature geothermal heat source." Applied Thermal Engineering 80 (2015): 1-9.

[7] Torresi M, Saponaro A, Camporeale SM, Fortunato B (2008). CFD analysis of the flow through tube banks of HRSG. In: Proceedings of the ASME Turbo Expo 2008: Power for Land, Sea and Air, June 9-13, 2008, Berlin, Germany, GT2008-51300

[8] Imran, Muhammad, et al. "Thermo-economic optimization of Regenerative Organic Rankine Cycle for waste heat recovery applications." Energy Conversion and Management 87 (2014): 107-118.

[9] Wang, Jiangfeng, et al. "Thermodynamic analysis and optimization of an (organic Rankine cycle) ORC using

low grade heat source." Energy 49 (2013): 356-365.

[10] Xi, Huan, et al. "Parametric optimization of regenerative organic Rankine cycle (ORC) for low grade waste heat recovery using genetic algorithm." Energy 58 (2013): 473-482.

[11] Bell, Ian H., et al. "Pure and pseudo-pure fluid thermophysical property evaluation and the open-source thermophysical property library CoolProp." Industrial & engineering chemistry research 53.6 (2014): 2498-2508.

[12] Camporeale S, Pantaleo A, Ciliberti P, Fortunato B, Cycle configuration analysis and techno-economic sensitivity of biomass externally fired gas turbine with bottoming ORC, Energy Conversion and Management 105 (2015) 1239–1250

[13] Camporeale SM, Ciliberti PD, Fortunato B, Torresi M, Pantaleo AM, (2015). Externally Fired Micro Gas Turbine and ORC Bottoming Cycle: Optimal Biomass/Natural Gas CHP Configuration for Residential Energy Demand, In: Proceedings of ASME Turbo Expo 2015: Power for Land, Sea and Air, June 15-19, 2015, Montréal, Canada,GT2015-43571.

[14] ENEA Working Group. Solar thermal energy production: guidelines and future programmes of ENEA. ENEA Report. Available at http://www.solaritaly.enea.it/Documentazione/Documentazione.php; 2001.

[15] Italian Ministry of Economic Development, Incentives for energy from electric not-photovoltaic renewable sources, Legislative decrees of 07.06.2016

[16] Turchi C, Mehos M, Ho C M, Holb G J, (2010) Current and future costs for parabolic trough and power tower systems in the US market, SolarPaces 2010, Perpignan, FR, September 21-24

[17] Giannuzzi, G.M.; Majorana, C.E.; Miliozzi, A.; Salomoni, V.A.L.; Nicolini, D. (2007), Structural design criteria for steel components of parabolic-trough solar concentrators. Journal of Solar Energy Engineering, Vol. 129, 382-390

[18] V.A. Salomoni, C.E. Majorana, G.M. Giannuzzi, A. Miliozzi, D. Nicolini (2010), New Trends in Designing Parabolic trough Solar Concentrators and Heat Storage Concrete Systems in Solar Power Plants, Solar Energy, Radu D Rugescu (Ed.), ISBN: 978-953-307-052-0, InTech.

[19] Herrmann, U.; Kelly, B.; Price, H. (2004). Two-tank molten salt storage for parabolic trough solar power plants. Energy, Vol. 29, No. 5-6, 883-893.

[20] Antonio M. Pantaleo, Sergio M. Camporeale, Adio Miliozzi, Valeria Russo, Nilay Shah, Christos N. Markides, Novel hybrid CSP-biomass CHP for flexible generation: Thermo-economic analysis and profitability assessment, Applied Energy, 2017, ISSN 0306-2619, http://dx.doi.org/10.1016/j.apenergy.2017.05.019.

[21] Badr, O., P. W. O'callaghan, and S. D. Probert. "Rankine-cycle systems for harnessing power from low-grade energy sources." Applied Energy 36.4 (1990): 263-292.

[22] ENEA Working Group. Solar thermal energy production: guidelines and future programmes of ENEA. ENEA Report. Available at http://www.solaritaly.enea.it/Documentazione/Documentazione.php; 2001.

PAPER 3

Hybrid solar-biomass combined Brayton/organic Rankine- cycle plants integrated with thermal storage: Techno- economic feasibility in selected Mediterranean areas

Antonio M Pantaleo[1,4,5]1, Sergio M Camporeale[2], Arianna Sorrentino[2], Adio Miliozzi[3], Nilay Shah[4], Christos N Markides[4,5]

1. Dipartimento DISAAT, Università degli Studi di Bari, Via Amendola 165/A 70125 Bari, Italy
2. Department , Polytechnic University of Bari, Via Orabona 4, 70125 Bari, Italy
3. Energy Technologies Department, ENEA, Casaccia Research Centre, Via Anguillarese, 301. 00123 S.M. di Galeria, Rome, Italy
4. Centre for Process Systems Engineering (CPSE), Imperial College London, South Kensington Campus, SW7 2AZ, London, UK
5. Clean Energy Processes (CEP) Laboratory, Imperial College London, South Kensington Campus, SW7 2AZ, London, UK

Division of work among authors

Thermodynamic calculations and energy balance have been done by Arianna Sorrentino (AS) in collaboration with Sergio M. Camporeale (SC). Adio Miliozzi (AM) was responsible for dimensioning and calculation of the solar plant. AS in cooperation with Antonio M. Pantaleo (AP) carried out the economical appraisal. The paper was written by AS and AP with the help of SC. Comments and supervision were provided by SC, Nilay Shah and Christos N. Markides.

Abstract

This paper presents a thermodynamic analysis and techno-economic assessment of a novel hybrid solar- biomass power-generation system configuration composed of an externally fired gas-turbine (EFGT) fuelled by biomass (wood chips) and a bottoming organic Rankine cycle (ORC) plant. The main novelty is related to the heat recovery from the exhaust gases of the EFGT via thermal energy storage (TES), and integration of heat from a parabolic-trough collectors (PTCs) field with molten salts as a heat-transfer fluid (HTF). The presence of a TES between the topping and bottoming cycles facilitates the flexible operation of the system, allows the system to compensate for solar energy input fluctuations, and in- creases capacity factor and dispatchability. A TES with two molten salt tanks (one cold at 200 o C and one hot at 370 o C) is chosen. The selected bottoming ORC is a superheated recuperative cycle suitable for heat conversion in the operating temperature range of the TES. The whole system is modelled by means of a Python-based software code, and three locations in the Mediterranean area are assumed in order to perform energy-yield analyses: Marseille in France, Priolo Gargallo in Italy and Rabat in Morocco. In each case, the thermal storage that minimizes the levelized cost of energy (LCE) is selected on the basis of the estimated solar radiation and CSP size. The results of the thermodynamic simulations, capital and operational costs assessments and subsidies (feed-in tariffs for biomass and solar electricity available in the Italian framework), allow estimating the global energy conversion efficiency and the investment profitability in the three locations. Sensitivity analyses of the biomass costs, size of PTCs, feed-in tariff and share of cogenerated heat delivered to the load are also performed. The results show that the high investment costs of the CSP section in the proposed size range and hybridization configuration allow investment profitability only in the presence of a dedicated subsidy framework such as the one available in the Italian energy market. In particular, the LCE of the proposed system is around 140 Eur/MWh (with the option to discharge the cogenerated heat) and the IRR is around 15%, based on the Italian electricity subsidy tariffs. The recovery of otherwise discharged heat to match thermal energy demand can significantly increase the investment profitability and compensate the high investment costs of the proposed technology.

Keywords: Biomass; Organic Rankine Cycle, concentrating solar panel, externally fired gas turbine.

1. Introduction

The increased utilization of renewable energy for the displacement of fossil-fuel consumption is an essential component of the transition to a low-carbon, sustainable energy future [76,77] and at the centre of the European Commission's 2030 energy strategy [1].

Solar and biomass are among the most widespread and promising renewable energy sources, however, solar energy is inherently intermittent and needs to be integrated with energy storage and programmable generation systems in order to match energy demand.

1.1. Literature review on hybrid solar-biomass and combined-cyle power plants

A hybrid Brayton solar/gas-fired plant in which a constant power output is ensured by natural-gas combustors was proposed in Ref. [2]. In this context, biomass can be an interesting alternative for compensating the fluctuations of solar energy. On the other hand, the necessity of a constant and reliable supply of biomass at an affordable price is one of the biggest challenges for the development of biomass power plants [3]. Hybridization of solar thermal with biomass combines two energy sources that complement one each other, both seasonally and diurnally [4]. Specifically, Hussain et al. [5] demonstrated that hybrid concentrating solar (CSP) and biomass power plants are technically viable alternatives to conventional fossil-fuelled plants. San Miguel at al. [6] used the life cycle assessment to highlight the environmental benefits of CSP hybridization by means of biofuels, instead of natural gas, including the environmental balances of biofuel production and transportation. The thermodynamic potential and a comparison of different types of solar-thermal collectors in the context of solar power-generation and cogeneration applications is considered in Ref. [78], where it is reported that the type of collector is strongly influenced by the characteristics of the solar resource. Parabolic trough collectors (PTCs) were found to be well suited to regions with good direct-solar irradiance conditions, but less so when diffuse irradiation accounts for a significant fraction of the total solar resource. Therefore, they are considered good options for hybridization, as they have good summer performance but poor performance at low

solar radiation levels, therefore offering promising options for integration with biomass energy during winter or during the night. Mishra et al. [7] compared various PTCs technologies in a solar biomass hybrid plant to choose the optimal one to match the thermal output. Nevertheless, the thermal inertia of biomass furnaces makes this technology suitable for base load operation but not for load-following options to meet variable energy demand. The integration of thermal energy storage (TES) can compensate these solar energy fluctuations and energy demand variations to overcome the individual drawbacks of solar and biomass as primary energy resources, thus facilitating smart and flexible operation strategies [8].

Organic Rankine cycle (ORC) technology is based on the Rankine cycle but employs organic working fluids and is particularly suit- able for the conversion of low-to-medium temperature heat [9] and for employment in small-to-medium scale applications [77]. Many thermodynamic and techno-economic feasibility studies on the employment of ORC technology in CHP applications have been reported in literature [10,79,80], including of working-fluid selection [11] and optimal cycle design, as well as studies specifically relating to solar applications [81,82], including with integrated TES [83,84]. Many ORC performance optimization methods have been proposed in literature. Conventional methods have been used in ORC optimization problems as in Ref. [12], where the steepest descendent method was adopted to minimize the ratio of total heat transfer areas and total net power. However, these methods are initialized in a way that can risk convergence to sub-optimal solutions. On the other hand, global optimization tools based on genetic algorithms (GAs) have been successfully adopted in heat transfer problems for their simplicity and robustness [13]. Xi et al. [14] analysed different ORC configurations with six working fluids adopting GA to maximize exergy efficiency, while Wang et al. [15] examined the effects of some thermodynamic design parameters on the power output and heat exchanger areas. Other ORC optimization problems have been solved by means of gradient-based methods [16], where a hybrid solar-biomass plant supplies heat to the ORC plant.

The performance of hybrid solar-biomass plant configurations under a variable solar input was studied by Srinivas & Reddy [17], who simulated a solar-biomass regenerative steam-Rankine cycle without TES, while Vidal & Martin [18] proposed the integration of biomass gasification in a CSP facility. In this case, the options of using syngas for hydrogen production and heat generation in a furnace, vs power generation in an open Brayton-cycle were compared, with the biomass section coupled to a tower-based CSP plant and a molten salt (MS) used as the heat transfer fluid (HTF). A general multi-criterion approach for selecting the most suitable CSP technology for hybridization with Rankine power plants using conventional (gas, coal) and alternative (biomass, wastes) fuels was suggested by Peterseim et al. [19], including key factors such as technology maturity, environmental impact, economics and site-specific solar yield. In Ref. [20], the same authors proposed a method for classifying CSP hybridization depending on the interconnections of the plant components, and including biomass, fossil fuel and geothermal sources. Other hybrid solar-biomass configurations are based on PTCs, backup boilers and Rankine cycles [21] using thermal oil as HTF [22] or MSs [23], the substitution of steam bleed regeneration with water preheating by solar energy [24] or Fresnel collectors [25] to increase temperatures. Some applications of CSP plants combined with gas turbines consider the use of solar towers or solar dishes with compressed air as HTF in internally fired cycle configurations [26]. More recently, Bai et al. [27] simulated a solar-biomass power generation system integrating a two-stage gasifier using two different types of solar col- lectors applied to drive thermochemical pyrolysis and gasification processes. In another study of interest, a mini hybrid CSP plant combining concentrating solar energy and biomass to drive an ORC was considered [28], in which PTCs were coupled to a biogas boiler used as backup. The results reported an improved annualized global electric efficiency with hybridization (from 3.4% to 9.6%). Integration of a PTC-based CSP to a CHP steam turbine was reported in Ref. [29], where a steam turbine plant was fed by sugarcane bagasse. Solar integration was considered for displacing the high- pressure steam extraction of a condensing-extraction steam turbine via feedwater preheating; operation in a

fuel-economy mode was employed to save bagasse during the harvesting period with use of the economized bagasse off-season. In this case, the hybridization of CSP with biomass allowed base-load generation, while solar thermal input facilitated the rational use of seasonal bagasse.

The use of biomass has been widely investigated in the literature as it provides added socio-economic and environmental benefits, especially when the organic by-products are also utilized [30]. In the case of small-to-medium scale CHP plants, this includes dual- fuelling of biomass and natural gas in externally/internally-fired gas turbines [31]. Applications in the tertiary and industrial sec- tors have been investigated in Ref. [32], while residential end-users have been analysed in Ref. [33]. The influence of part-load performance on optimal EFGT operation was investigated in Ref. [34], while the improved energy performance and profitability of bottoming ORCs has been investigated in different energy-demand segments from technical [35,80] and exergo-economic [36] points of view. The literature on ORC systems and working-fluid selection for waste-heat recovery is also extensive [37]. Oyewunmi et al. [38,39] analysed the effect of working-fluid mixtures on the efficiency and power output of ORC systems by using the molecular- based statistical associating fluid theory (SAFT), specifically, the SAFT-VR Mie equation of state for the prediction of the working- fluid properties (The interested reader can also refer to extensions of these approaches to a group-contribution version of SAFT referred to as SAFT-g Mie [85,86], which can be used for simultaneous working-fluid design and overall ORC system performance optimization). Economic analyses have also been performed by the same authors, in Ref. [40] in relation to the use of working-fluid mixtures, and in Ref. [87] in relation to supercritical cycles. More recently, Prattico' et al. [41] investigated a small solar-powered ORC plant in a rural application with a focus on optimizing the heat- source temperature, while a combined cycle with a 1.3 MW biomass EFGT topping cycle and 0.7 MW bottoming ORC plant was proposed in Ref. [42]. Furthermore, previous research from the same authors has addressed the integration of PTCs and molten salt TES with biomass

combustion in externally fired gas turbines (EFGT) [43], estimating the profitability of such hybridization options in the Italian energy policy framework.

1.2 Contents of innovation of the proposed plant

This paper progresses beyond the hybrid EFGT ORC system proposed in Ref. [43], presenting a novel CHP plant based on in- dependent "power blocks" (PBs), which comprise: electric power generation (gas turbine and ORC), thermal energy sources (biomass furnace and CSP plant), and energy storage (a thermal storage as depicted in Fig. 1). The proposed configuration is characterized by a high degree of flexibility and can be integrated to additional (and different) power blocks such as gen-sets, electric energy storage (electric batteries), wind turbines or photovoltaic modules. The main novelty is the connection of thermal sources (exhaust gas from the topping cycle and from the CSP) and thermal sinks (bottoming ORC and thermal users) to the TES that can compensate the fluctuations of the solar input as well as electricity and/or heat demand.

Several TES typologies can be used to recover heat from relatively high temperature: a critical review of technologies and materials is proposed in Ref. [44]. In this work, considering the range of temperatures available from EFGT and PTC [44], the two-tank technology that uses MSs as HTF and heat storage medium has been selected. This technology, referred as 'sensible heat storage' with direct heating, has the advantage of a relatively low-cost medium for storage and fluid vector, and indirect heating arrangements that need additional heat exchangers for charge and discharge of the thermal storage. Even if low cost material is chosen, the size of the TES needs to be optimized to minimize exergy losses when heat is recovered from the thermal sources to the storage and when the heat extracted from the storage is transferred to the bottoming thermal sinks.

The selected MSs mixture determines the operating range of the TES. The minimum temperature at which the MS mixture remains liquid in the cold tank determines the minimum temperature of heat storage.

The novelty of the proposed plant scheme relies on the hybrid combined configuration that offers promising opportunities for flexible operational strategies

and coupling of solar and biomass sections. In particular, the adoption of a combined cycle with a biomass fired EFGT and a bottoming ORC that is fed by solar energy and heat discharged from the topping turbine, potentially allows an independent operation of the system with only one of the two sources, which could occur in case of low solar radiation, high biomass costs or modulation of the electric output for load following. Moreover, the high temperature of the cogenerated heat allows matching on site thermal energy demand or coupling to another ORC that can operate at lower temperature, so increasing the electric efficiency or flexibility of the heat/electricity output.

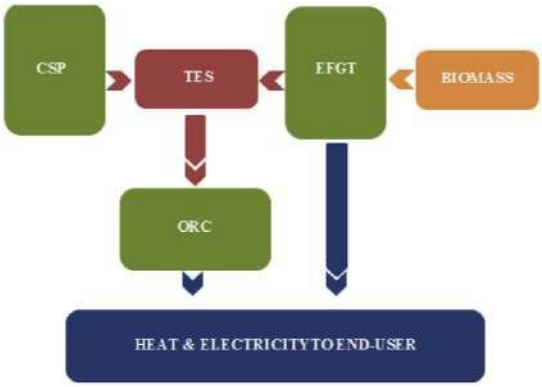

Fig. 1. Power blocks and energy flows through the proposed plant.

The paper is structured as follows: in the second section, the thermodynamic description of the topping EFGT, bottoming ORC and of the solar plant, including the TES, is provided, and the simulation model adopted to predict the performance of the solar system connected to the TES is also described; in Section 3, energy and exergy balances of the system at design condition are reported; in Section 4 the energy yield analysis in different plant locations and thermal storage size is presented; in section 5 the costs assessment and the hypotheses for the economic analysis are presented, while the results are reported in Section 6 and the conclusions are drawn in Section 7.

2. Plant description

In this section, the combined-cycle system components are described. Fig. 2 shows the plant layout of the three blocks that compose the proposed configuration and which are detailed hereafter.

2.1 Biomass EFGT section

The topping cycle is a biomass-fired EFGT (Fig. 2(a)). The thermodynamic cycle is characterized by an inter-refrigerated compression (A-C) with overall pressure ratio of 10; a gas-gas heat exchanger (High Temperature Heat Exchanger, HTHE) transfers the heat of the flue gas exiting the biomass furnace to the compressed air (C-D) that is heated to a turbine inlet temperature (TIT) of 800 o C. This relatively low temperature is chosen to keep low the cost of heat exchanger that can be made of steel. The air is then expanded in the turboexpander (D-E): the turbine outlet temperature is 390 o C. The heat of the air exiting the turbine is recovered and transmitted to the molten salts flowing in the heat exchanger indicated as Heat Recovery Molten Salts Heat Exchanger (HRMSHE) in Fig. 2(a). Since the minimum temperature of the cold tank is 200 oC, sensible heat can be further recovered from the gas for cogeneration. The thermodynamic cycle is represented by mean of a Temperature-entropy diagram, shown in Fig. 3.

The air in the biomass combustion is taken directly from the ambient. Since the two gas circuits (circuit of the working air flowing into the turbine and circuit of the combustion air flowing into the furnace) are decoupled, the proposed scheme allows a flexible regulation of the air-to-fuel ratio, taking into account the furnace characteristics, the lower heating value of the biomass, its moisture content, etc. It is also possible to have a partial flue gas recirculation, in order to lower the temperature of the hot gas entering the HTHE and avoid that high metal temperatures deteriorate the molecular structure of the MSs.

2.2 CSP and TES section

The solar collectors are based on the ENEA technologies of PTCs largely described in Refs. [45e47], while a numerical simulation of the PTC performance is proposed in Ref. [48]. The main characteristic is the use of MSs as HTF instead of synthetic

oil. This presents two main advantages: lower environmental impact and fire risks and higher maximum temperature that can be raised up to about 500 o C. The main drawback of MSs is the risk of freezing that occurs at about 120 o C; however, they can be considered liquid only at temperatures higher than 200 oC [49].

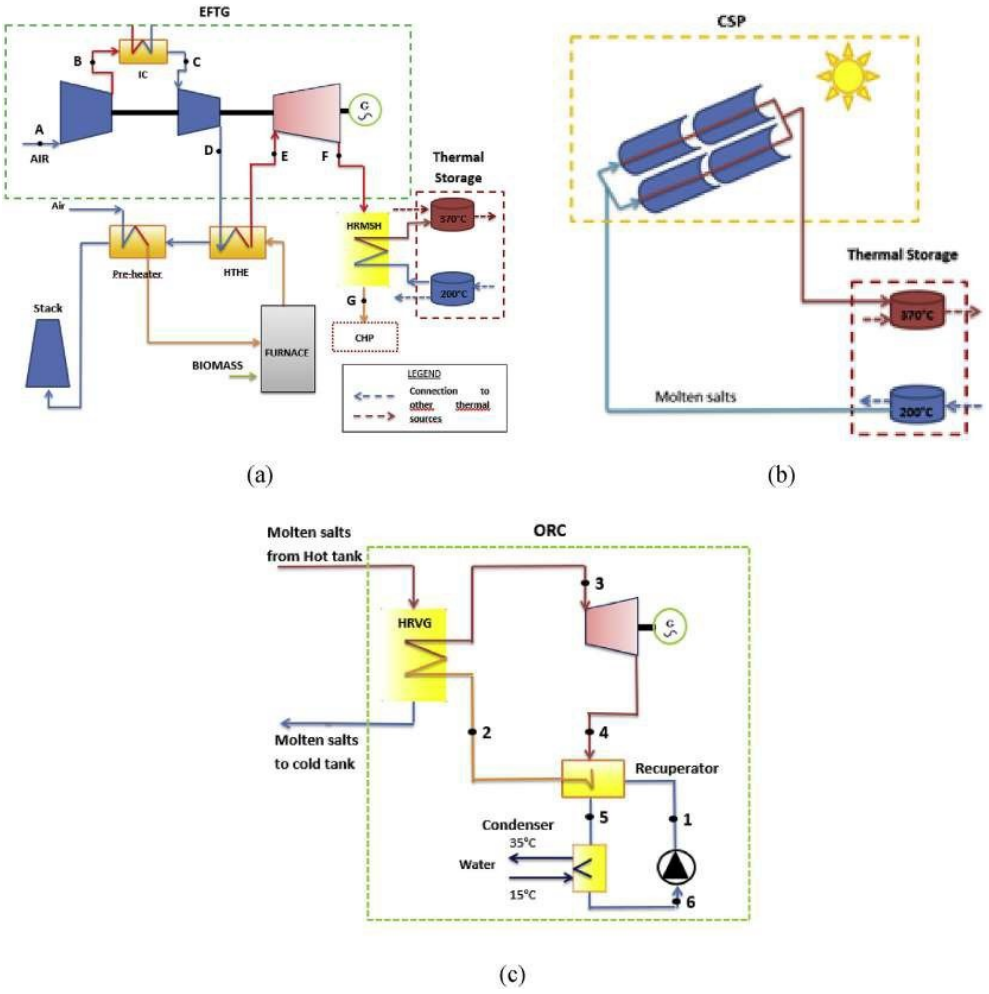

Fig. 2. Layout of the power blocks that compose the plant: (a) EFGT; (b) CSP with TES; (c) ORC plant.

A mixture of MSs (lithium, sodium and potassium nitrates) is chosen for both the HTF and the TES medium. This scheme is generally referred as “Direct Heating” TES [50] because it does not need a heat exchanger to transfer heat from the solar plant to the thermal storage, so avoiding the related costs. MSs flow in the solar

collectors during the day but also at night, because continuous recirculation can avoid freezing in the circuit. However, heat losses from the solar collectors are generally low at night. In the event of a lack of heating from the sun, the temperature can be restored using some heaters inside the two tanks.

Minimum and maximum temperatures of the PTC are therefore equal to those of the TES: the max temperature is limited to 370 o C, in order to recover heat from the EFGT while the min temperature cannot be lower than 200 o C to avoid risk of freezing for the molten salts.

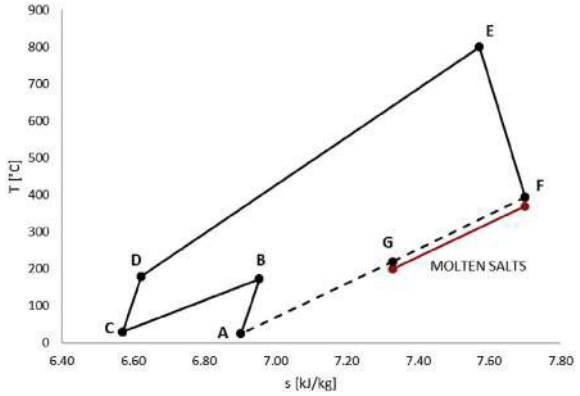

Fig. 3. T-s diagram of the EFGT plant

The CSP consists of one or more lines of collectors in a cascade configuration: the number of collectors of each line is evaluated to raise the temperature of the salts flowing in the receiver from 200 to 370 o C, with a standard direct normal irradiance (DNI) of 800 W/ m2 [51]. The solar collectors considered in this work have been lengthily tested in the ENEA facilities [52], and are characterized by a width of 5.9 m and a length of 12 m that determines a useful intercepting area of 67.3 m^2, equal to the 95% of the geometric area. The collectors are controlled by a central driving unit and form a Solar Collector Assembly (SCA). A single SCA includes eight col- lectors for a total length of 96 m. The collector axis is supposed to have a N-S orientation and an E-W track axis. Within such hypotheses, the average photothermal efficiency of the solar collectors is $\eta_{sol,PTC}$ =73% which includes a cleaning efficiency of 95% and a solar field availability of 99%. For each collector line, considering the cross section of the receiver and assuming a fluid velocity of 1.2 m/s, a MS flow rate of 6 kg/s is obtained and the overall length is 506 m. This means that each line is composed by 6 collectors of 96 m, with an intercepted area of about 3230 m^2 per each line and thermal power output of 1.885 MW. The

results of the design of the solar collectors' line are summarized in Table 1. Considering the scheme of Fig. 2, the share of energy input (solar/biomass) can be chosen considering the local availability of biomass and solar energy.

Description	Value
Intercepting area (m2)	3230
Ground area (m2)	9075
Overall photo-thermal efficiency	0.73
Thermal power output (MW)	1.895

Table 1 Performance of a single line of solar collectors under rated conditions

2.3 ORC section

The bottoming ORC recovers heat from MSs flowing from the Hot Tank to the Cold Tank of the TES as shown in Fig. 2(c). Since the heat is available at high temperature (from 370 to 200 °C) a recuperative configuration with superheating is chosen for the organic cycle. A pump (6-1) compresses the fluid up to the evaporating pressure and supplies it to the recuperator (1-2) that preheats the working fluid. Heat is supplied to the ORC plant in a heat exchanger between MSs and organic fluid heat recovery Vapour Generator (HRVG) (2-3) and then electric power is produced by the expansion of the organic fluid in the turbine (3-4). Finally, the hot organic vapour exiting from the turbine preheats the fluid entering in the recuperator (4-5) and condenses in a water condenser (5-6) until the inlet pump conditions. Selection of the working fluid is a crucial aspect in ORC analysis. Dry fluids, with a positive slope of the saturation curve in the *T-s* diagram, show a better thermal efficiency [53] with respect to other working fluids. Among dry fluids, Toluene is chosen because it shows a relatively high critical temperature and good performance at temperature ranges higher than 300 °C [54]. Moreover, Toluene has good environmental and safety properties, with both ozone depletion potential (ODP) and global warming potential (GWP) equal to zero.

The ORC parameters have been designed in order to meet the operating conditions of the MSs. A single-objective genetic algorithms (GA) based

optimization is performed, to maximize the thermal efficiency of the cycle. A GA procedure starts from a randomly initial population that through genetic operators and stochastic selection, mutation and crossover, generates other populations by combining the best individuals [13]. The process ends when the global optimal value of the objective function is found. GAs involve a search from a population of solutions and not from a single point, hence convergence to sub-optimal solutions is prevented.

An in-house code in Phytoon language has been adopted for the parametric single-objective optimization process. In the code, a set of equations have been implemented to model each ORC component. The thermodynamic properties of the organic fluid have been evaluated by means of Coolprop library [55]. The objective function was the ORC thermal efficiency maximization:

$$\eta_{\mathrm{ORC}} = \frac{\dot{W}_{\mathrm{exp}} - \dot{W}_{\mathrm{pump}}}{\dot{Q}_{\mathrm{ORC,in}}}, \tag{1}$$

where W˙_exp and W˙_pump are the expander output power and pump input power, and Q˙_in is the thermal input of the molten salt stream coming from the Hot Tank (370°C) and the returning temperature to the Cold Tank (200 °C). In this study, the evaporating pressure P_{ev}, the turbine inlet temperature T_TIT and the pinch point temperature difference in the HRVG are considered as optimization parameters. The optimization problem has been solved under the following constraints: 0.4P_c≤P_ev≤0.9P_c, where P_c is the critical pressure of Toluene; $T_{\mathrm{TIT}} < T_{\mathrm{HOTTANK}}$ $7\ \mathrm{K} \leq \Delta T_{\mathrm{PP}} \leq 10\ \mathrm{K}$; minimum temperature difference in the RHE recuperator, $\Delta T_{min,RHE} \geq 5K$. Only subcritical cycles have been considered. Further thermodynamic assumptions for the ORC cycle are summarized in Table 2.

The convergence in the single-objective optimization problem was reached after 13 generations, each generation made by 200 individuals. The T-s diagram of the cycle is shown in Fig. 4 where the red line represents MSs temperature profile while the blue line represents the cooling water temperature profile, respectively.

Table 2. Basic calculation hypotheses for the ORC plant.

Description	Value
Pump isentropic efficiency	0.75
Pump mechanical efficiency	0.96
Turbine isentropic efficiency	0.80
Turbine mechanical efficiency	0.96
Electric generator efficiency	0.95
Condenser temperature	40 °C

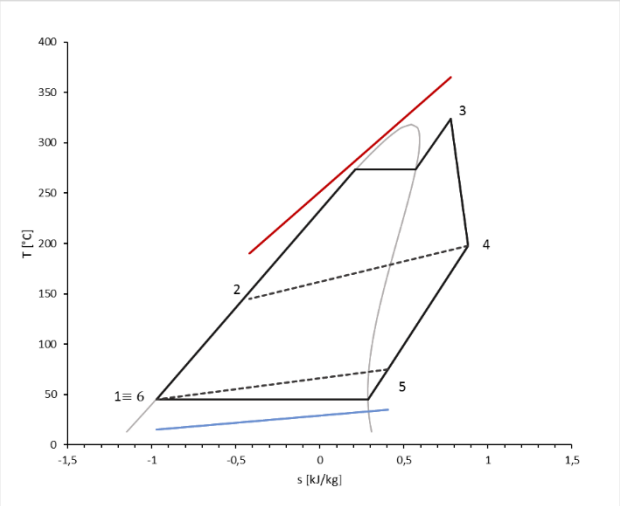

Figure 5. T-s diagram of the ORC plant obtained from the optimization.

Table 3. Results of the optimization process.

Description	Value
Evaporating pressure	21.7 bar
Turbine inlet temperature	322 °C
Pinch point temperature difference in HRVG	7.06
Cycle thermal efficiency	30.4%

Results are summarized in Table 3.

Under the optimal set of operating conditions, the cycle thermal efficiency results equal to 30.4% and the ORC electric efficiency is $\eta_{el,orc}$ = 29%, considering electric generator efficiency. The state points in Fig. 4 are correspondent to the state points in Fig. 2 (c).

3. Design-point performance

This section analyses the design point performance of the plant. Considering the scheme of Fig.2, the share of biomass and solar energy inputs can be chosen considering this local availability. The aim of this section is to determine the rated power for the different plant components and to set properly the overall solar field size. For a better understanding of the energy conversion process, a first law energy analysis is firstly carried out; then, an exergy analysis is carried out in order to detect the main causes of irreversibility for the plant and suggest the most profitable modifications to improve the energy conversion efficiency.

3.1 First law analysis at the design point

Let's consider first the EFGT including the biomass furnace **Errore. L'origine riferimento non è stata trovata.**(a). The rated lower heating value (LHV) input produced by the biomass combustion is:

$$\dot{E}_{biom} = \dot{m}_{biom} LHV_{biom} \,, \tag{2}$$

where $\dot{m}_{biom}$ is the biomass flow and LHV_{biom} is lower heating value of the biomass equal to 4.18 kWh/kg. The biomass combustion energy is partially transmitted to the compressed air flowing in the HTHE. The biomass furnace efficiency is expressed by:

$$\eta_{fur} = \frac{\dot{Q}_{HTHE}}{\dot{E}_{biom}}. \tag{3}$$

This efficiency is about 79,6% due to the relatively high energy losses for sensible heat of the exhaust gas and unburnt fraction of the biomass.

The net electric power output of the EFGT is:

$$\dot{W}_{net,EFGT} = \eta_{gen,el}\left(\dot{W}_t - \dot{W}_{c,I} - \dot{W}_{c,II}\right) \quad (4)$$

where $\eta_{gen,el}$ is the electric generator efficiency, $\dot{W}_t$ is the turbine power output, $\dot{W}_{c,I}$ and $\dot{W}_{c,II}$ are respectively the power input of first and second compressor stages. The available heat flow at the turbine exit $\dot{Q}_{av}$ is the heat flow that could be recovered when the gas is cooled to the ambient temperature. Therefore $\dot{Q}_{av}$ can be evaluated from the gas temperature at the turbine exit T_F and the ambient temperature T_{amb} from:

$$\dot{Q}_{av} = \dot{m}_g \, c_{p,g}(T_F - T_{\mathrm{amb}}) \, , \quad (5)$$

where $\dot{m}_g$ and $c_{p,g}$ are the mass flow and specific heat at constant pressure of the air working in the turbine, respectively. The heat of the air exiting the turbine is recovered in the HRMSHE (**Errore. L'origine riferimento non è stata trovata.**a) and transferred to the MSs to supply heat to the TES. The thermal flow $\dot{Q}_{rec}$ that can be recovered in the HRMSHE is determined by the MS temperature in the Cold Tank. Considering a Cold Tank temperature $T_{COLD\,TANK}$= 200°C, and assuming $\Delta T_{min} = 20°C$ between hot and cold fluids at the cold end of the HRMSHE, the temperature of the gas exiting the heat exchanger results $T_G = 220°C$ and the heat flow recovered is:

$$\dot{Q}_{rec} = \dot{m}_g \, c_{p,g}(T_F - T_G) \, . \quad (6)$$

We will assume that, at the design point, the heat flow $\dot{Q}_{rec}$ will be entirely delivered to the bottoming ORC cycle and no thermal energy will be stored or discharged. Further heat can be recovered from the air exiting the HRMSHE at the temperature T_G =220°C and used to serve on site heating demand.

We consider the additional solar contribution to the thermal input of the ORC Power Block (ORC_PB). It is worth noting that in the proposed scheme the share of the solar input can be varied in relation to the local disposability of the energy sources, solar and biomass. The total thermal input to the ORC at design condition is:

$$\dot{Q}_{\mathrm{orc,in}} = \dot{Q}_{\mathrm{rec}} + \dot{Q}_{\mathrm{th,sol,ORC\_PB}}\,, \tag{7}$$

where $\dot{Q}_{\mathrm{th,sol,ORC\_PB}}$ is the additional thermal power delivered to the ORC power block produced by solar plant. Then, let's consider the solar multiple (SM) of the solar plant. Considering a design point value for the Direct Normal Irradiance , the thermal power generated by the solar field at the design point, $\dot{Q}_{th,\mathrm{solar\_field}}$, is related to the total intercepting area A_c and the efficiency $\eta_{\mathrm{sol,PTC}}$ of the solar collectors that compose the solar field by

$$\dot{Q}_{th,\mathrm{solar\_field}} = \eta_{\mathrm{sol,PTC}} \cdot A_c \cdot \mathrm{DNI}\,. \tag{8}$$

The Solar Multiple is the ratio of the thermal power generated by the solar field at the design point, $\dot{Q}_{th,\mathrm{solar\_field}}$, to the thermal power input of the power block at reference condition $\dot{Q}_{\mathrm{th,sol,ORC\_PB}}$:

$$\mathrm{SM} = \frac{\dot{Q}_{th,\mathrm{solar\_field}}}{\dot{Q}_{\mathrm{th,sol,ORC\_PB}}}\,. \tag{9}$$

Therefore, the SM is a measure of the excess thermal power produced by the solar field at the design point that cannot be absorbed by the power block and should be delivered to the TES. Therefore, the thermal power delivered to the TES at the design point is:

$$\dot{Q}_{th,\mathrm{TES}} = \dot{Q}_{th,\mathrm{solar\_field}} - \dot{Q}_{\mathrm{th,sol,ORC\_PB}}\,. \tag{10}$$

According to these assumptions, at the design point with biomass + solar input contribution, the combined cycle net power output is:

$$\dot{W}_{el,tot} = \dot{W}_{net,EFGT} + \dot{W}_{net,ORC}\,. \tag{11}$$

The net electric efficiency is the ratio of the produced electric power $\dot{W}_{el,tot}$ and the sum of biomass and solar input power:

$$\eta_{\mathrm{el}} = \frac{\dot{W}_{el,tot}}{\dot{E}_{\mathrm{biom}} + \dot{E}_{\mathrm{sol}}}\,, \tag{12}$$

where $\dot{E}_{\mathrm{sol}}$ is the input of solar energy, evaluated from the part of the solar thermal power delivered to the ORC power block:

$$\dot{E}_{\mathrm{sol}} = \frac{\dot{Q}_{\mathrm{th,sol,ORC\_PB}}}{\eta_{\mathrm{sol,PTC}}} = A_r \cdot DNI\,. \tag{13}$$

where A_r is the reference area related to the part of the solar thermal power delivered to the ORC. It is worthwhile to show that $SM = A_c/A_r$.

The energy balance of the whole plant is reported in the energy flow scheme in Figure 6. As far as concerns the biomass input, the same EFGT proposed in Ref. [12] with a thermal power input $\dot{E}_{biom} = 9050\ kW$. The thermal input to the gas cycle is given by the heat flux in the HTHE, $\dot{Q}_{HTHE} = 7201\ kW$, with a relatively low efficiency of the furnace due to the sensible heat of the exhaust gas. Based on the hypotheses detailed in Ref. [12], the net power output of the EFGT, calculated from Eq. (5), is $\dot{W}_{net,EFGT}$ = 1388 kW while $\dot{Q}_{av}$ is calculated from Eq. (6) results equal to 4043 kW.

The heat flow $\dot{Q}_{av}$ is partly recovered and transferred to the MSs flowing in the HRMSHE. The heat flow recovered is $\dot{Q}_{rec}$ = 1890 kW. At the design point, we assume that such heat flow is entirely transferred to the ORC power block and does not contribute to the energy storage.

We revert now to the solar plant. In this work, it has been also assumed that the additional contribution of the solar field will be the 30% of the total rated thermal input to the ORC power block, corresponding to a thermal power $\dot{Q}_{\mathrm{th,sol,ORC\_PB}}$ = 900 kW. The total input to the ORC resulting from Eq. (7) is hence $\dot{Q}_{\mathrm{orc,in}}$ = 2,780 kW while, considering $\eta_{el,orc}$ of the optimal cycle, the electric power output $\dot{W}_{net,ORC}$ is 800 kW.

Let's then consider the solar field considering, at the design point, a DNI of 800 W/m^2. Under such conditions, a single line of solar collectors generates a thermal power output of 1.885 MW. Then, considering the thermal power

delivered to the power block, $\dot{Q}_{\mathrm{th,sol,ORC\_PB}} = 0.900$ MW, we can reasonably examine two scenarios:

- **Scenario no. 1:** 1 line of solar collectors, SM= 1.885MW/ 0.900 MW = 2.1
- **Scenario no. 2:** 2 lines of solar collectors, SM = 2 · 1.885MW/ 0.900 MW = 4.2

Figure 6 shows the scenario with SM = 2.1. In such case, from Eq. (7), the excess heat produced by the solar field and delivered to the TES is $\dot{Q}_{th,\mathrm{TES}}$ = 985 kW. The overall plant net electric power output results $\dot{W}_{el,tot} = \dot{W}_{net,EFGT} + \dot{W}_{net,ORC}$ = 2,188 kWe while the thermal power output available for cogeneration is $\dot{Q}_{cog}$ =2,152 kWt at 220 °C. In the case of no solar contribution [12] and with a direct heat recovery of the heat available $\dot{Q}_{av}$ from EFGT, $\dot{Q}'_{\mathrm{orc,in}} = 2{,}413$ kW the gas can be cooled to 104°C. Consequently the $\dot{W}'_{net,ORC}$ results 700kW and the total electric power output is $\dot{W}'_{el,tot}$ =2,083 kWe and the thermal power output for cogeneration is of 963 kWt. The modelling results report a net electric efficiency of 21.5% for the 100% biomass case.

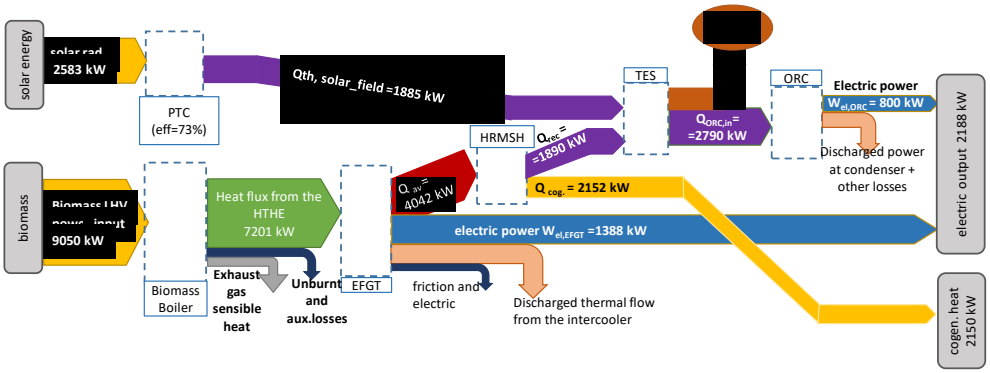

Figure 6. Energy flows at the design point.

3.2 Second law analysis

The main limit of the energy analysis is that it does not provide information about irreversibility of the system. Exergy (or "second law") analysis, which is based on the second law of thermodynamics **Errore. L'origine riferimento non è stata trovata.**, provides information on inefficiency of the different processes in order to identify components that cause the largest exergy losses.

Exergy is the maximum work we can obtain from a fluid until it reaches the "dead-state" condition (T_0 = 298.15 K, P_0 = 1 atm = 1.01325 bar). Unlike energy, exergy is not conservative. Exergy per unit mass can evaluated as the sum of a "physical" and a "chemical" component **Errore. L'origine riferimento non è stata trovata.**:

$$e_x = e_x^{ph} - e_x^{ch} . \tag{14}$$

"Physical exergy" (e_x^{ph}) gives the potential work that could be obtained from the fluid due to its thermodynamic state (temperature and pressure) and can be calculated from:

$$e_x^{ph} = h - h_0 - T_0(s - s_0) , \tag{15}$$

where *h* and *s* represent enthalpy and entropy of the fluid at the considered state point and at the dead-state, respectively. In the present work, the mechanical terms corresponding to kinetic and gravity potential energy will be neglected. "Chemical exergy" (e_x^{ch}.) is a function of the material stream composition; for a gas mixture, supposed ideal, it can be calculated as **Errore. L'origine riferimento non è stata trovata.**

$$e_x^{ch} = \sum_{j=1}^{N} x_i \cdot e_{x,j}^{ch,\mathbf{0}} + R\, T_0 \sum_{j=1}^{N} x_j \ ln\, x_j , \tag{16}$$

where x_j and $e_{x,j}^{ch,0}$ are mole fraction and standard chemical exergy of substance *j* that compose the stream, respectively, evaluated at the dead state. The chemical exergy can be evaluated from the standard Gibbs free energy as shown in Ref. **Errore. L'origine riferimento non è stata trovata.** that gives also the values for several substances. For the biomass, the physical exergy can be neglected since the biomass

is delivered to the furnace at ambient conditions while the chemical exergy can be evaluated from its lower heating value (LHV) from:

$$e_{x,biom}^{ch} = \beta \cdot LHV_{biom}\,, \tag{17}$$

where the coefficient β can be evaluated from the chemical composition of the biomass. Here, we assume $\beta = 1.06$.

Considering steady-state conditions, for every component of the plant, a control volume can be defined in order to identify mass, work and heat flows that cross the volume. The exergy balance can be expressed as:

$$\sum_{in} \dot{m} \cdot e_x + \dot{E}_x^Q = \sum_{out} \dot{m} \cdot e_x + \dot{W}_{act} + \dot{I}\,, \tag{18}$$

where $\dot{E}_x^Q$ is the net exergy transfer rate associated with the heat transfer flows $\dot{Q}_i$ from heat sources at temperature T_i placed in the surroundings

$$\dot{E}_x^Q = \sum_{i=1}^{N} \dot{Q}_i \left(1 - \frac{T_0}{T_i}\right), \tag{19}$$

$\dot{W}_{act}$ is the actual rate of work produced by the component and $\dot{I} = T_0 \dot{S}_{\mathrm{gen}}$ is the "irreversibility" or the rate of work lost due to the entropy rate generated, $\dot{S}_{gen}$, due to the irreversibility within the control volume as well as those associated to the irreversible heat transfer with the heat sources.

For the solar field we consider the radiation $\dot{E}_{\mathrm{sol}} = A_r \cdot DNI$ intercepted by the reference area A_r (see Eq. (13). The maximum useful work rate available from radiation, $\dot{E}_x^{rad}$ can be calculated from Petela's formula:

$$\dot{E}_x^{\mathrm{rad}} = A_r\, DNI \left(1 - \frac{T_0}{T_{\mathrm{sol}}}\right), \tag{20}$$

where T_{sol} is the solar temperature (4350 K) which is approximately 3/4 of the blackbody temperature of sun **Errore. L'origine riferimento non è stata trovata.**. The thermal exergy transferred from the receiver to the working fluid due to the incident radiation can be expressed as:

$$\dot{E}_{x,sol}^Q = \eta_{\mathrm{sol,PTC}}\, A_r\, DNI \left(1 - \frac{T_0}{T_{lm}}\right), \tag{21}$$

where T_{lm} is the log-mean temperature of inlet and outlet molten salt stream flowing in the receiver. It is worth to recall here that the inlet temperature of the molten salts is the temperature of cold tank and the outlet temperature should be equal to that of the hot tank.

Considering the overall plant, there are two exergy inputs: the solar exergy input is $\dot{E}_x^{\mathrm{rad}}$given by Eq. (20) while the biomass exergy input $\dot{E}_x^{biom}$ is related to mass flow rate of biomass $\dot{m}_{biom}$ by:

$$\dot{E}_x^{biom} = \dot{m}_{biom}\, e_{x,biom}^{ch}\,. \tag{22}$$

The overall exergy output is given by the mechanical actual power output $\dot{W}_{act}$that is the sum of the mechanical power output of the EFGT and ORC:

$$\dot{W}_{act} = \dot{W}_{EFGT} + \dot{W}_{ORC}\,. \tag{23}$$

The subscript "act" recalls that the quantity is referred to the actual irreversible process to be distinguished from the ideal reversible process. As usual, in the present exergy analysis, friction and electric losses will not be considered as they are not involved in the thermodynamic conversion process. Therefore, it is possible to define the second law efficiency from:

$$\eta_{II} = \frac{\dot{W}_{act}}{\dot{W}_{rev}}, \tag{24}$$

where:

$$\dot{W}_{rev} = \dot{E}_x^{biom} + \dot{E}_x^{rad}\,, \tag{25}$$

is the reversible power output that could be ideally produced in a totally reversible process. The difference between $\dot{W}_{rev}$ and $\dot{W}_{act}$is due to the sum of the irreversibility rate or destroyed exergy in the M plant components:

$$\dot{W}_{rev} - \dot{W}_{act} = \dot{I}_{TOT} = \sum_{k=1}^{M} \dot{I}_k\,. \tag{26}$$

The analysis of the irreversibility rate $\dot{I}_k$ in the k component, allows one to identify the root causes that originate the reduction of the actual work rate with respect to the reversible work rate.

Table 4. Exergy accounting for the plant components.

Component	Exergy input	Exergy output	Exergy destroyed
EFGT	**Biomass** $\dot{E}_x^{biom} = 9593$ kW	**Mechanical power output** $\dot{W}_{EFGT} = 1623$ kW **Thermal exergy to molten salts circuit** $\dot{E}_x^Q = 893.8\ kW$ **Thermal exergy for cogeneration** $\dot{E}_x^Q = 98.1\ kW$	$\dot{I} = 6978.1\ kW$
Solar collectors	**Solar irradiance** $\dot{E}_x^{\mathrm{rad}} = 1149.2$ kW	**Thermal exergy to molten salts circuit** $\dot{E}_x^Q = 484.5\ kW$	$\dot{I} = 664.7 kW$
Molten salts circuit	**Thermal exergy** $\dot{E}_x^Q = 893.8$ kW (from EFGT) $\dot{E}_x^Q = 484.5$ kW (from solar collectors)	**Thermal exergy to ORC** $\dot{E}_x^Q = 1270$ kW	$\dot{I} = 108.3\ kW$
ORC	**Thermal exergy** $\dot{E}_x^Q = 1270$kW	**Mechanical power output** $\dot{W}_{ORC} = 846.5$ kW	$\dot{I} = 423.5\ kW$

The exergy analysis results are summarized in Table 4 and, by applying Eq. (25), it is possible to evaluate the second law efficiency of the whole system that is equal to $\eta_{II,ORC} = 0.37$. The main source of actual work reduction in the whole configuration is the EFGT whose irreversibility is 87% of the total exergy losses.

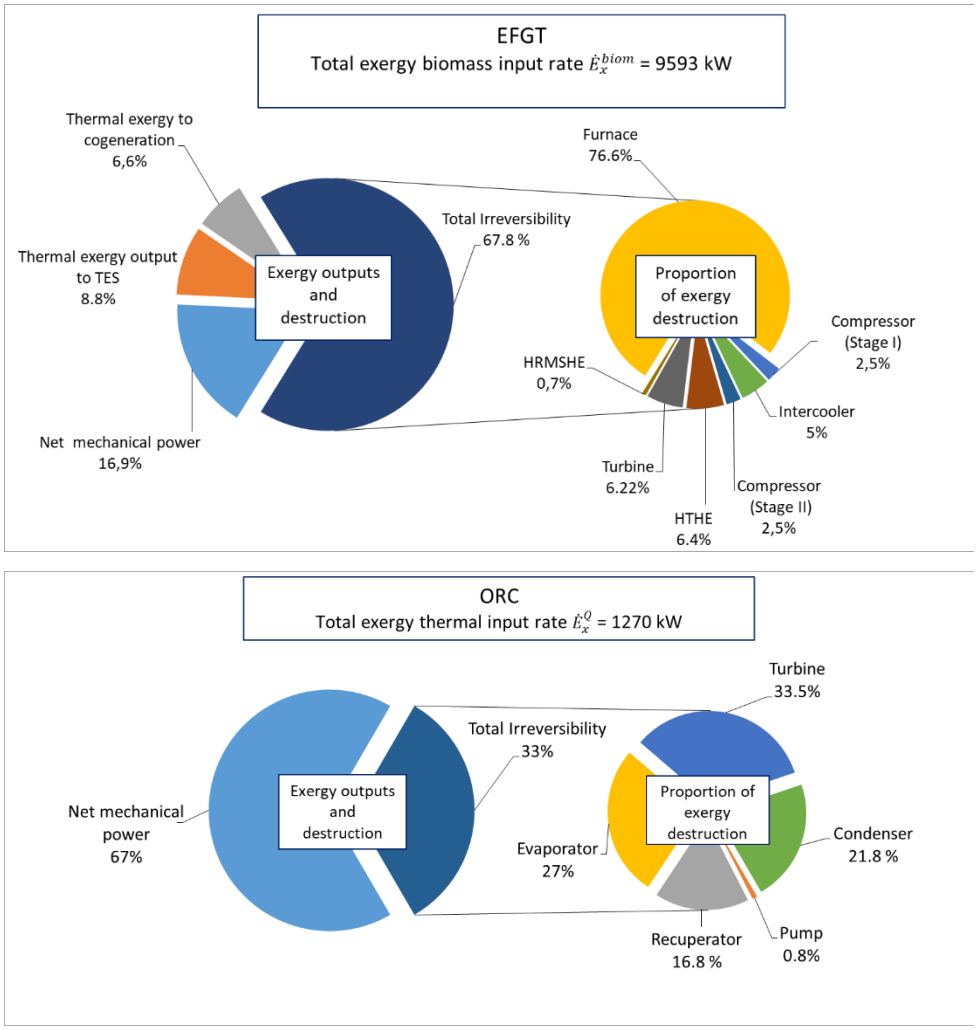

Figure 6. Exergy balances at design point in the EFGT (top) and ORC (bottom).

At the same time, Fig. 6(a) and (b) show exergy output and destruction in the EFGT and ORC section, respectively. In particular, pie graphs on the left-hand side show exergy output and irreversibility referred to the exergy input, while the right-hand side pie chart show exergy destruction proportion caused by each component of the cycle. The second law efficiency for the main subsystems results equal to $\eta_{II,EFGT} = 0.35$ for EFGT section and $\eta_{II,ORC} = 0.67$ for the ORC. In Fig. 6(a) is it possible to see that the low value of the second law efficiency for the EFGT depends mainly on the biomass exergy input wasted in the furnace which accounts 77% of the total

irreversibility, mainly due to the low temperature of the compressed air flowing in the HTHE and the exergy losses with the exhaust gas. On the other hand, ORC can convert most of the thermal input exergy in mechanical power and only the 33% is lost in irreversibility. The main sources of irreversibility in the ORC are the turbine and the evaporator that are respectively equal to 33.5% and 27% of the total losses. Very low is the exergy destruction due the heat exchange with the molten salt circuit of the TES, due to the choice of the scheme with "direct heat exchange" in which molten salts act as heat transfer fluid and heat storage medium.

4. Annual energy analysis

The analysis of the yearly electricity generated by the solar/biomass hybrid system has been carried out, considering different values of SM and TES capacities. In order to analyse the influence of the annual solar radiation on the annual energy plant production, three different locations in Fig. 7(a) have been selected.

- **Case P**: Priolo Gargallo (Siracusa, Italy, Latitude 37°08'04" N, Longitude 15°03'00"E, 30 m a.s.l.);
- **Case M**: Marseilles (France, Latitude 43°17'49'' N, Longitude 5°22'51'' E, 28 m a.s.l.);
- **Case R**: Rabat (Morocco, Latitude 34°00'47'' N, Longitude 6°49'57'' W, 46 m a.s.l.);

The DNI for each site has been evaluated by means of the software Meteonorm that provides accurate and representative solar radiation for any location on earth, using satellite data **Errore. L'origine riferimento non è stata trovata.** has been carried out. The methodology proposed in Ref. **Errore. L'origine riferimento non è stata trovata.** has been adopted to estimate the reduction coefficient of the direct normal irradiance DNI (kWh/m^2 month) and aperture normal irradiance (ANI) (kWh/m^2 month) in Figure 7(b).

Table 5. Acronyms of the examined cases.

Solar Multiple (SM)	Priolo	Marseilles	Rabat
2.1	P1	M1	R1

4.2	P2	M2	R2

The cases studies under investigation are reported in Table 5.

An hourly basis simulation on the solar field productivity has been carried out to analyse the energy performance of the system. A minimum DNI of 200 W/m2 have been considered as operational limit.

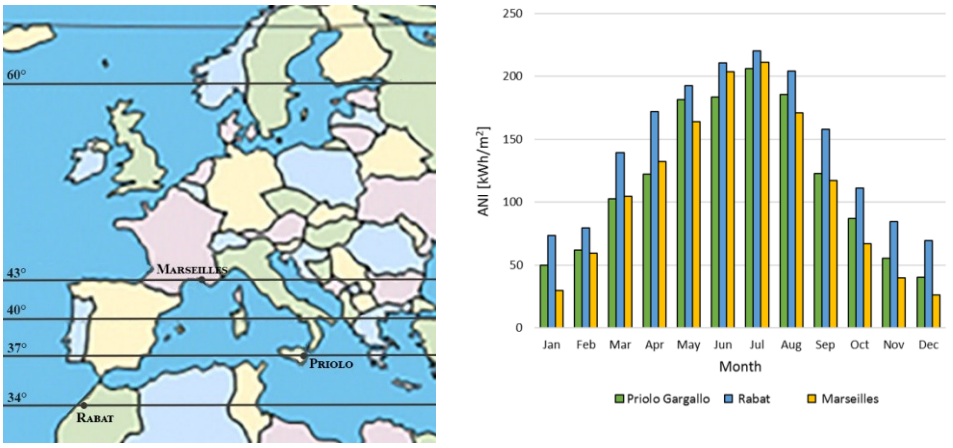

(a) (b)

Figure 7. (a) Site map from METEONORM **Errore. L'origine riferimento non è stata trovata.**. (b) Monthly ANI for each site **Errore. L'origine riferimento non è stata trovata.**.

The TES capacity has been expressed in hours t_s given by the ratio of the maximum energy that can be stored $E_{\mathrm{TES_MAX}}$ to the solar contribution to the thermal input of the ORC, $\dot{Q}_{\mathrm{th,sol,ORC\_PB}}$ which is set to 900 kW:

$$t_s = \frac{E_{\mathrm{TES\_MAX}}}{\dot{Q}_{\mathrm{th,sol,ORC\_PB}}} \qquad (27)$$

Thermal losses are neglected (adiabatic system) and when the thermal storage is full, the excess energy is dissipated. For each location, both the solar field with SM = 2.1 and that one with SM = 4.2 (1 and 2 lines of collectors) have been considered.

Figure 8 reports the time plot of the solar energy output, the quantity delivered to the ORC, delivered to the TES and dissipated, for the 21st of June, in the case R1 for a TES capacity t_s = 2 h (i.e., $E_{\mathrm{TES\_MAX}}$ = 1800 kWh). When the thermal power produced by the solar field is higher than the max thermal energy to be supplied to

the ORC plant, the energy excess is delivered to the TES. If the stored energy reaches the maximum (1800 kWh), the excess of energy is dissipated. During the night, when solar energy falls down, the stored thermal energy is supplied to the ORC plant.

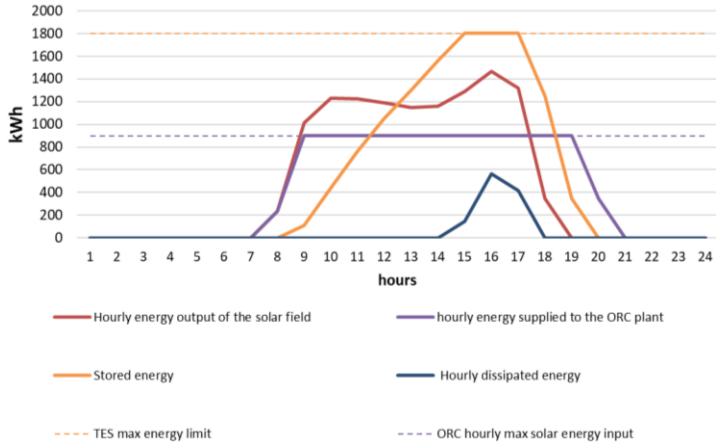

Figure 8. Energy performance of the solar plant connected to the TES for 21st June.

The Annual Energy Production (AEP) is calculated assuming a baseload operation of 8,040 hours per year for the biomass EFGT and bottoming ORC, and the solar energy production evaluated on the basis of the TES capacity and the value of SM of the solar field. The electricity production is expressed in terms of equivalent operating hours:

$$h_{eq} = \frac{AEP}{\dot{W}_{el,tot}} . \qquad (28)$$

The effect of the TES capacity on the equivalent operating hours is shown in Fig.9 while Fig. 10 reports the amount of the solar energy dissipated in a year. As expected, the higher is the TES capacity the higher are the equivalent operating hours. On the other hand, the dissipated solar energy decreases when TES capacity increases. In Scenario 1, there is no dissipation of solar energy when the TES has a capacity higher than 12 hours while in Scenario 2 the amount of dissipated solar energy increases to 5-10% according to the location. Fig. 11 reports the percentage of electricity produced by the ORC section as percentage of the total electricity produced in a year.

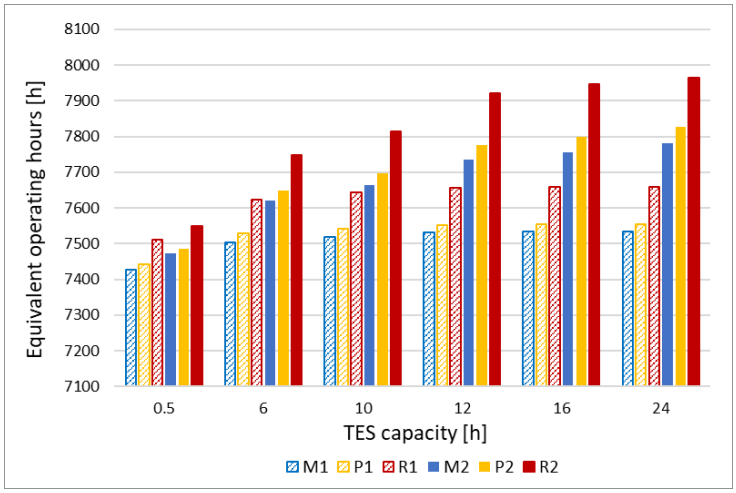

Figure 9. Equivalent operating hours of the solar section at different TES capacity.

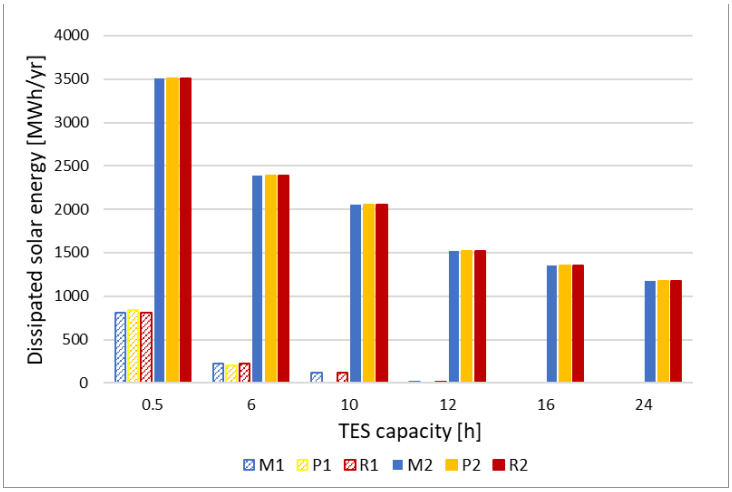

Figure 10. Amount of dissipated solar energy in a year at different TES capacity.

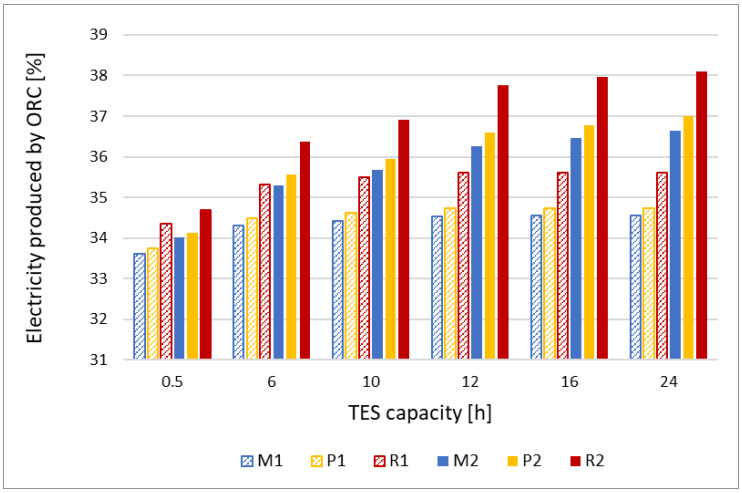

Figure 11. Percentage of electricity produced by the ORC section respect to the total annual electricity produced by the system, at different TES capacity.

The influence of the TES capacity on the annual electricity generation is reported in Fig 12. In the scenario of single collector line (SM of 2.1), increasing the TES capacity from 6 to 8 h has a limited effect on the produced electric energy, with an increase lower than 5%, while for TES capacity higher than 12 h the further electric energy production is negligible, as from Fig. 12.

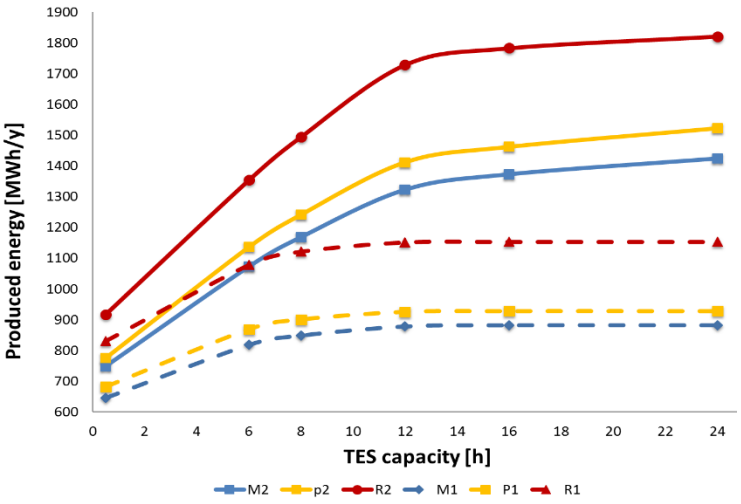

Figure 12. Annual electricity produced by the ORC with solar input as function of TES capacity.

In the case of 2 collector lines, the influence of TES capacity on the generated electricity is similar and, as also shown in Fig. 12, the advantage of a TES with a capacity higher than 12 h is negligible.

5. Cost analysis and economic assumptions

The cost analysis has been carried out assuming investment cost data from manufacturers and interviews to operators, as described in Ref. [12]. In particular, the costs of the biomass furnace have been taken from Uniconfort (Global biomass boilers) **Errore. L'origine riferimento non è stata trovata.**, the EFGT from Solar Turbines (Saturn 20) **Errore. L'origine riferimento non è stata trovata.**, the PTC from the pilot Archimede CSP plant **Errore. L'origine riferimento non è stata trovata.** and TES **Errore. L'origine riferimento non è stata trovata.** and from available literature **Errore. L'origine riferimento non è stata trovata.-Errore. L'origine riferimento non è stata trovata.**.

The component cost of the bottoming ORC plant has been estimated according to correlations in Seider et al. **Errore. L'origine riferimento non è stata trovata.**:

$$C = (F) \cdot exp\{C_0 + C_1 \cdot \ln(S) + C_2 \cdot [\ln(S)]^2\} \qquad (29)$$

where S is the size factor for each component and C_0, C_1, C_2 are the cost coefficients. The value used in the equation are listed in Table 7. The Obtained cost figures for the ORC are compared with data from Turboden **Errore. L'origine riferimento non è stata trovata.**.

For the CSP section, the PTCs and TES costs are derived from NREL cost figures **Errore. L'origine riferimento non è stata trovata.**, according to the lessons learnt from ENEA/Enel Archimede project **Errore. L'origine riferimento non è stata trovata.**. Unitary PTC costs of 250 Eur/m^2 and TES costs of 40 kEur/MWh are assumed. The annual operation and maintenance (O&M) costs are assumed 3.5% of the turnkey cost. In all scenarios, the biomass cost (wood chip) is 50 Eur/t at 40% moisture content and LHV of 2.8 kWh/kg. This relatively low cost of wood chips in comparison to market price figures of 80-120 Eur/t reflects the fact that high moisture content biomass locally produced and with a low collection radius is here considered, to be dried via high temperature heat discharged by the cogeneration

plant, following the assumptions in Refs. [25,35,36]. The ash discharge costs are accounted for by assuming unitary cost of 70 Eur/t ash. Personnel costs are taken as 268 kEur/yr [12].

Table 7. Component factors used in Eq. (29).

Component	**F**	**S**	C_0	C_1	C_2
Pump	2.7	$\dot{V}\sqrt{H}$($m^3s^{-1}m^{1/2}$)	9.0073	0.4636	0.0519
Turbine	1.0	$\dot{W}_t$ (kW)	6.5106	0.8100	0
Heaters/Cooler	1.0	HTA (m^2)	10.106	-0.4429	0.0901
Evaporator/Condenser	1.0	HTA (m^2)	9.5638	0.5320	-0.0002

Table 8. Capex and Opex costs. Optimized TES capacity is assumed.

Case study	**Only biomass**	**Scenario no. 1**	**Scenario no. 2**
Turn-key cost (kEur) I	4,700	5,740	6,780
- Biomass EFGT section I_{EFGT}	2,800	2,800	2,800
- CSP section I_{CSP}	-	807	1,614
- TES section I_{TES}	-	216	432
- Bottoming ORC I_{ORC}	1,200	1,200	1,200
- Engineering, building and installation I_{EBI}	700	700	700
Specific upfront cost (kEur/kWe)	2.26	2.63	3.1
O&M costs $C_{O\&M}$ (kEur/y)	487	520	523
Biomass cost C_B (kEur/y)	1285	1285	1285
Total Opex (kEur/yr)	2,285	2,263	2,350

The TES cost depends on its capacity, and in Table 5 the cost figures of the optimal TES capacity of 6 and 12 h respectively for scenarios 1 and 2 are considered, as described in the next section.

From Table 8, the total predicted turnkey cost is lowest at 4.7 MEur for the biomass-only plant (first column) that does not have a solar field, and is highest at 6.7 MEur for scenario 2, which features significant TES (with SM of 4.2). The upfront specific costs (in kEur/kWe) varies from 2.3 kEur/kWe for the biomass-only plant to 3.1 kEur/kWe for the hybrid plant of scenario 2. Opex, on the other hand, varies from a high of 2.28 MEur/yr for the biomass-only plant to 2.35 MEur/yr for the hybrid plant of scenario 2, given the added O&M costs for the solar section required in the former.

The levelized cost of electricity (LCE) is calculated from:

$$LCE = \frac{f_a \cdot (I_{EFGT} + I_{CSP} + I_{TES} + I_{ORC} + I_{EBI}) + C_{O\&M} + C_B}{E_G}, \qquad (30)$$

where f_a is the annuity factor given by:

$$f_a = \frac{r}{1 - \left(\frac{1}{1+r}\right)^l}, \qquad (31)$$

and where r is the discount rate and i the economic lifetime (years).

The financial appraisal of the investment is carried out assuming the following hypotheses: (i) 20 years of operating life and FiT duration for renewable electricity; no 're-powering' throughout the 20 years; zero decommissioning costs, straight line depreciation of capital costs over 20 years; (ii) maintenance costs, fuel supply costs, electricity and heat selling prices held constant (in real 2018 values); (iii) cost of capital (net of inflation) equal to 5%, corporation tax neglected, no capital investments subsidies. In order to compare the investment profitability in different location, the electricity sales revenues are calculated assuming the Italian subsidy framework. This is due to the fact that there are no specific support mechanisms for such hybrid biomass-solar CHP systems in France and Morocco. In the latter case, some support measures in the form of capital grants could be available, according to energy policy scenarios or specific CSP projects in development **Errore. L'origine riferimento non è stata trovata.**, while in the case of France there are some feed in tariffs for biomass or solar installations which however do not specifically address hybrid configurations and concentrating solar power **Errore. L'origine riferimento non è stata trovata.**. With these assumptions, the electricity is sold to the grid at the

feed-in electricity price available in the Italian energy market for the whole plant lifetime [15], which is 180 and 296 Eur/MWh respectively for biomass electricity (assuming the use of lignocellulosic by-products in the form of wood chips from forestry harvesting) and CSP electricity [15]. These figures are valid in the considered power size range, TES size, adoption of best available technologies for emission abatement, and use of agricultural by-products from local and sustainable supply chains. The same assumptions were made for the other two locations, with the aim to assess the influence of different solar radiation on economic performance. A sensitivity analysis to the feed in tariff has been included to assess the influence of subsidies on investment profitability. The further revenues from sales of cogenerated heat at high temperature (1,890 kWt at 220 °C) are included in a specific sensitivity analysis, that reports the financial profitability variation at different share of cogenerated heat valorization to match local thermal energy demand, and when varying the heating selling price. The cogeneration option represents a significant increase of revenue in case of high temperature heat demand availability. The Net present value (NPV) and the Internal Rate of Return (IRR) are the economic indices assumed to appreciate the investment profitability. The NPV is calculated from Eq. (21), being $(CFi)_{\text{dis}}$ the discounted cash flow in year l, and I is the total turnkey cost:

$$NPV = \sum_{i=1}^{l} (CF_i)_{\text{dis}} - I \,. \quad (32)$$

6. Techno-economic results

6.1 Levelized cost of energy and sensitivity to TES capacity

The TES capacity for each site has been selected in order to minimize the LCE, which is reported for each site in Fig. 13. LCE reaches its minimum value for a TES capacity equal to 6 h and 12 h respectively for the single and double collectors line scenario.

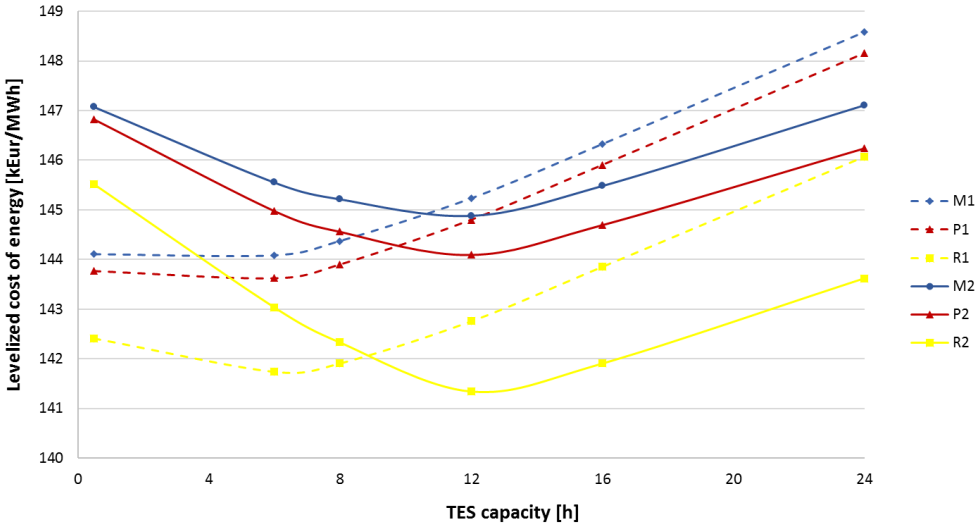

Figure 13. LCE as function of the TES capacity for the three locations and two solar-field sizes (see acronyms in Table 2).

These capacity values reflect the trade-offs between the higher investment costs and higher production rate when increasing the thermal storage size.

These optimal TES capacities have been assumed for the energy balances and economic profitability analyses reported the next sub-section.

6.2 Energy performance and profitability analysis results

The energy performance analysis and the profitability assessment have been performed considering a TES with a capacity respectively of 6 and 12 h for the scenarios with 1 and 2 lines of collectors, which is the size that minimizes the LCE.

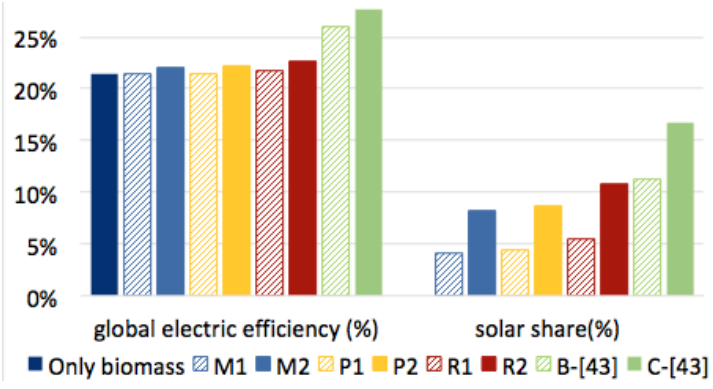

Figure 14. Energy performance results and solar share for the different scenarios. Cases B and C represent the system configuration proposed in Ref. ***Errore. L'origine riferimento non è stata trovata.*** *with small and large PTC and TES size respectively.*

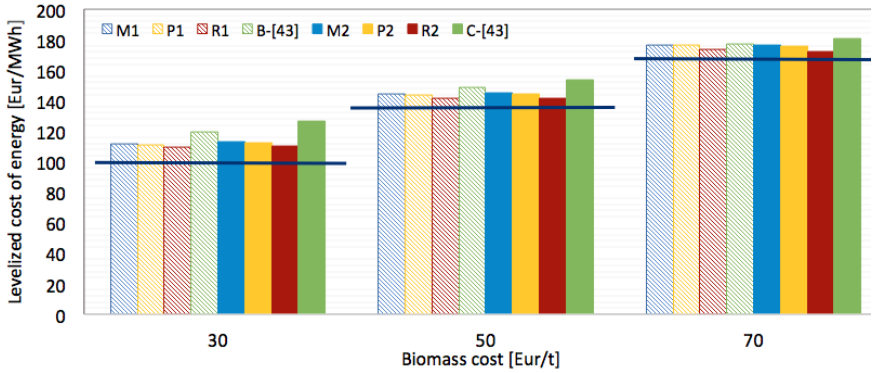

Figure 15. LCE as function of biomass cost. Cases B and C represent the system configuration proposed in Ref. ***Errore. L'origine riferimento non è stata trovata.*** *with small and large PTC and TES size. The black horizontal line represents the scenario of only biomass EFGT+ORC [43].*

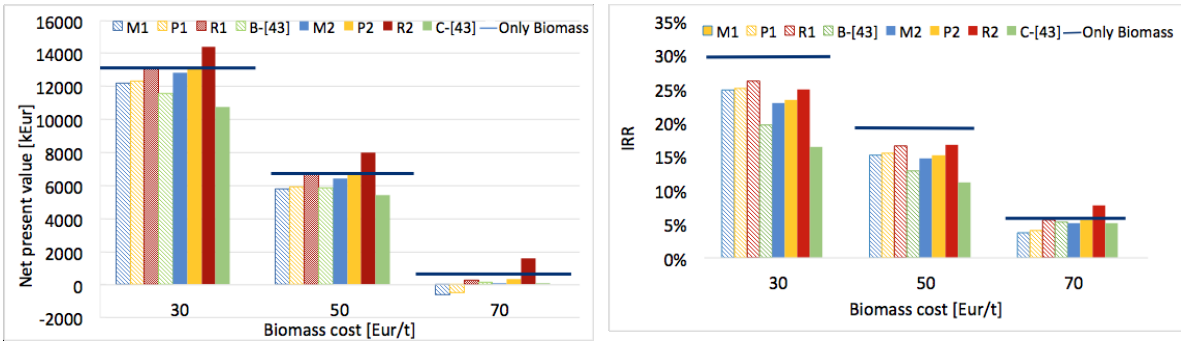

(a) (b)

Figure 16. (a) NPV and (b) IRR as a function of biomass supply cost for the different scenarios, and including the results of configuration ***Errore. L'origine riferimento non è stata trovata.*** *at small and large solar field sizing (B and C) and of configuration [42] with only biomass section.*

The results are compared to those ones of a plant with 100% biomass fuel already examined in Ref. [42] and to the different hybrid configuration analysed in Ref. [43], which assumes the location of Priolo Gargallo for the solar resource analysis (cases B and C of Fig 14 and 15, respectively with 8,600 and 12,900 m2 of PTC area).

In this case, the solar input from the same typology of PTCs and TES is provided to the topping gas turbine at 550 °C, so reducing the biomass consumption, but with a PTC size about 2 times larger than in the configuration here proposed. This justifies the higher LCE of the configuration proposed in Ref. **Errore. L'origine riferimento non è stata trovata.**, despite of the higher global electric efficiency (due to the higher solar share). The global electric efficiency and the solar share at different locations and SM are reported in Fig. 14. The solar share represents the ratio of energy input from solar resource vs the total energy input to the system. Figure15 reports the LCE for the proposed case studies, and a comparison with the hybrid solar-biomass system configuration proposed in Ref. **Errore. L'origine riferimento non è stata trovata.**.

For each case study, a sensitivity analysis to the biomass purchase price is considered. A baseload operation strategy is assumed to calculate the annual electric output, given that renewable CHP plants are eligible for feed-in tariffs (FiT) in the Italian energy market. The NPV and IRR of the investment at different biomass supply costs are reported in Fig. 16.

The proposed hybridization of the biomass EFGT with CSP presents higher global electric efficiency (in comparison to only biomass case), due to the solar energy input, in particular at higher SM level. As can be seen from Fig 15, LCE values are reduced on respect to **Errore. L'origine riferimento non è stata trovata.**, and the lower costs of the proposed configuration are due to the lower solar section size and costs, that balance their lower conversion efficiency on respect to the configuration [43]. Rabat is the location with the lowest LCE, due to the highest solar energy radiation and system producibility. However, all hybrid configurations present LCE higher than the one of only biomass fuel, demonstrating that the proposed CSP hybridization needs specific subsidies to be competitive with other renewable energy sources. For the only biomass scenario, LCE values range between 100 and 170 Eur/MWh at different biomass fuel costs, while for the best location of Rabat these values range between 110 and 174 Eur/MWh.

NPV ranges between 14,000 kEur (Rabat at high solar field size) to -600 kEur (Marseille with low solar field size) and IRR values from 25% (Rabat at low solar field size) down to 3.7% (Marseille at low solar field size). The hybridization of the biomass EFGT with CSP increases the global electricity efficiency, due to the solar energy input, but reduces both NPV and IRR in all the scenarios. In fact, despite the increased global energy efficiency of the solar input, and the higher electricity selling price of the solar based fraction on respect to biomass based one, the investment costs of the PTCs with MSs as HTF are very high and make this investment not competitive. This is more evident at higher solar shares where the larger PTC solar-array areas (and consequently higher investment costs) reduce the IRR but not the NPV.

In general, the results indicate the reduced IRR of CSP integration into biomass plants, due to the high investment costs of the former, are not compensated by the higher global energy conversion efficiency and additional electricity sale revenues. However, these results are not completely reflected in the NPV which is higher that the biomass-only case at the location of Rabat and the larger solar field (R2 of Fig. 16-a). Moreover, for biomass cost of 50 Eur/t or lower, the NPV and IRR of the system configuration here proposed result higher than the correspondent values of Ref. **Errore. L'origine riferimento non è stata trovata.**. On the other hand, for a biomass cost of 70 Eur/t the plant configuration in locations as Marseilles or Priolo Gargallo present negative NPV, except for the two collectors line scenario. Finally, the LCE and investment profitability is highly influenced by the biomass cost, and at values higher than 70 Eur/t (which are common on the market if no fuel source is available at low cost close to the premises of the plant) the difference between performance of only-biomass and hybrid systems decreases remarkably. Solar hybridization of biomass CHP could be hence an interesting option in case of suitable feed in prices for solar based electricity generation, relatively high costs of biomass fuel supply and perspectives of cost reduction for CSP capital costs.

In Figure 17, a sensitivity analysis of IRR and NPV to the variation of feed in price is reported. Feed in prices of 20% lower than the baseline correspond to average

electricity costs for industrial or large commercial consumers (150 Eur/MWh) in Italy, included generation, transmission, measurement and dispatchment costs. This scenario corresponds to onsite power generation to match local electricity demand with revenues achieved as avoided electricity purchase. As can be seen, this scenario is not profitable with the considered investment costs and in light of the conversion efficiencies that could be achieved. A different result would be achieved when using also the cogenerated heat at medium-high temperature to match on site energy demand.

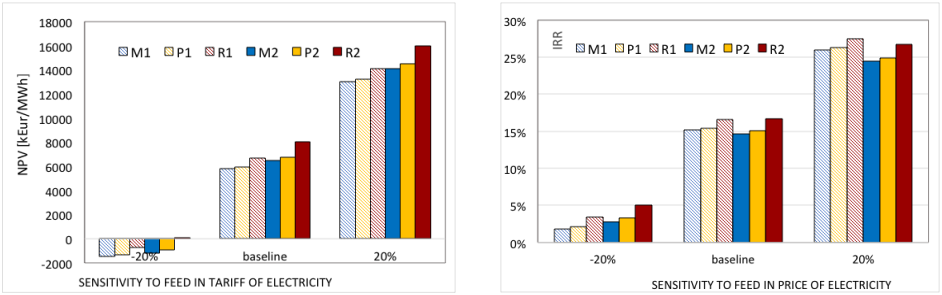

(a) (b)

Figure 17. Sensitivity of NPV (a) and IRR (b) to the feed-in tariff.

In this case, the further revenues from thermal energy sales increase the investment profitability, as reported in Fig 18, and in agreement with the results proposed in Refs. [37,43] for similar configurations. In particular, Fig 18 reports the NPV and IRR when using the discharged heat from the plant (2100 kWt at 200°C) to match heating demand (hot water at 70-90 °C) and with the assumption to sell the thermal energy at 40 Eur/MWh (bottom graphs, variation of equivalent operating hours in cogeneration mode in the range 0 – 5,000 h/year) or to have 3,000 equivalent hours/year in CHP mode operation (down graphs, variation of thermal energy selling price from 0 to 60 Eur/MWh).

variation of thermal energy selling price from 0 to 60 Eur/MWh).

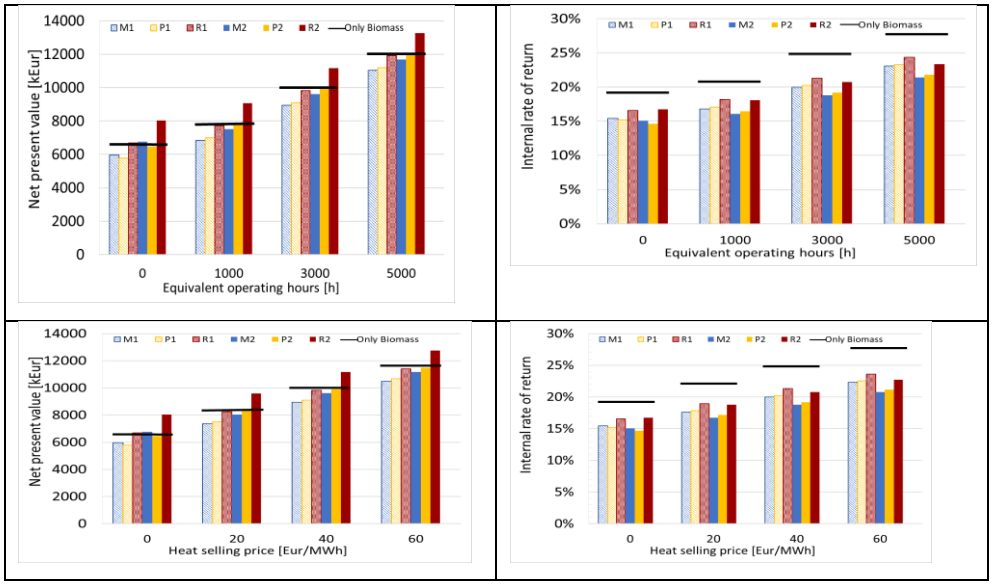

Figure 18: Sensitivity of NPV and IRR to the equivalent operating hours in cogeneration option (top) and to the heating selling price (down).

7. Conclusions

A thermodynamic and economic analysis has been performed on a hybrid (solar-biomass) combined-cycle system composed of an externally fired gas-turbine (EFGT) fuelled by biomass (wood chips) and a bottoming organic Rankine cycle (ORC) plant. In order to improve the flexibility of the overall system, heat is removed from the exhaust gases of the EFGT via the use of thermal energy storage (TES), with the thermal energy storage also receiving heat from a field of linear parabolic-trough collectors (PTCs) with molten salts used as a heat-transfer fluid (HTF). Heat from the TES is transferred the ORC plant and to thermal end-users, as and when requested. The thermal input of the EFGT is 9 MW, with a power output of 1.3 MW, while the ORC plant has an electric output of 700 or 800 kW with or without the solar hybridization configuration. Thermodynamic modelling was performed assuming two CSP sizes, and the energy performance results report higher global conversion efficiencies when using CSP integration while the thermo-economic analysis reports a higher investment NPV when integrating solar energy, due to the increased electricity generation and higher value of solar-based electricity.

A comparison with a previously proposed solar-biomass hybrid solution with a higher temperature (550 °C) available to the CSP working fluid and direct solar energy input to the topping EFGT demonstrates a higher profitability of the system configuration proposed in the present work. Another advantage of this configuration is the availability of high-grade heat for cogeneration from the bottoming ORC plant that can improve the profitability of the overall system when a suitable heat demand is available, as reported in the sensitivity analysis. The future steps of this research will focus on the quantification of the techno-economic advantages of the proposed system configuration in terms of higher generation flexibility. In particular, a more detailed analysis can include specific simulation of thermal and electrical load-following operating modes for the hybrid CHP system, in order to match specific energy-demand profiles. Moreover, a key research question arises from the need to assess off-design operation and part-load performance of the components (EFGT, CSP and ORC) and of the whole-system. Finally, a systematic procedure for the optimization of the size of the various components on the basis of key techno-economic factors such as solar irradiance and collector efficiency, biomass availability and supply costs, and energy demand profiles would be useful to support investment decisions.

Acknowledgements

This work was supported by the UK Engineering and Physical Sciences Research Council (EPSRC) [grant number EP/P004709/1] and DFID through the Royal Society-DFID Africa Capacity Building Initiative. The support of ENEA, Department of Energy Technologies, Division DTE-BBC, who funded the fellowship of Arianna Sorrentino in the field of "Development of biomass uses for distributed heat and power generation" is also kindly acknowledged. Data supporting this publication can be obtained on request from cep-lab@imperial.ac.uk.

The authors would like to thank the Organizing Committee of the 4th International Seminar on ORC Power Systems ORC2017 (13-15 September 2017, Milan, Italy) for awarding this paper the Best Paper Award presented at ORC2017.

References

[1] European Commission web site: https://ec.europa.eu/energy/en/topics/ energy-strategy-and-energy-union/2030-energy-strategy (accessed 26-1- 2018).

[2] R.P. Merch,ana, M.J. Santosb, A. Medinac, A. Calvo Herna,ndezd, Multi-stage configurations for central receiver hybrid gas-turbine thermosolar plants, in: Proceedings of ECOS, 2018.

[3] B. Coelho, A. Oliveira, P. Schwarzbo€zl, A. Mendes, Biomass and central receiver system (CRS) hybridization: integration of syngas/biogas on the atmospheric air volumetric CRS heat recovery steam generator duct burner, Renew. Energy 75 (2015) 665e674.

[4] J.D. Nixon, P.K. Dey, P.A. Davies, The feasibility of hybrid solar-biomass power plants in India, Energy (2012) 541e554. October.

[5] C.M.I. Hussain, B. Norton, A. Duffy, Technological assessment of different solar- biomass systems for hybrid power generation in Europe, Renew. Sustain. Energy Rev. (2016).

[6] G. San Miguel, B. Corona, Hybridizing concentrated solar power (CSP) with biogas and biomethane as an alternative to natural gas: analysis of environ- mental performance using LCA, Renew. Energy 66 (2014) 580e587.

[7] A. Mishra, N. Chakravarty, N. Kaushika, Thermal optimization of solar biomass hybrid cogeneration plants, J. Sci. Ind. Res. 65 (4) (2006) 355e363.

[8] M. Liu, N.H. Tay, S. Bell, M. Belusko, R. Jacob, G. Will, W. Saman, F. Bruno, Review on concentrating solar power plants and new developments in high temperature thermal energy storage technologies, Renew. Sustain. Energy Rev. 53 (2016) 1411e1432.

[9] Y. Takahisa, F. Tomohiko, A. Norio, M. Koichi, Design and testing of the organic Rankine cycle, Energy (March 2001) 239e251.

[10] M. Uris, J.I. Linares, E. Arenas, Techno-economic feasibility assessment of a biomass cogeneration plant based on an Organic Rankine Cycle, Renew. En- ergy 66 (2014) 707e713.

[11] R. Rayegan, Y.X. Tao, A procedure to select working fluids for Solar Organic Rankine Cycles (ORCs), Renew. Energy 36 (2011) 659e670.

[12] H.D. Madhawa Hettiarachchi, G. Mihajlo, W.M. Worek, I. Yasuyuki, Optimum design criteria for an organic Rankine cycle using low temperature geothermal heat sources, Energy 32 (2007) 1698e1706.

[13] L. Gosselin, M. Tye-Gingras, F. Mathieu-Potvin, Review of utilization of genetic algorithms in heat transfer problems, Int. J. Heat Mass Tran. (2009) 2169e2218.

[14] H. Xi, M. Li, C. Xu, Y. He, Parametric optimization of regenerative organic Rankine cycle (ORC) for low grade waste heat recovery using genetic algo- rithm, Energy (2013) 473e482.

[15] J. Wang, Z. Yan, M. Wang, S. Ma, Y. Dai, Thermodynamic analysis and opti- mization of an (organic Rankine cycle) ORC using low grade heatsource, En- ergy 49 (2013) 356e365.

[16] M. Petrollese, J. Oyekale, V. Tola, D. Cocco, Optimal ORC configuration for the combined production of heat and power utilizing solar energy and biomass, in: Proceedings of ECOS, 2018.

[17] T. Srinivas, B.V. Reddy, Hybrid solar-biomass power plant without energy storage, Case Stud. Therm. Eng. 2 (2014) 75e81.

[18] M. Vidal, M. Martin, Optimal coupling of a biomass based polygeneration system with a concentrated solar power facility for the constant production of electricity over a year, Comput. Chem. Eng. 72 (2015) 273e283.

[19] J.H. Peterseim, S. White, A. Tadros, U. Hellwig, Concentrated solar power hybrid plants, which technologies are best suited for hybridisation? Renew. Energy 57 (2013) 520e532.

[20] J.H. Peterseim, S. White, A. Tadros, U. Hellwig, Concentrating solar power hybrid plants - enabling cost effective synergies, Renew. Energy 67 (2014) 178e185.

[21] A,. Pe,rez, N. Torres, Solar parabolic trough e biomass hybrid plants: a cost efficient concept suitable for places in low irradiation conditions, in: Solar- PACES Conference, 2010.

[22] L. Schnatbaum, Biomass utilization for Co firing in parabolic trough power plants, in: SolarPACES Conf, 2009.

[23] V. Piemonte, M. De Falco, P. Tarquini, A. Giaconia, Life Cycle Assessment of a high temperature molten salt concentrated solar power plant, Sol. Energy 85 (5) (2011) 1101e1108, https://doi.org/10.1016/j.solener.2011.03.002.

[24] A. Amoresano, G. Langella, S. Sabino, Optimization of solar integration in biomass fuelled steam plants, Energy Proced. 81 (2015) 390e398.

[25] J.H. Peterseim, A. Tadros, S. White, U. Hellwig, F. Klostermann, Concentrated solar power/energy from waste hybrid plants e creating synergies, in: Solar- PACES Conference, 2012.

[26] European Concentrated Solar Thermal Road-mapping, 2005. SES6-CT-2003- 502578, DLR, http://www.promes.cnrs.fr/uploads/pdfs/ecostar/ECOSTAR. Roadmap.pdf.

[27] Z. Bai, O. Lium, J. Lei, H. Hong, H. Jin, New solar-biomass power generation system integrated a two-stage gasifier, Appl. Energy (2016). https://doi.org/ 10.1016/j.apenergy.2016.06.

[28] J. Soares, A.C. Oliveira, Numerical simulation of a hybrid concentrated solar power/biomass mini power plant", Appl. Therm. Eng. (2016). https://doi.org/10.1016/j.applthermaleng.2016.06.180.

[29] E.K. Burin, L. Buranello, P. Lo Giudice, T. Vogel, K. Grner, E. Bazzo, Boosting power output of a sugarcane bagasse cogeneration plant using parabolic trough collectors in a feedwater heating scheme, Appl. Energy 154 (2015) 232e241, 2015.

[30] A. Pantaleo, A. Pellerano, M.T. Carone, Potentials and feasibility assessment of small scale CHP plants fired by energy crops in Puglia region (Italy), Biosyst. Eng. 102 (3) (2009) 345e359, https://doi.org/10.1016/ j.biosystemseng.2008.12.002.

[31] G. Riccio, D. Chiaramonti, Design and simulation of a small polygeneration plant cofiring biomass and natural gas in a dual combustion micro gas turbine (BIO_MGT), Biomass Bioenergy 33 (11) (2009) 1520e1531.

[32] A.M. Pantaleo, S.M. Camporeale, N. Shah, Thermo-economic assessment of externally fired micro-gas turbine fired by natural gas and biomass: appli- cations in Italy, Energy Convers. Manag. 75 (2013) 202e213.

[33] A.M. Pantaleo, S. Camporeale, N. Shah, Natural gasebiomass dual fuelled microturbines: comparison of operating strategies in the Italian residential sector, Appl. Therm. Eng. 71 (2) (2014) 686e696.

[34] S. Camporeale, F. Turi, M. Torresi, B. Fortunato, A. Pantaleo, A. Pellerano, Part load performances and operating strategies of a natural gas-biomass dual fuelled microturbine for CHP operation, J. Eng. Gas Turbines Power 137 (12) (2015).

[35] S. Barsali, R. Giglioli, G. Ludovici, D. Poli, A micro combined cycle plant for power generation from solid biomass: Coupling EFMGT and ORC, in: 19th European Biomass Conference, ETA-WIP, Berlin, 2011.

[36] A. Bagdanavicius, R. Sansom, N. Jenkins, G. Strbac, Economic and exer- goeconomic analysis of micro GT and ORC cogeneration systems, in: ECOS 2012, 2012, pp. 1e11.

[37] G. Qiu, Selection of working fluids for micro-CHP systems with ORC, Renew. Energy 48 (2012) 565e570.

[38] O.A. Oyewunmi, A.I. Taleb, A.J. Haslam, C.N. Markides, An assessment of working-fluid mixtures using SAFT-VR Mie for use in organic Rankine cycle systems for waste-heat recovery, Comput. Therm. Sci. 6 (4) (2014) 301e316, https://doi.org/10.1615/.2014011116.

[39] O.A. Oyewunmi, A.I. Taleb, A.J. Haslam, C.N. Markides, On the use of SAFT-VR Mie for assessing large-glide fluorocarbon working-fluid mixtures in organic Rankine cycles, Appl. Energy 163 (2016) 263e282, https://doi.org/10.1016/ j.apenergy.2015.10.040.

[40] O.A. Oyewunmi, C.N. Markides, Thermo-economic and heat transfer optimi- zation of working-fluid mixtures in a low-temperature organic Rankine cycle system, Energies 9 (6) (2016) 1e21, https://doi.org/10.3390/en9060448, 448.

[41] L. Prattico', L. Toccia, E. Sciubba, Performance assessment of a solar-powered Organic Rankine Cycle for combined heat and power generation in small size rural applications, in: Proceedings of ECOS, 2018.

[42] S. Camporeale, A. Pantaleo, P. Ciliberti, B. Fortunato, Cycle configuration analysis and techno-economic sensitivity of biomass externally fired gas turbine with bottoming ORC, Energy Convers. Manag. 105 (2015) 1239e1250.

[43] A. Pantaleo, S. Camporeale, A. Miliozzi, V. Russo, C.N. Markides, N. Shah, Novel hybrid CSP-biomass CHP for flexible generation: Thermo-economic analysis and profitability assessment, Appl. Energy 204 (2017) 994e1006, https:// doi.org/10.1016/j.apenergy.2017.05.019.

[44] H. Zhang, B. Jan, G. C,aceres, D. Jan, Y. Lv, Thermal energy storage: recent developments and practical aspects, Prog. Energy Combust. Sci. 53 (2016) 1e40. ISSN 0360e1285, https://doi.org/10.1016/j.pecs.2015.10.003.

[45] ENEA Working Group, Solar Thermal Energy Production: Guidelines and Future Programmes of ENEA, 2001. ENEA Report. Available at: http://www. solaritaly.enea.it/Documentazione/Documentazione.php.

[46] Technology Roadmap, Concentrating Solar Power, International Energy Agency, 2010.

[47] G.M. Giannuzzi, C.E. Majorana, A. Miliozzi, V.A.L. Salomoni, D. Nicolini, Structural design criteria for steel components of parabolic-trough solar concentrators, J. Sol. Energy Eng. 129 (2007) 382e390.

[48] V.A. Salomoni, C.E. Majorana, G.M. Giannuzzi, A. Miliozzi, D. Nicolini, in: Radu D. Rugescu (Ed.), New Trends in Designing Parabolic Trough Solar Concen- trators and Heat Storage Concrete Systems in Solar Power Plants, Solar En- ergy, InTech, 2010. ISBN: 978-953-307-052-0.

[49] R.W. Bradshow, D.R. Meeker, High temperature stability of ternary nitrate molten salts for solar thermal energy systems, Sol. Energy Mater. (1990) 51e60.

[50] U. Herrmann, B. Kelly, H. Price, Two-tank molten salt storage for parabolic trough solar power plants, Energy 29 (5e6) (2004) 883e893.

[51] H. Hottel, B. Woertz, Thermal theory and Modeling of Solar Collectors, MIT press, Cambridge, MA, 1990.

[52] ENEA web Site: www.solaritaly.enea.it (accessed 20-12-2017).

[53] P.J. Mago, L.M. Chamra, K. Srinivasan, C. Somayaji, An examination of regen- erative organic Rankine cycles using dry fluids, Appl. Therm. Energy (2008) 998e1007.

[54] R. Chacartegui, D. Sa,nchez, J.M. Mun~oz, T. Sa,nchez, Alternative ORC bottoming cycles FOR combined cycle power plants, Appl. Energy (2009) 2162e2170.

[55] I.H. Bell, J. Wronski, S. Quolin, V. Lemort, Pure and pseudo-pure fluid ther- mophysical property evaluation and the open-source thermophysical prop- erty library CoolProp, Ind. Eng. Chem. Res. 53 (6) (2014) 2498e2508.

[56] M.J. Moran, H.N. Shapiro, D.D. Boettner, M.B. Bailey, Fundamentals of Engi- neering Thermodynamics, John Wiley & Sons, 2010.

[57] T.J. Kotas, The Exergy Method of Thermal Plant Analysis, Elsevier, 2013.

[58] F. Gharagheizi, M. Mehrpooya, Prediction of standard chemical exergy by a three descriptors QSPR model, Energy Convers. Manag. 48 (2007) 2453e2460.

[59] M. Mehrpooya, M. Khalili, M. Mehdi Moftakhari Sharifzadeh, Model devel- opment and energy and exergy analysis of the biomass gasification process (Based on the various biomass sources), Renew. Sustain. Energy Rev. 91 (2018) 869e887. ISSN 1364e0321, https://doi.org/10.1016/j.rser.2018.04.076.

[60] H. Li, X. Zhang, L. Liu, R. Zeng, G. Zhang, Exergy and environmental assess- ments of a novel trigeneration system taking biomass and solar energy as co- feeds, Appl. Therm. Eng. 104 (2016) 697e706. ISSN 1359e4311, https://doi. org/10.1016/j.applthermaleng.2016.05.081.

[61] Web site Irradiation data: http://www.meteonorm.com.

[62] M. Sengupta, A. Habte, S. Kurtz, A. Dobos, S. Wilbert, E. Lorenz, T. Stoffel,

[63] D. Renne,, C. Gueymard, D. Myers, S. Wilcox, P. Blanc, R. Perez, Best Practices Handbook for the Collection and Use of Solar Resource Data for Solar Energy Applications, February 2015. Technical Report, NREL/TP-5D00-63112.

[64] Uniconfort website: https://www.uniconfort.com (accessed 20-1-2018) and personal communications.

[65] Solar Turbines website: https://mysolar.cat.com (accessed 25-1-2018) and personal communications.

[66] Archimede solar power plant, https://en.wikipedia.org/wiki/Archimede_ solar_power_plant.

[67] S. Sau, N. Corsaro, T. Crescenzi, C. D'Ottavi, R. Liberatore, S. Licoccia, V. Russo,

[68] P. Tarquini, A.C. Tizzoni, Techno-economic comparison between CSP plants presenting two different heat transfer fluids, Appl. Energy 168 (2016) 96e109.

[69] V. Russo, CSP plant thermal-hydraulic simulation, Energy Proced. 49 (2014) 1533e1542. Proceedings of the SolarPACES 2013 International Conference.

[70] Italian Ministry of Economic Development, Incentives for energy from electric not-photovoltaic renewable sources, Legislative decrees of 07.06.2016.

[71] R. Sterrer, S. Schidler, O. Schwandt, P. Franz, A. Hammerschmid, ScienceDirect Theoretical Analysis of the Combination of CSP with a Biomass CHP-plant Using ORC-technology in Central Europe, vol. 49, 2014, pp. 1218e1227. http://doi.org/10.1016/j.egypro.2014.03.131.

[72] S.S. Mostafavi Tehrani, R.A. Taylor, K. Nithyanandam, S.A. Ghazani, Annual comparative performance and cost analysis of high temperature, sensible thermal energy storage systems integrated with a concentrated solar power plant, Sol. Energy 153 (2017) 153e172.

[73] W.D. Seider, J.D. Seader, D.R. Lewin, Product & Process Design Principles: Synthesis, Analysis and Evaluation, John Wiley & Sons, Hoboken, NJ, USA, 2009.

[74] Turboden Web Site www.turboden.com and personal communications.

[75] C. Turchi, Parabolic Trough Reference Plant for Cost Modeling with the Solar Advisor Model (SAM), July 2010. Technical Report, NREL/TP-550-47605.

[76] Renewable Energy and Energy Efficiency in Morocco, Moroccan-German En- ergy Partnership PAREMA, 2016. Report available at: http://dkti-maroc.org/ wp-content/uploads/sites/61/2016/11/PAREMA_sme-re-ee-morocco.pdf.

[77] Legal Resources on Renewable Energy web site: http://www.res-legal.eu/ search-by-country/france/single/s/res-e/t/promotion/aid/feed-in-tariff-tarif- dachat/lastp/131/(accessed 26-1-2018).

[78] C.N. Markides, The role of pumped and waste heat technologies in a high- efficiency sustainable energy future for the UK, Appl. Therm. Eng. 53 (2) (2013) 197e209, https://doi.org/10.1016/j.applthermaleng.2012.02.037.

[79] C.N. Markides, Low-concentration solar-power systems based on organic Rankine cycles for distributed-scale applications: overview and further de- velopments, Front. Energy Res. 3 (2015) 1e16, https://doi.org/10.3389/ fenrg.2015.00047. Article Number 47.

[80] J. Freeman, K. Hellgardt, C.N. Markides, An assessment of solarethermal col- lector designs for small-scale combined heating and power applications in the United Kingdom, Heat Transf. Eng. 36 (14-15) (2015) 1332e1347, https:// doi.org/10.1080/01457632.2015.995037.

[81] O.A. Oyewunmi, C.J.W. Kirmse, A.M. Pantaleo, C.N. Markides, Performance of working-fluid mixtures in ORC-CHP systems for different heat-demand seg- ments and heat-recovery temperature levels, Energy Convers. Manag. 148 (2017) 1508e1524, https://doi.org/10.1016/j.enconman.2017.05.078.

[82] M.A. Chatzopoulou, C.N. Markides, Thermodynamic optimisation of a high- electrical efficiency integrated internal combustion engineeorganic Rankine cycle combined heat and power system, Appl. Energy 226 (2018) 1229e1251, https://doi.org/10.1016/j.apenergy.2018.06.022.

[83] J. Freeman, K. Hellgardt, C.N. Markides, An assessment of solar-powered organic Rankine cycle systems for combined heating and power in UK do- mestic applications, Appl. Energy 138 (2015) 605e620, https://doi.org/ 10.1016/j.apenergy.2014.10.035.

[84] J. Freeman, K. Hellgardt, C.N. Markides, Working fluid selection and electrical performance optimisation of a domestic solar-ORC combined heat and power system for year-round operation in the UK, Appl. Energy 186 (2017) 291e303, https://doi.org/10.1016/j.apenergy.2016.04.041.

[85] J. Freeman, I. Guarracino, S.A. Kalogirou, C.N. Markides, A small-scale solar organic Rankine cycle combined heat and power system with integrated thermal energy storage, Appl. Thermal Eng. 127 (2017) 1543e1554, https:// doi.org/10.1016/j.applthermaleng.2017.07.163.

[86] A. Ramos, M.A. Chatzopoulou, J. Freeman, C.N. Markides, Optimisation of a high-efficiency solar-driven organic Rankine cycle for applications in the built environment, Appl. Energy 228 (2018) 755e765, https://doi.org/10.1016/ j.apenergy.2018.06.059.

[87] M.T. White, O.A. Oyewunmi, A.J. Haslam, C.N. Markides, Industrial waste-heat recovery through integrated computer-aided working-fluid and ORC system

PAPER 4

Distributed heat and power generation: Thermo-economic analysis of Biomass-fired Rankine cycle systems with molten salts as heat transfer fluid

Arianna Sorrentino[1,2], Antonio M. Pantaleo[2,3], Sergio M Camporeale[1], Christos N. Markides[2], Giacobbe Braccio[4]

1. *Department DMMM, Polytechnic of Bari, Via Orabona 4, 70125 Bari, Italy*
2. *Clean Energy Processes (CEP) Laboratory, Department of Chemical Engineering, Imperial College London, South Kensington Campus, London SW7 2AZ, UK*
3. *Department DISAAT, University of Bari, Via Amendola 165/A 70125 Bari, Italy*
4. *ENEA-National Agency for New Technology, Energy, and Environment, Policoro (MT) 75025, Italy*

Division of work among authors

Thermodynamic calculations have been done by Arianna Sorrentino (AS) under the supervision of Sergio M. Camporeale (SC). AS in cooperation with Antonio M. Pantaleo (AP) carried out the economical appraisal. The paper was written by AS and AP with the help of SC. Comments and supervision were provided by SC, Christos N. Markides and Giacobbe Braccio

Abstract

Distributed cogeneration systems can be used to serve onsite energy demands in industrial and commercial buildings. In market segments with highly variable heat-demand patterns, the thermal plant is often composed of a boiler that is operated at part load in case of low thermal demands. To improve the plant flexibility and its overall energy efficiency, the biomass boiler can be coupled to a combined heat and power (CHP) generation system, as an alternative to a heat-only plant. In this work, three thermodynamic configurations are compared:
(A) a biomass furnace that acts as a heat-source for a steam Rankine cycle (ST) plant coupled to an organic Rankine cycle (ORC) engine; (B) the same as Case A but without the bottoming ORC; and (C): the same as Case A but without the steam cycle. All configurations assume the cogeneration of heat and power to match onsite energy demands. The plant adopts a molten salt (MS) circuit to transfer heat from the biomass furnace to the power generation system. The energy analysis assumes a ternary MS mixture operating up to 450 °C and with minimum temperature of 200 °C. Two organic fluids (Pentafluoropropane R245fa and Toluene) are considered, based on the temperature of heat available to the ORC engine. In the combined cycle of Case A, R245fa is selected and the maximum cycle temperature is 130 °C, with a global electrical efficiency of 16.6%. In Case C, when only the ORC system is used with Toluene as the working fluid, the electrical efficiency is 18.8% at the higher turbine inlet temperature of 330 °C. Production of hot water for cogeneration at different temperature levels is also considered. Based on the results of the thermodynamic simulations, upfront and operational costs assessments, and feed-in tariffs for renewable electricity, energy efficiency and investment profitability are estimated.

Keywords: CHP, cogeneration, biomass, concentrating solar, ORC, combined cycle, bottoming cycle

1. Introduction

A sustainable, secure and competitive energy supply represents the main pillar of the EU energy policy. In addition to the "20-20-20" energy policy goals, the EC has introduced new and ambitious targets of renewable energy penetration (27% of internal energy consumption), greenhouse gas (emissions abatement of 40% compared to 1990 levels) and energy efficiency (27% of energy savings) by 2030 [1]. In this context, small-scale biomass-fired Combined Heat and Power (CHP) systems can contribute to all these goals, including the development of decentralised energy generation, avoidance of electricity networks energy losses, increased energy security. Moreover, bioenergy could provide added socioeconomic and environmental benefits when organic by-products are recovered and further income to the rural sector if domestic biomass supply chains are developed [2]. In particular, small-scale CHP plants operated by Energy Service Companies (ESCOs) to match onsite energy demand can be promising for the tertiary sector, which is commonly affected by high energy demand intensity and costs, and for the industrial sector, in particular in case of energy- intensive processes, concurrent heat and power demand, and high tariffs of electricity and heating [3].

The use of biomass in small-scale CHP plants has been widely investigated in literature, including, among the others, aspects such as biomass upgrading and processing technologies, logistics of supply, optimization of CHP plants sizing, location and operation. In the field of lignocellulosic biomass, the available technologies for small-scale CHP (100 kWe to 1 MWe size) include: (i) biomass pre-processing through gasification coupled to both Internal Combustion Engine (ICE) [4,5] and Micro Gas Turbine (MGT) [6], included pyrolysis [7], and (ii) direct combustion in grate or fluidized bed boilers to feed externally-fired MGT [8,9], Stirling [10,11] or Organic Rankine Cycle (ORC) engines [12,13]. An overview of biomass combustion for small-scale CHP is provided in Ref. [14], and in Ref. [15] a review of small-scale biomass gasification coupled to different engines and turbines is proposed, while in Ref. [5] the technical and economic issues of decentralized

CHP through biomass gasification are reviewed. Further comparisons between biomass gasification-ICE and combustion- ORC are proposed in Ref. [16], while Ref. [17] investigates the bottoming ORC coupled to a syngas- fed ORC. Other options of combined use of biomass and natural gas into small-scale CHP by means of externally fired micro turbines are explored in Refs. [18-20]. The influence of part load efficiencies on optimal operation of such biomass/natural gas fired MGT has been investigated in Ref. [21]. A bottoming ORC could also be coupled to both MGT and ICE in order to increase the electric efficiency of the system but reducing the temperature of heat available for cogeneration. Several researches aimed to quantify the benefits of this ORC bottoming cycle coupled to a MGT [22,23].

In some cases, biomass furnaces are coupled to ORC plants via diathermic oils as heat transfer fluids (HTFs). The main novelty of this work relies on the use of molten salts (MSs) as an alternative HTF for different plant configurations and their use as thermal storage, using the well-known "two tanks" technology. In power generations plants energy storage not only reduces the mismatch between supply and demand but also improves the performance and reliability of energy systems [29]. In this paper the two tank MS storage aims to decouple the biomass boiler operation (that should be kept constant at rated power avoiding part load modulation) and the CHP system, that can be designed and operate in load following mode to match onsite heat and power demand. On the other hand, the advantages of MSs instead of oils are related to the lower cost of the fluid, the absence of safety issues (there are no fire risks), the environmental friendly characteristics of MSs (no environmental hazards in case of leakages). Possible integration with CSP plant is a further feature of MS technology. Unfortunately, besides these favourable characteristics, there are some issues related to the control of the plant, in particular the start-up and shut-down operation, due to the relatively high temperature of MS freezing. Depending on the composition of the MSs, freezing may occur at a temperature variable around 150-250 °C. To accommodate these temperatures, the biomass combustion hot gases have to exit the MS cold tank with a high sensible heat content, which increases the

stack losses, unless this heat is recovered for preheating the combustion air or delivered to thermal users.

ORCs are much more suited than conventional steam Rankine cycles for small and micro plants from a few dozen to some hundreds kWe. A relevant factor that could influence the selection of optimal technology is the temperature of heat demand for cogeneration. For this purpose, it is possible to use a combined cycle composed by a topping steam cycle and a bottoming ORC cycle. This scheme can be used as alternative to a simple ORC plant in order produce heat at higher temperature. In this paper, the thermodynamic analysis of a combined cycle composed by a steam turbine (ST) and a bottoming ORC (Case A) in comparison to only ST (Case B) or only ORC (Case C) is described, considering the influence of the energy demand patterns. A thermoeconomic methodology for financial appraisal of different thermodynamic cycle configurations is applied to different energy demand segments considering a simplified representation of energy demand, a costs assessment and discounted cash flow analysis. This methodology is applied to the case of 1 MWt biomass boilers coupled to ST and/or ORC generation systems (corresponding electric output of 100-200 kWe). The economic profitability of the investments is based on thermoeconomic methodologies [30] in light of the Italian policy measures for renewable heat and electricity generation and high efficiency CHP [31]. Three different energy demand patterns (industrial, tertiary and residential) are compared, and the results allow quantifying some of the key factors for the integration of bottoming ORC into ST for small-scale CHP.

2. Systems configurations and modelling

The layout of the proposed combined cycle with biomass section, intermediate thermal energy storage circuit and cogeneration section is reported in Fig. 1.

Fig. 1. Layout of the system configuration in the hypotheses of steam turbine and bottoming ORC (Case A).

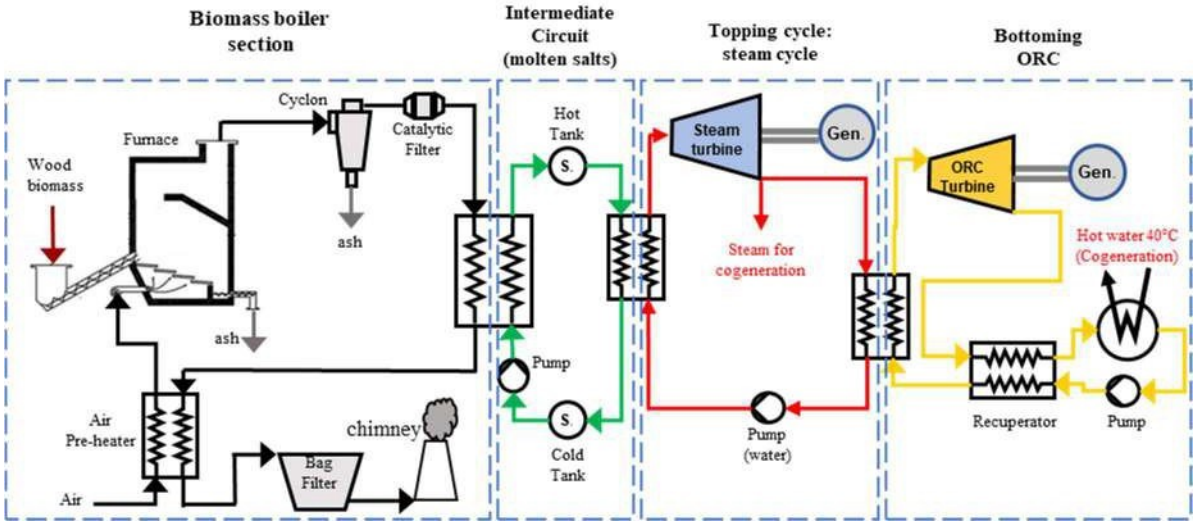

In this work, we consider a combined cycle composed by a ST topping cycle and an ORC bottoming cycle that can convert part of the heat from the ST in useful work. This cycle (Case A) is compared to the separate use of ST (Case B) and ORC (Case C). The reduced volume of steam and the production of steam at a pressure not higher than 20 bar make the steam expander compact. In Case A, the steam inlet conditions to the ST are 220 °C and 20 bar, and at outlet temperature of 150 °C the steam is conveyed to the evaporator of the ORC plant. The organic fluid is then vaporized and brought to the thermodynamic condition requested for the admission in the turbine. The water exiting the condenser still has a temperature suitable for low temperature heat demand (residential end users heat demand at 40 °C). The bottoming cycle is an ORC in a recuperative configuration. Recuperative heat exchangers are widely used in these cycles, to recover the heat of the organic fluid after the turbine expansion. In particular, the ORC can be described as follows. A pump supplies the organic fluid to the recuperator that pre-heats the fluid recovering the thermal energy from the fluid exiting the turbine. The evaporator produces the

evaporation of the organic fluid up to the requested condition, by recovering the heat from the topping cycle. Thus, the vapour flows in the turbine connected to a high-speed electric generator. At the exit of the turbine, the organic fluid goes to the hot side of the recuperator where it is cooled to a temperature a little higher than the condensation temperature. Finally, the condenser closes the thermodynamic cycle.

The condensation temperature of the ORC section is assumed of about 45 °C in order to maximize the electric efficiency of the cycle. Consequently, the condensation heat can be used only for low temperature cogeneration. In case of high temperature heat demand, the bottoming ORC is not compatible with the CHP configuration and an evaporative cooling tower or an air condenser is needed to dispose of the waste heat.

Based on the low steam temperature at the turbine outlet (143°C), refrigerants can be examined as suitable working fluids for the ORC. In particular, Pentafluoropropane R245fa has been selected for this application. It has thermodynamic properties compatible with the heat source and it is a "dry fluid" with a dry expansion in the turbine, thus avoiding the drop generation that can damage turbine blades. Moreover, it is not subject to greenhouse gas emission regulations as it does not damage the ozone layer, and it is non-flammable, non-toxic, and has satisfactory thermal stability [32].

Thermodynamic simulations were performed in Cycle-Tempo for both the ST and ORC sections. The obtained values for Case A have been validated through the data supplied by Ingeco [33] that described a similar plant but a different type of boiler.

In Case C, the ORC is directly connected to the MS circuit, thus the organic fluid has to exploit a heat source with a higher temperature (450 °C). For this case, Toluene proves to be a suitable working fluid because it is chemically stable in the range of temperature considered [34] and meets environmental and safety requirements. The T-s diagrams of the ORC in Case A and in Case C are reported in Fig. 2.

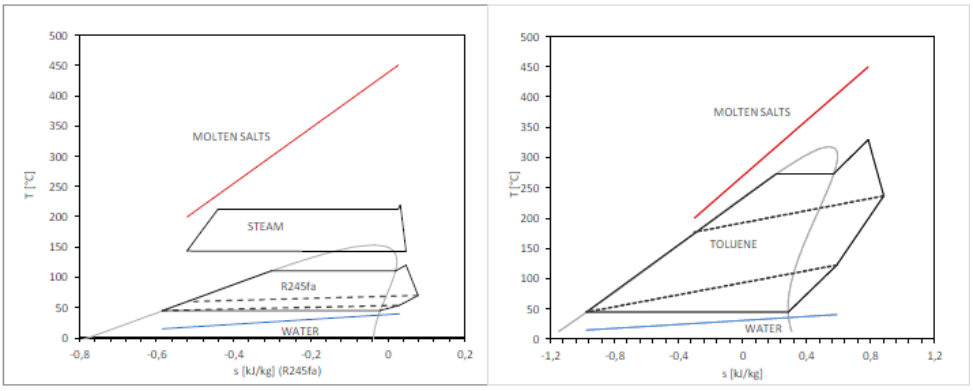

Fig. 2. ORC T-s diagrams for Case A with R245fa as the working fluid (left) and Case C with Toluene as the working fluid (right).

The temperature profiles of MSs are represented by the red line while the cooling water flowing in the condenser is indicated by a blue line. Further technical input parameters and modelling results are reported in Table 1.

The input data for Case D are the same of Case A when the plant operates in CHP mode with low temperature heat demand or in only electricity mode (bottoming ORC switched on), and the same of Case B when the plant operates in CHP mode with high temperature heat demand (tertiary and industrial end users, bottoming ORC switched off).

Table 1. Technical parameters and results of the thermodynamic analysis.

Case study	Unit	Cases A, D	Case B	Case C
Net electric power output (ISO)	kW	189	99	210
Total thermal power input	kW	1,136	966	1,114
Net thermal power output (for CHP)	kW	790	737	806
Shaft power	kW	203	104	231
Net-electric efficiency (ISO)	%	16.6	10.3	18.8
Temperature at (top) turbine exit	°C	143	111	237
Temperature at (bot) turbine exit	°C	77	-	-
Mass flow rate (top)	kg/s	0.410	0.337	1.832
Mass flow rate (bottoming)	kg/s	3.78	-	-
Maximum cycle temperature	°C	220	220	330

Other parameters used in the thermodynamic simulations: biomass boiler efficiency = 88%; mechanical/isentropic efficiency all turbines = 90/75%; electrical genset efficiency = 92%.

3.Technoeconomic assessment

The assessment of global energy efficiency of each case study is carried out considering the three different end-user categories of industrial (i), tertiary (t) and residential (r) heat demand. The operating hours of the plants (baseload operation mode) are assumed 7,500 (in agreement with data from manufacturer [35]), while the useful cogeneration heat is calculated assuming heat demand of 4,000/1,800/1,200 hours/year at temperature of 110/90/35 °C, respectively for industrial/tertiary/residential consumers.

In order to carry out the profitability assessment, the main cost items and biomass consumption values in Table 2 are assumed. The turnkey investment and operational costs are personal estimates from manufacturers and case studies data. The O&M costs are 20 Eur/MWh and include the handling and maintenance of the biomass furnace and storage system. Biomass ash discharge costs are accounted for assuming unitary cost of 70 Eur/t of ash. The following additional input data are assumed: LHV of biomass of 4.18 kWh/kg; cost of biomass of 80 Eur/t; electric internal consumption for operation of the CHP plant equal to 5%; biomass electricity feed-in tariff of 287 Eur/MWh [30]; heat selling price = 60/80/100 Eur/MWh respectively for industrial, tertiary and residential end users.

Table 2. CAPEX, OPEX and biomass consumption for the selected case studies.

Description	**Cases A, D**	**Case B**	**Case C**
Biomass consumption (t/year)	2,036	1,731	1,995
Total upfront cost (kEur) [3,4], of which:	1,170	840	990
- Steam Turbine	220	220	-
- ORC generator	330	-	370
- Biomass boiler, HEX, gas treatment	480	480	480
- Intermediate HTF circuit and MS system	80	80	80
- Engineering, development, insurance	60	60	60
Specific upfront cost (kEur/kW)	6.18	8.46	4.71
Operational cost included fuel (kEur/yr)	191.26	153.34	191.12

The financial appraisal of the investment is carried out assuming the following assumptions: (i) an operational lifetime of 20 year with no 're-powering' over this

lifetime and zero decommissioning costs; (ii) the maintenance and fuel supply costs, and electricity and heat selling prices are held constant of the lifetime (in real 2018 values); (iii) the feed-in tariff for biomass electricity is available over the entire lifetime of the project; (iv) the capital assets depreciate linearly over 20 years; and (v) the cost of capital (net of inflation) is equal to 8%, corporation tax can be neglected, and the capital investments and income do not benefit from any support.

4.Results and discussion

The global conversion efficiency of the selected case studies in different end-user segments is reported in Fig. 3 (ratio of useful heat + electricity generated vs. input biomass energy). The industrial energy demand presents the highest global efficiency because of the high heat demand rate, and Case study B, which maximizes the heat available to the load, appears the most suitable technology in this market segment, followed by Case D where the plant operational flexibility (switch on/off the ORC on the basis of the heat demand) makes the difference in comparison to Cases A and C. The same conclusions can be drawn for the tertiary end user segment, being the global energy efficiency lower in comparison to the industrial end user typology because of the reduced heat demand. The market segment of residential customers is the only one where the low temperature heat discharged by the ORC cycle is compatible with the cogeneration (35 °C of heat demand), hence the plant can maximize the electric efficiency and at the same time operate in CHP configuration. This is the only market segment where the global efficiency of Case C is higher than in the other cases. Despite these conversion efficiencies appear quite low if compared to average values for large scale CHP (usually well above 75%), an accurate comparison should take into account the benefits of onsite small-scale generation and use of renewable sources (biomass).

The results of the financial appraisal are reported in Fig. 4. The IRR results appear similar to the global energy efficiency ones. For industrial end-users, the steam turbine CHP (Case B) and the combined cycle with the option to switch off the ORC to maximize the heat delivered to the load (Case D) present the highest IRR, while Cases A and C are less profitable. However, considering the industrial demand

segment, the NPV is the highest for Case D, and this is due to the higher investment cost and higher revenues in comparison to Case B. The flexible combined cycle (Case D) is the most profitable option also in the tertiary market segment, which both in terms of the IRR and in terms of the NPV is higher than in Case B.

Fig. 3. Conversion efficiency (ηCHP) (left) and discounted payback time

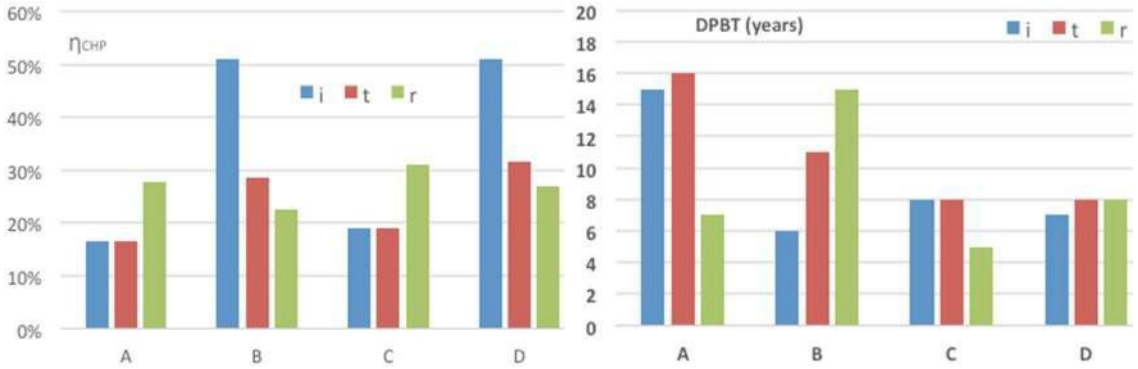

(DPBT) (right) for CHP Cases A to D and industrial (i), tertiary (t) and residential (r) users.

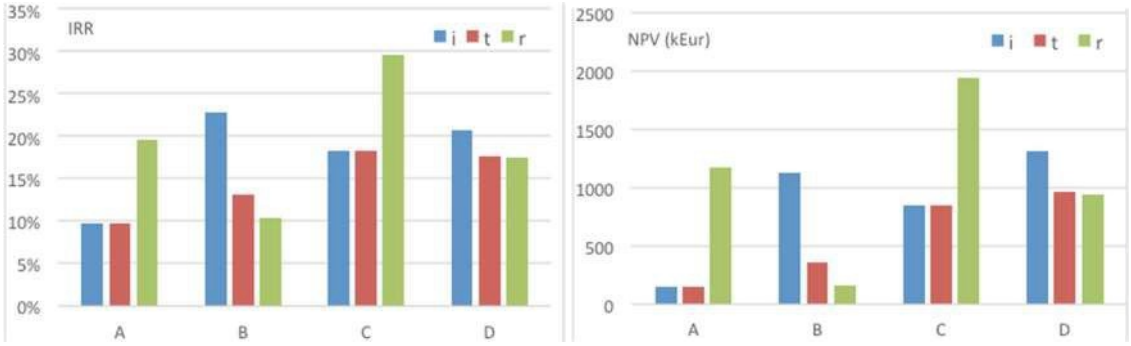

Fig. 4. IRR (left) and NPV (right) of the investment for the 4 case studies and 3 different energy demand segments.

5.Conclusions

In this paper, a thermo-economic comparison of the following biomass-CHP configurations/cases is presented: (A) boiler + ST + bottoming ORC, (B) boiler + ST, (C) boiler + ORC, and (D) configuration (A) with option to switch on or off the bottoming ORC on the basis of the heat demand available. The focus is on a 1 MWt

biomass boiler, and the plants are operated to serve residential (r), tertiary (t) and industrial (i) heat demand. The thermodynamic cycles are modelled by Cycle-Tempo, while the energy demand is modelled by simplified indicators (temperature of heat demand, equivalent hours of heat demand per year).

On the basis of the results of thermodynamic simulations, upfront and operational costs estimates, and Italian energy policy scenario (feed-in tariffs for biomass electricity), the maximum global energy efficiency and investment profitability is estimated, for each CHP configuration and energy demand segment. The highest conversion efficiency, obtained in case of industrial end users and Case B (only steam turbine) results slightly above 50%, while the option of ORC switching (Case D) makes the difference in comparison to Case A for industrial and residential market segments. The separate ORC cycle (Case C) presents a promising conversion efficiency (around 18%), which is even higher than that one of the combined cycle of Case A, due to the relatively high temperature of heat available from the intermediate HTF with molten salts.

For this reason, Case C is found here to be the most profitable option when low temperature heat demand, such as in residential sector, is available, and the maximization of electric output of the CHP system does not influence the availability of low temperature heat to match the thermal energy demand. The results show that the end user energy demand is a key factor to select the optimal CHP configuration. In particular, ORC cycles (both bottoming in a combined cycle and stand alone) appear to be profitable in case of low temperature heat demand, otherwise a flexible ORC is preferred to match the heat demand. For industrial users, a simpler configuration without ORC can be more competitive than a flexible ORC, on the basis of upfront costs, discount rate and feed-in tariffs. Further simulations to select the optimal ORC turbine output temperature should be carried out, in order to investigate the trade off between electric efficiency and temperature of heat demand, and to optimize the size of intermediate thermal storage and CHP systems, to facilitate baseload operation of the biomass boiler and at the same time smart load following operation of the CHP.

References

[1] European Commission website. Available at: http://ec.europa.eu/clima/news/articles/news_2014102401_en.htm accessed Nov 2014

[2] Pantaleo, A., Pellerano, A., Carone, M.T. (2009). Potentials and feasibility assessment of small scale CHP plants fired by energy crops in Puglia region (Italy), Biosystems Engineering 102(3), 345-359. doi:10.1016/j.biosystemseng.2008.12.002.

[3] Pantaleo, A., Candelise, C., Bauen, A., Shah, N. (2014). ESCO business models for biomass heating and CHP: Profitability of ESCO operations in Italy and key factors assessment, Renewable and Sustainable Energy Reviews 30, 237-253.

[4] Sridhar, G., Sridhar, H.V., Dasappa, S. (2005). Green electricity from biomass fuel producer gas engine, in Proceedings of 14th European Biomass Conference, Paris.

[5] Buragohain, B., Mahanta, P., Moholkar, V.S. (2010). Biomass gasification for decentralized power generation: The Indian perspective, Renewable and Sustainable Energy Reviews 14(1), 73-92. doi:10.1016/j.rser.2009.07.034.

[6] Janssen, R., Grimm, H.P., Helm, P., Pigaht, M. (2005). Biofuel burning microturbines – Current status and future perspectives, in Proceedings of 14th European Biomass Conference, Paris.

[7] Chiaramonti, D., Oasmaa, A., Solantausta, Y. (2007). Power generation using fast pyrolysis liquids from biomass, Renewable and Sustainable Energy Reviews 11(6), 1056-1086. doi:10.1016/j.rser.2005.07.008.

[8] Cocco, D., Deiana, P., Cau, G. (2006). Performance evaluation of small size externally fired gas turbine (EFGT) power plants integrated with direct biomass dryers, Energy 31(10-11), 1459- 1471. doi:10.1016/j.energy.2005.05.014.

[9] Datta, A., Ganguly, R., Sarkar, L. (2010). Energy and exergy analyses of an externally fired gas turbine (EFGT) cycle integrated with biomass gasifier for distributed power generation, Energy 35(1), 341-350.

[10] Ferreira, A.C.M., Nunes, M.L., Martins, L.A.S.B. (2012). A review of Stirling engine technologies applied to micro-cogeneration systems, in Proceedings of 25th ECOS, Palermo.

[11] Kong, X. (2004). Energy efficiency and economic feasibility of CCHP driven by Stirling engine, Energy Conversion and Management 45(9-10), 1433-1442.

doi:10.1016/j.enconman.2003.09.009.
[12] Dong, L., Liu, H., Riffat, S. (2009). Development of small-scale and micro-scale biomass-fuelled CHP systems – A literature review, Applied Thermal Engineering 29(11-12), 2119-2126. doi:10.1016/j.applthermaleng.2008.12.004.
[13] Chacartegui, R., Sánchez, D., Muñoz, J.M., Sánchez, T. (2009). Alternative ORC bottoming cycles for combined cycle power plants, Applied Energy 86(10), 2162-2170. doi:10.1016/j.apenergy.2009.02.016.
[14] Míguez, J.L., Morán, J.C., Granada, E., Porteiro, J. (2012). Review of technology in small-scale biomass combustion systems in the European market, Renewable and Sustainable Energy Reviews 16(6), 3867-3875. doi:10.1016/j.rser.2012.03.044.
[15] Bocci, E., Sisinni, M., Moneti, M., Vecchione, L., Di Carlo, A., Villarini, M. (2014). State of art of small scale biomass gasification power systems: A review of the different typologies, Energy Procedia 45, 247-256.
[16] Rentizelas, A., Karellas, S., Kakaras, E., Tatsiopoulos, I. (2009). Comparative techno-economic analysis of ORC and gasification for bioenergy applications, Energy Conversion and Management 50(3), 674-681. doi:10.1016/j.enconman.2008.10.008.
[17] Kalina, J. (2011). Integrated biomass gasification combined cycle distributed generation plant with reciprocating gas engine and ORC, Applied Thermal Engineering 31(14-15), 2829-2840. doi:10.1016/j.applthermaleng.2011.05.008.
[18] Riccio, G., Chiaramonti, D. (2009). Design and simulation of a small polygeneration plant cofiring biomass and natural gas in a dual combustion micro gas turbine (BIO_MGT), Biomass and Bioenergy 33(11), 1520-1531.
[19] Pantaleo, A.M., Camporeale, S.M., Shah, N. (2013). Thermo-economic assessment of externally fired micro-gas turbine fired by natural gas and biomass : Applications in Italy, Energy Conversion and Management 75, 202-213.
[20] Pantaleo, A.M., Camporeale, S., Shah, N. (2014). Natural gas-biomass dual fuelled microturbines: Comparison of operating strategies in the Italian residential sector, Applied Thermal Engineering 71(2), 686-696.
[21] Camporeale, S.M., Fortunato, B., Torresi, M., Turi, F., Pantaleo, A.M., Pellerano, A. (2014). Part load performances and operating strategies of a natural gas-biomass dual fuelled microturbine for CHP generation, in Proceedings of ASME Turbo Expo, Dusseldorf.

[22] Barsali, S., Giglioli, R., Ludovici, G., Poli, D. (2011). A micro combined cycle plant for power generation from solid biomass: Coupling EFGT and ORC, in Proceedings of 19th European Biomass Conference, Berlin.

[23] Bagdanavicius, A., Sansom, R., Jenkins, N., Strbac, G. (2012). Economic and exergoeconomic analysis of micro GT and ORC cogeneration systems, in Proceedings of 25th ECOS, Perugia.

[24] Preißinger, M., Heberle, F., Brüggemann, D. (2012). Exergetic analysis of biomass fired double- stage organic Rankine cycle (ORC), in Proceedings of 25th ECOS, Perugia.

[25] Chen, H., Goswami, D.Y., Stefanakos, E.K. (2010). A review of thermodynamic cycles and working fluids for the conversion of low-grade heat, Renewable and Sustainable Energy Reviews 14(9), 3059-3067, doi:10.1016/j.rser.2010.07.006.

[26] Drescher, U., Bruggemann, D. (2007). Fluid selection for the organic Rankine cycle (ORC) in biomass power and heat plants, Applied Thermal Engineering 27, 223-228.

[27] Camporeale S, Ciliberti P, Fortunato B, Torresi M, Pantaleo A. Externally Fired Micro-Gas Turbine and Organic Rankine Cycle Bottoming Cycle: Optimal Biomass/Natural Gas Combined Heat and Power Generation Configuration for Residential Energy Demand. ASME. J. Eng. Gas Turbines Power. 2016;139(4):041401-041401-10. doi:10.1115/1.4034721.

[28] Kusterer, K., Braun, R., Bohn, D. (2014). Organic Rankine cycle working fluid selection and performance analysis for combined application with a 2 MW class industrial gas turbine, in Proceedings of ASME Turbo Expo, Düsseldorf.

[29] Sharma, A., Tyagi, V.V., Chen, C.R., Buddhi, D. (2009). Review on thermal energy storage with phase change materials and applications, Renewable and Sustainable Energy Reviews 13, 318- 345.

[30] Al-Sulaiman F.A., Dincer I., Hamdullahpur F. (2013). Thermoeconomic optimization of three trigeneration systems using organic Rankine cycles: Part I – Formulations, Energy Conversion and Management 69, 199-208.

[31] Ministry Decree 5-09-2011 on incentives for high efficiency cogeneration in Italy (in Italian).

[32] Kang, S.H. (2012). Design and experimental study of ORC (organic Rankine cycle) and radial turbine using R245fa working fluid, Energy 41, 514-524.

[33] Ingeco project. Available at: http://www.verticale.net/sistemi-di-cogenerazione-a-ciclo-combinato

[34] Lai, N.A. Wendland, M., Fischer, J. (2011). Working fluids for high-temperature organic Rankine cycles, Energy 36, 199-211.
[35] Personal information with Progeco Srl.

PAPER 5

Energy performance and profitability of biomass boilers in the commercial sector: A case study in the UK

Arianna Sorrentino[1], Antonio M. Pantaleo[2,4], *, Niccolò Le Brun[4], Salvador Acha[4], Christos N. Markides[4], Giacobbe Braccio[3] , Emanuele Fanelli [3], Sergio M Camporeale[1]

1. *Department DMMM, Polytechnic of Bari, Via Orabona 4, 70125 Bari, Italy*
2. *Department DISAAT, University of Bari, Via Amendola 165/A 70125 Bari, Italy*
3. *ENEA-National Agency for New Technology, Energy, and Environment, Policoro (MT) 75025, Italy*
4. *Clean Energy Processes (CEP) Laboratory, Department of Chemical Engineering, Imperial College London, South Kensington Campus, London SW7 2AZ, UK*

Division of work among authors

Thermodynamic calculations have been done by Arianna Sorrentino (AS) under the supervision of Sergio M. Camporeale (SC). AS done the optimization of the system. AS in cooperation with Antonio M. Pantaleo (AP) carried out the economical appraisal. The paper was written by AS and AP with the help of SC. Comments and supervision were provided by the remaining authors.

Abstract

Commercial buildings or shopping malls are characterized by large thermal and electrical energy consumptions with high variability of energy demand. Therefore, there is a large interest to explore novel renewable energy generation systems for these applications. A novel flexible configuration of biomass-fired CHP system with organic Rankine cycle (ORC) is here proposed and applied to the case study of food retail buildings in the UK. The proposed configuration adopts a molten salt (MS) circuit to transfer heat from the biomass furnace to the ORC plant. A thermal Energy Storage (TES) is proposed to improve the flexible operation of the plant and reduce the size of the biomass boiler. Molten salts have been preferred to thermal oil as they have no fire risks and low environmental impact and can be used as medium for a Two Tank TES with a "direct heating" scheme. The plant has been analysed using real input data from a biomass boiler installation, conversion efficiency and heat demand from the store. The model is informed by hourly energy costs and electricity feed in tariff in order to define optimal size and operation of the bottoming ORC for the specific case study of large commercial energy end user in the UK. The results show that the use of thermal storage in a biomass-fired ORC plant can improve the boiler efficiency and reduce the biomass consumption in thermal-load following operating mode and increase the investment profitability.

Keywords: CHP; biomass; molten salts; thermal energy storage; distributed generation;

Introduction

Commercial buildings represent an important thermal and electrical energy demand segment, characterized by highly variable energy demand. To satisfy their energy demand and reduce primary energy consumption, small size combined heat and power (CHP) generation systems are possible solutions [1]. These cogeneration units form a large segment of the distributed generation (DG) market [2], presenting several advantages from environmental and economic point of view.

Biomass boilers are suitable technologies to reduce greenhouse gas emissions and increase the share of renewable energy sources. The use of biomass as substitute to fossil fuel in small-scale CHP plants has been widely investigated in literature. Available technologies for small-scale CHP (from 100 kWe to 1 MWe size) using lignocellulosic biofuel include: (i) biomass pre-processing through gasification coupled to both Internal Combustion Engine (ICE) [3] and Micro Gas Turbine (MGT) [4], included pyrolysis [5], and (ii) direct combustion in grate or fluidized bed boilers to feed externally-fired MGT [6] or Stirling [7] also for trigeneration application [8]. Another commercially available solution for biomass CHP is represented by Organic Rankine Cycle (ORC) engines [11]. ORCs are similar to the steam-driven Rankine turbine cycle, except that they are able to exploit low-temperature heat sources because of the use of an organic working fluid as medium for the turbine instead of water. The biomass ORC plants market has grown thanks to the reliability of the technology but also thanks to the policy mechanism of incentives available in many European countries [10]. A review on application of ORC in small and micro scale biomass CHP is presented in ref. [11]. In ref.[12], an assessment of the energy performance of biomass boilers coupled to an ORC under real operating conditions is showed.

Biomass boilers are generally characterised by difficulties when requested to be operated during rapid transients for load following: a longer time period to ignite the fuel and reach rated output respect to gas or oil boilers [13], lower performances and higher emissions at part load [14]. A thermal energy storage (TES) connected to a biomass boiler could allow decoupling boiler operation and thermal energy output modulation for load following. In the recent years, the development of energy storage

technologies has increased the interest on this option [15]. Thermal energy can be stored as latent heat, sensible heat or thermochemical energy. Sensible heat storage (SHS) is the most common store method. For low-temperature SHS water appears to be the best liquid available because it is inexpensive and has a high specific heat, but in case of temperature higher than 100°C diathermic oil, liquid metals or molten salts (MS) are preferred[16]. In particular, MSs show a number of advantages for applications at temperature higher than 250°C such as in the case of concentrating solar plants [17]. At these temperatures, MSs have the advantages of a high heat capacity, high density, high thermal stability, relatively low cost and low vapor pressure. The low vapor pressure results in storage designs without pressurized vessels [17]. Moreover, MSs represent also a good alternative as heat transfer fluid (HTF) to thermal oil as they have no fire risks and low environmental impact.

In this paper, a cogenerative plant composed by a biomass boiler connected to an ORC generation system and a TES selected to compensate the energy fluctuations has been analysed as possible solution to satisfy a supermarket heat demand. Real heat demand patterns in UK have been used. The main novelty relies on the biomass boiler decoupling from the load by means of a two-tanks MS TES that provide the required heat to ORC, avoiding part load operation. An economic assessment has been carried out to compare this solution to: (i) a standard configuration, where the biomass boiler is directly coupled to the ORC, (ii) a scenario where only the biomass boiler and the TES are considered and (iii) the baseline scenario where the heat is supplied to the store through the hot water produced by the boiler (currently adopted solution).

TES and ORC technology description

The layout of the plant is shown in Fig.1. The plant is composed by a biomass boiler, an intermediate circuit that uses Molten salts as HTF directly connected to a Two Tank thermal storage, an ORC operated as cogeneration unit because the heat flux discharged from the condenser is directly supplied to the thermal end users of the commercial building. The considered biomass boiler is a moving grate furnace fed by wood pellets. Unlike normal biomass boilers that produce steam or hot water, the

proposed boiler heats molten salts by means of flue gases exiting the combustion chamber flow in a heat exchanger where MS are heated up to the temperature of the hot tank. The MS selected is a mixture of lithium, sodium and potassium nitrates that can operate up to 500°C without chemical decomposition and reach 120°C without freezing [18]. MSs have been used not only as HTF but also as energy storage medium. In this work, considering the high temperature of the flue gas, a temperature of 450 °C has been chosen for the Hot Tank, while a temperature of 200°C has been chosen for the cold tank to avoid excess work for the circulating pump. Thanks to the relatively high temperature interval (450-200=250°C), the energy stored per mass unit is relatively high with savings for the costs of tanks and storage medium. The ORC analyzed receive the thermal input from molten salts. Since the temperature of the hot tank is relatively high, a recuperative configuration has been selected for the system.

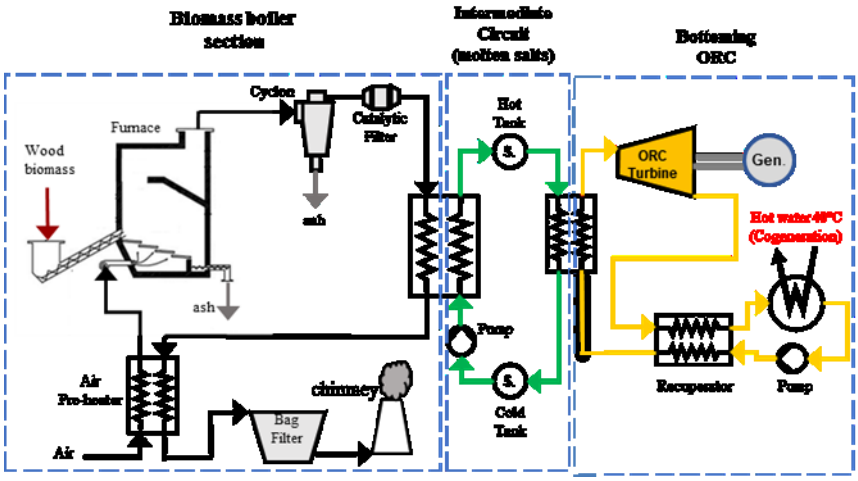

Fig. 1 Layout of the system configuration

According to the characteristic of the thermal source, Toluene proves to be a suitable working fluid because it is chemically stable in the range of temperature considered [19], [20] and meets environmental and safety requirements. It is a “dry fluid” with a dry expansion in the turbine, thus avoiding the drop generation that can damage turbine blades. The main thermodynamic properties of the ORC are summarized in Table 1 while a T-s diagram can be found in Fig.2. The condenser temperature has

been selected to match the water temperature requested by the thermal users. Other parameters used in the thermodynamic simulations are: biomass boiler efficiency = 88%; mechanical/isentropic efficiency all turbines = 90/75%; electrical genset efficiency = 92%.

Thermal energy storage: sizing and operating conditions selection

The food retail sector interest in sustainability goals is fast increasing, and a number of operators in the UK is keen to decarbonize its business and to reduce energy consumption [21]. To pursue these goals, several biomass boilers have been installed in different stores to supply the required heat, also motivated by the introduction of the non- domestic renewable heat incentive (RHI)[22] by the UK government. These boilers are constantly monitored and data on electric and thermal demand are recorded every half hour. In this paper heat demand patterns of three days, in summer, winter and mid-season shown in Fig.3, have been used to size the TES and carry out the economic assessment. All the calculations have been done under the hypothesis of heat load following condition.

Table 1. Thermodynamic properties of the ORC

Description	Value
Organic fluid	Toluene
Evaporating pressure	25 bar
Inlet turbine temperature	330°C
Condenser Temperature	85 °C
Net electric efficiency (η_{el})	18.8 %

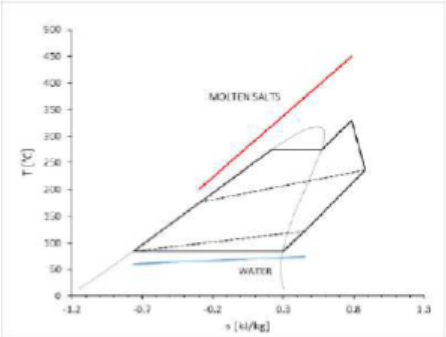

Fig. 2 ORC T-s diagram

TES has been sized in winter conditions, represented in Fig. 3 in orange, when the heat required is maximum for a time period of 24 hours. The analysis starts evaluating the mean value of the heat required by the ORC, blue line in Fig. 3. Remembering that data are available for every 30 minutes, the mean of the heat required by the ORC is equals to $Q_{mean,\ req}$ =159 kWh and, based on this, a biomass boiler of 350 kW is assumed to satisfy the demand. A

biomass boiler of 500 kW should be selected in case of absence of TES to meet the peak demand equal to 234 kW, in fig.3. $Q_{mean,\ req}$ is slightly higher than the mean of the heat profile, orange line in Fig. 3, due to the conversion efficiency of the ORC. The size of the storage to satisfy the heat demand can be obtained from the integral curve in Fig. 4, obtained by the equation (1):

$$Q(t) = \int_0^T (Q_{mean,req} - Q_{req})dt \qquad (1)$$

where:

- Q(t) is the heat sent to the TES at the time t;
- T is the time period considered, equal to 24 hours;
- Q_{req} is the heat required by the ORC.

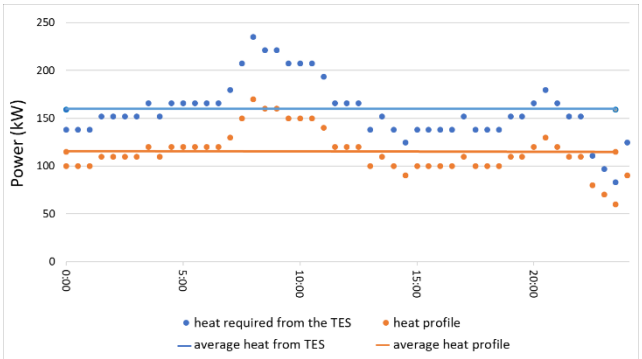

Fig. 3. Heat demands pattern and heat required from the TES

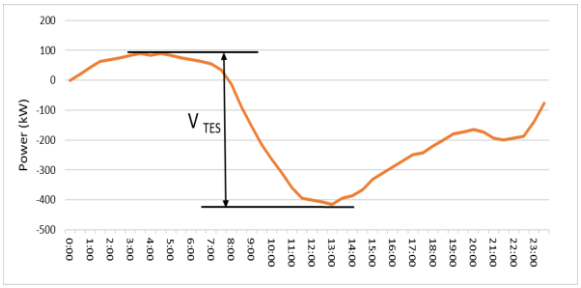

Fig. 4. Integral curve for TES size evaluation

Once the TES and the biomass boiler size are defined, it is possible to analyze the operating conditions of the biomass boilers in summer and mid-season conditions. The choice of the furnace operating mode has been done according to the following principles, in order to reduce the emissions and increase the efficiency:

- the furnace should be turned off at part load lower than 50%;
- from two ignition cycles a time interval of at least one hour should be considered.

A preliminary optimization of the furnace operating condition has been done by a trial and error strategy. ORC heat demand can be satisfied by the biomass boiler operating as summarized in table 2:

Table 2. Biomass boiler operating conditions with TES

	Winter	Mid-season	Summer
Load [%]	100	60	100
Total working hours [h]	24	12	4
Time between two ignitions [h]	0	12	10*
Average biomass consumption [t/day]	2.23	0.74	0.69

*Two ignitions considered

The evaluation of the biomass consumption has been done considered the boiler part load efficiency as declared by the manufacturer. An ORC of 100 kW has been selected in both cases considering the characteristics of the TES and of the biomass boiler.

Table 3. Technical parameters of the case study

case study	Biomass boiler size [kWt]	TES [kWh]	ORC [kWe]
TES	350	550	100
No TES	500	0	100

In table 3. the technical parameters of the considered plants are summarized

Technoeconomic assessment

In order to carry out the profitability assessment, the main cost items and biomass consumption values in Table 3 are assumed. A configuration where the biomass boiler and the TES are connected without an ORC is here added to complete the analysis. The turnkey investment and operational costs are personal estimates from manufacturers and case studies data. The operation and maintenance (O&M) costs are 5% of investment cost and include the handling and maintenance of the biomass furnace, personnel and biomass storage cost. Biomass ash discharge costs are accounted for assuming unitary cost of 70 Eur/t of ash (10% content in the biomass). The following additional input data are assumed: lower heating value (LHV) of biomass of 4.18 kWh/kg; cost of biomass of 80 Eur/t; electric internal consumption for operation of the CHP plant equal to 5%; avoided cost of electricity from on-site ORC generation of 220 Eur/MWh [23]; heat selling price of 80 Eur/MWh for tertiary end users.

Table 3. CAPEX, OPEX and biomass consumption for the selected case studies.

Description	**TES**	**No TES**	**No ORC**
Biomass consumption (t/year)	151	281	151
Total upfront cost (kEur) of which:	385	400	200
- ORC generator	185	185	0
- Biomass boiler, HEX, gas treatment	134	185	134
- Intermediate HTF circuit and MS system	36	0	36
- Engineering, development, insurance	30	30	30
Specific upfront cost (kEur/kWt)	1.10	0.80	0.57

The financial appraisal of the investment is carried out assuming the following assumptions: (i) an operational lifetime of 20 year with no 're-powering' over this

lifetime and zero decommissioning costs; (ii) the maintenance and fuel supply costs, and electricity and heat selling prices are held constant of the lifetime (in real 2018 values); (iii) the feed-in tariff for biomass electricity is available over the entire lifetime of the project; (iv) the capital assets depreciate linearly over 20 years; and (v) the cost of capital (net of inflation) is equal to 5%, corporation tax can be neglected, and the capital investments and income do not benefit from any support. The equivalent operating hours for electricity production, assuming a thermal load following operating mode, are respectively 767 (biomass boiler + TES + ORC and biomass boiler + TES) and 680 (biomass boiler + TES) per year. The analysis has been done on a seasonal base, hence the number of days considered are 75/76/161 respectively in winter, summer and mid-seasons.

Results

In fig.5 the levelized cost of heat and electricity (LCE) is reported for the three case-studies. The fuel costs are allocated to the heat generation, while the investment and operational costs of the boiler and ORC system are allocated respectively to the heat and electricity generated. The presence of the TES results in a lower value of LCE considering both electricity and heat costs. The higher cost of the configuration with no TES is due to the thermal load-following condition which limit electricity production.

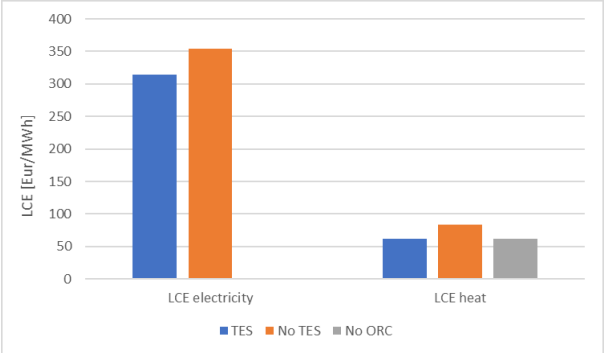

Fig. 5. Levelized cost of electricity and heat

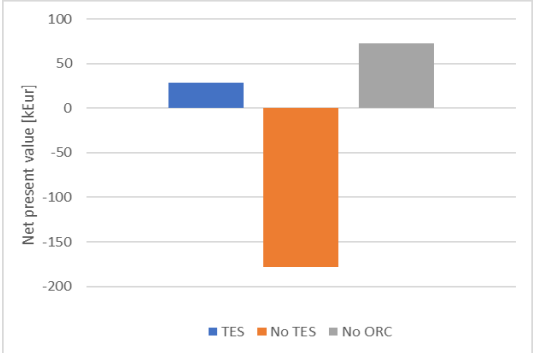

Fig. 6. Net present value

The net present value (NPV), in Fig. 6, is negative only in the case of no TES. This is due to a low number of operating hours (10% of the annual total) in view of significant investment related to the ORC.

The economic indices are displayed in Fig 7-9. The internal rate of return (IRR) in Fig. 7 and the Profitability Index of Fig 8 confirm the considerations done for the NPV: in a thermal-load following mode, considering the low amount of electricity produced, coupling an ORC to a biomass boiler by means of a TES does not increase the investment profitability.

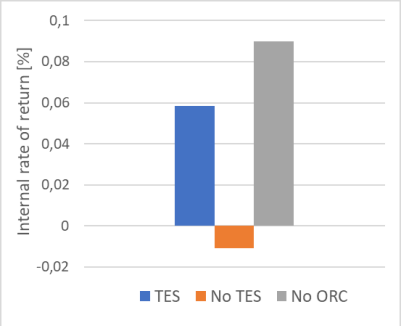

Fig.7. Internal rate of return

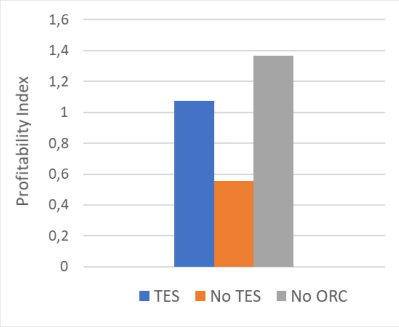

Fig.8. Profitability index

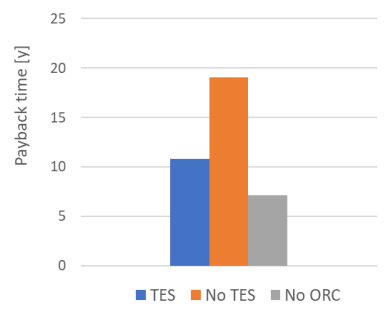

Fig.9. Not discounted payback time

Profitability index of the biomass boiler + TES + ORC configuration is also more profitable than biomass boiler + ORC without the thermal storage, since this allows higher global conversion efficiency due to the peak shaving effect of the thermal storage buffer. The Payback time of fig. 9 confirms the advantages of a TES in biomass- fired ORC plant since payback time is almost 50% lower than the one with no TES, and the option of only heating generation without the bottoming ORC presents the lowest PBT.

Conclusions

In this paper, a thermo-economic comparison of the following biomass-CHP configurations is proposed: biomass boiler + TES + ORC, boiler + ORC and boiler +TES. The plants are operated to serve commercial heat demand in thermal load following mode. Real data from one of the Sainsbury's store

have been used to size the TES and the biomass boiler and select the operating conditions of the plant. On the basis of the results of thermodynamic simulations and upfront and operational costs estimate, the investment profitability is evaluated, for each configuration. The main conclusions are:

- Coupling the biomass boiler with a TES allows the boiler to work at higher part load conditions and consequently at higher global energy efficiency, with a lower biomass consumption and reduced emission. The economic analysis suggests that this solution presents a higher profitability on respect to the solution without thermal storage;
- A bottoming ORC is not profitable in a thermal-load following operating mode since the low amount of electricity production does not allows recovering the investment costs.

Further simulations to select the optimal ORC turbine output temperature should be carried out, in order to investigate the trade-off between electric efficiency and temperature of heat demand, and to optimize the size of intermediate thermal storage and CHP systems, to facilitate baseload operation of the biomass boiler and at the same time smart load following operation of the CHP

References

[1] M. Casisi, A. Pinamonti, M. Reini, "Optimal lay-out and operation of combined heat and power (CHP) distributed generation systems", Energy 34(2009) 2175-2183;

[2] G. Pepermansa, J. Driesenb , D. Haeseldonckxc , R. Belmansc , W. D'haeseleer, "Distributed generation: definition, benefits and issues", Energy Policy 33 (2005) 787–798;

[3] Buragohain, B., Mahanta, P., Moholkar, V.S. (2010). Biomass gasification for decentralized power generation: The Indian perspective, Renewable and Sustainable Energy Reviews 14(1), 73-92. doi:10.1016/j.rser.2009.07.034;

[4] Janssen, R., Grimm, H.P., Helm, P., Pigaht, M. (2005). Biofuel burning microturbines – Current status and future perspectives, in Proceedings of 14th European Biomass Conference, Paris;

[5] Chiaramonti, D., Oasmaa, A., Solantausta, Y. (2007). Power generation using fast pyrolysis liquids from biomass, Renewable and Sustainable Energy Reviews 11(6), 1056-1086. doi:10.1016/j.rser.2005.07.008;

[6] Cocco, D., Deiana, P., Cau, G. (2006). Performance evaluation of small size externally fired gas turbine (EFGT) power plants integrated with direct biomass dryers, Energy 31(10-11), 1459-1471. doi:10.1016/j.energy.2005.05.014.;

[7] Ferreira, A.C.M., Nunes, M.L., Martins, L.A.S.B. (2012). A review of Stirling engine technologies applied to micro-cogeneration systems, in Proceedings of 25th ECOS, Palermo;

[8] Kong, X. (2004). Energy efficiency and economic feasibility of CCHP driven by Stirling engine, Energy Conversion and Management 45(9-10), 1433-1442. doi:10.1016/j.enconman.2003.09.009;

[9] H. Liu, Y. Shao, J. Li, "A biomass-fired micro-scale CHP system with organic Rankine cycle (ORC) e Thermodynamic modelling studies", biomass and bioenergy 35(2011) 3985-3994;

[10] A. Guercio, R. Bini, "Biomass-fired Organic Rankine Cycle combined heat and power systems", https://doi.org/10.1016/B978-0-08-100510-1.00015-6;

[11] Dong, L., Liu, H., Riffat, S. (2009). Development of small-scale and micro-scale biomass-fuelled CHP systems – A literature review, Applied Thermal Engineering 29(11-12), 2119-2126. doi:10.1016/j.applthermaleng.2008.12.004;

[12] D. Prando, M. Renzi, A. Gasparella, M. Baratieri, "Monitoring of the energy performance of a district heating CHP plant based on biomass boiler and ORC generator", Applied Thermal Engineering 79 (2015) 98-107;

[13] Duncan M Faulkes, "Modelling the optimum thermal store and biomass boiler size for a small communal heating scheme", Building Serv. Eng. Res. Technol. 2016, Vol. 37(2) 136–147;

[14] V.K. Verma , S. Bram , G. Gauthier , J. De Ruyck, “Performance of a domestic pellet boiler as a function of operational loads: Part-2”, Biomass and bioenergy 35(2011);

[15] Atul Sharma, V.V. Tyagi , C.R. Chen , D. Buddhi, “Review on thermal energy storage with phase change materials and applications”, Renewable and Sustainable Energy Reviews 13 (2009) 318–345;

[16] U. Herrmann, D.W. Kearney, “Survey of Thermal Energy Storage for Parabolic Trough Plants.”, ASME J Sol Energy Eng. 124 (2002) 145-151;

[17] T. Bauer, N. Breidenbach, N. Pfleger, D. Laing, M Eck, “Overview of molten salt storage systems and material development for solar thermal power plants”, Conference: World Renewable Energy Forum 2012

[18] R.W. Bradshow, D.R. Meeker, “High temperature stability of ternary nitrate molten salts for solar thermal energy systems”, Solar Energy materials (1990), 51-60.

[19] Lai, N.A. Wendland, M., Fischer, J. (2011). Working fluids for high-temperature organic Rankine cycles, Energy 36, 199-211;

[20] A. Sorrentino, A. M. Pantaleo, S. Camporeale, N. Markides, G. Braccio, “Distributed heat and power generation: Thermo-economic analysis of Biomass-fired Rankine cycle systems with molten salts as heat transfer fluid”, (submitted);

[21] N. Le Brun, S. Acha, C. N. Markides, N. Shah, “Techno-economic potential of small-scale ORC systems applied to supermarkets”, (under review) Thermal Science and Engineering Progress;

[22] Renewable heat incentive website: https://www.gov.uk/non-domestic-renewable-heat-incentive;

[23] Al-Sulaiman F.A., Dincer I., Hamdullahpur F. (2013). Thermoeconomic optimization of three trigeneration systems using organic Rankine cycles: Part I – Formulations, Energy Conversion and Management 69, 199-208.